

A LABORATORY STUDY OF THE ROLE OF GEOTECHNICAL  
FABRIC AS A SEPARATION MEDIUM IN A  
SOIL FABRIC SYSTEM

By

JOHN KEVIN KING

"

Bachelor of Science in Civil Engineering

Oklahoma State University

Stillwater, Oklahoma

1979

Submitted to the Faculty of the Graduate College  
of the Oklahoma State University  
in partial fulfillment of the requirements  
for the Degree of  
MASTER OF SCIENCE  
July, 1981

Thesis  
1981  
K532  
00p.2

Dedicated to everyone who  
had faith in me.



A LABORATORY STUDY OF THE ROLE OF GEOTECHNICAL  
FABRIC AS A SEPARATION MEDIUM IN A  
SOIL FABRIC SYSTEM

Thesis Approved:

*L. Allen Haliburton*  
Thesis Adviser

*Ronald R. Snethen*

*James V. Parker*

*Norman D. Durham*  
Dean of the Graduate College



## PREFACE

This report discusses conclusions reached after analyzing data collected from research conducted for the United States Air Force Office of Scientific Research under grant AFOSR-79-0087. I am very grateful for the opportunity to participate in this research.

Companion research was conducted by graduate student, Mr. Jack D. Lawmaster. Portions of preliminary testing were conducted by Mr. Lawmaster and undergraduate student, Mr. Page Maxson. Clerical work involved in preparation of this thesis was performed by Ms. Charlene Fries and Ms. Barbara Vick.

I would like to express my gratitude to all of the above mentioned people for their assistance in conducting the research and/or preparing the report.

I would like to express my gratitude also to my committee members Dr. J. V. Parcher and Dr. D. R. Snethen for their assistance and careful review of the manuscript. I am especially grateful to my major advisor, Dr. T. A. Haliburton, for his guidance and assistance during this project.

A very special thanks to my wife, Leslie and my parents for their love and sometimes impatient understanding.

## TABLE OF CONTENTS

| Chapter  | Page |
|--|------|
| I. INTRODUCTION . . . . .                          | 1    |
| Geotechnical Fabric . . . . .                      | 1    |
| Statement of Problem . . . . .                     | 2    |
| Scope of Research . . . . .                        | 3    |
| II. LITERATURE SURVEY . . . . .                    | 4    |
| Introduction . . . . .                             | 4    |
| Snaith and Bell (5) . . . . .                      | 4    |
| T. A. Haliburton and Jack Fowler (6) . . . . .     | 5    |
| Bender and Barenberg (7) . . . . .                 | 6    |
| Summary . . . . .                                  | 7    |
| III. MATERIAL, EQUIPMENT, AND PROCEDURES . . . . . | 8    |
| Fabrics Evaluated in Testing Program . . . . .     | 8    |
| Testing Program . . . . .                          | 8    |
| Details of Uniaxial Tension Testing . . . . .      | 11   |
| Details of Creep Testing . . . . .                 | 11   |
| Details of Direct Shear Testing . . . . .          | 13   |
| Details of Separation Testing . . . . .            | 15   |
| IV. RESULTS AND DISCUSSION . . . . .               | 22   |
| Selection of Geotechnical Fabrics . . . . .        | 22   |
| Separation Tests . . . . .                         | 26   |
| V. CONCLUSIONS AND RECOMMENDATIONS . . . . .       | 32   |
| Conclusions . . . . .                              | 32   |
| Literature Survey . . . . .                        | 32   |
| Preliminary Testing . . . . .                      | 32   |
| Separation Testing . . . . .                       | 33   |
| Recommendations for Further Research . . . . .     | 34   |
| BIBLIOGRAPHY . . . . .                             | 35   |
| APPENDIX - FIGURES AND TEST RESULTS . . . . .      | 36   |

## LIST OF TABLES

| Table   | Page |
|---|------|
| I. Fabrics Used in Initial Testing . . . . .  | 9    |
| II. Soil-Fabric Friction Values Fabric Warp Direction . . . . .   | 24   |
| III. Warp Direction Physical Properties of Geotechnical Fabrics<br>Used in Separation Testing Program . . . . . | 25   |

## LIST OF FIGURES

| Figure  | Page |
|---|------|
| 1. Photographs of Bidim C-34-Warp Direction in Tension Testing of (Left to Right) Start, 10 Percent Strain, Failure, and Rebound . . . . .                  | 12   |
| 2. Schematic Diagram of Separation Testing Equipment . . . . .  | 14   |
| 3. Schematic Diagram of Separation Model Test Box . . . . .   | 17   |
| 4. Separation Experiment Test Box Containing Kaolinite Subgrade, with Geotechnical Fabric Anchored in Place . . . . .                                       | 18   |
| 5. Separation Experiment Test Box with 0.5-in.-dia Ball Bearing Aggregate Placed Over Geotechnical Fabric . . . . .   | 20   |
| 6. Separation Experiment Test Setup, Ready for Conduct of Testing . . . . .   | 21   |
| 7. Displacement vs. Number of Loading Cycle Relationships for the Four Test Fabrics Used in Separation Experiment . . . . .                                 | 28   |
| 8. Underside of Geolon 66475 Fabric After Separation Testing, Showing Kaolinite Subgrade Smeared on the Fabric . . . . .                                    | 30   |
| 9. Photographs of Bidim C-34-Warp Direction in Tension Testing at (Left to Right) Start, 10 Percent Strain, Failure, and Rebound . . . . .                  | 37   |
| 10. Photographs of Bidim C-34-Fill Direction in Tension Testing at (Left to Right) Start, 10 Percent Strain, Failure, and After "Elastic" Rebound . . . . . | 38   |
| 11. Stress-Strain Data for Bidim C-34 in Uniaxial Testing . . . . .   | 39   |
| 12. Photographs of Typar 3401-Warp Direction in Tension Testing at (Left to Right) Start, 10 Percent Strain, Failure, and After "Elastic" Rebound . . . . . | 40   |
| 13. Photographs of Typar 3401-Fill Direction in Tension Testing at (Left to Right) Start, 10 Percent Strain, Failure, and After "Elastic" Rebound . . . . . | 41   |
| 14. Stress-Strain Data for Typar 3401 in Uniaxial Testing . . . . .   | 42   |

| Figure   | Page |
|--|------|
| 15. Photographs of Celanese 500X-Warp Direction in Tension Testing at (Left to Right) Start, 10 Percent Strain, Failure, and After "Elastic" Rebound . . . . . | 43   |
| 16. Photographs of Celanese 500X-Fill Direction in Tension Testing at (Left to Right) Start, 10 Percent Strain, Failure, and After "Elastic" Rebound . . . . . | 44   |
| 17. Stress-Strain Data for Celanese 500X in Uniaxial Testing . . .   | 45   |
| 18. Photographs of Nicolon 66475-Warp Direction in Tension Testing at (Left to Right) Start, 10 Percent Strain, Failure, and After "Elastic" Rebound . . . . . | 46   |
| 19. Photographs of Nicolon 66475-Fill Direction in Tension Testing at (Left to Right) Start, 10 Percent Strain, Failure, and After "Elastic" Rebound . . . . . | 47   |
| 20. Stress-Strain Data for Nicolon 66475 in Uniaxial Testing . . .   | 48   |
| 21. Photographs of Celanese 600X-Warp Direction in Tension Testing at (Left to Right) Start, 10 Percent Strain, Failure, and After "Elastic" Rebound . . . . . | 49   |
| 22. Photographs of Celanese 600X-Fill Direction in Tension Testing at (Left to Right) Start, 10 Percent Strain, Failure, and After "Elastic" Rebound . . . . . | 50   |
| 23. Stress-Strain Data for Celanese 600X in Uniaxial Testing . . .   | 51   |
| 24. Photographs of Diamond 8-Warp Direction in Tension Testing at (Left to Right) Start, 10 Percent Strain, Failure, and After "Elastic" Rebound . . . . .     | 52   |
| 25. Photographs of Diamond 8-Fill Direction in Tension Testing at (Left to Right) Start, 10 Percent Strain, Failure, and After "Elastic" Rebound . . . . .     | 53   |
| 26. Stress-Strain Data for Diamond 8 in Uniaxial Testing . . . . .   | 54   |
| 27. Photographs of Special 400-Warp Direction in Tension Testing at (Left to Right) Start, 10 Percent Strain, Failure, and After "Elastic" Rebound . . . . .   | 55   |
| 28. Photographs of Special 400-Fill Direction in Tension Testing at (Left to Right) Start, 10 Percent Strain, Failure, and After "Elastic" Rebound . . . . .   | 56   |
| 29. Stress-Strain Data for Special 400 in Uniaxial Testing . . . . .   | 57   |

| Figure   | Page |
|--|------|
| 30. Photographs of Retain 72-Warp Direction in Tension Testing at (Left to Right) Start, 10 Percent Strain, Failure, and After "Elastic" Rebound . . . . .       | 58   |
| 31. Photographs of Retain 72-Fill Direction in Tension Testing at (Left to Right) Start, 10 Percent Strain, Failure, and After "Elastic" Rebound . . . . .       | 59   |
| 32. Stress-Strain Data for Retain 72 in Uniaxial Testing . . . . .   | 60   |
| 33. Photographs of Stitchbond 1375-Warp Direction in Tension Testing at (Left to Right) Start, 10 Percent Strain, Failure, and After "Elastic" Rebound . . . . . | 61   |
| 34. Photographs of Stitchbond 1375-Fill Direction in Tension Testing at (Left to Right) Start, 10 Percent Strain, Failure, and After "Elastic" Rebound . . . . . | 62   |
| 35. Stress-Strain Data for Stitchbond 1375 in Uniaxial Testing . . . . .   | 63   |
| 36. Photographs of Fibretex 150-Warp Direction in Tension Testing at (Left to Right) Start, 10 Percent Strain, Failure, and After "Elastic" Rebound . . . . .    | 64   |
| 37. Photographs of Fibretex 150-Fill Direction in Tension Testing at (Left to Right) Start, 10 Percent Strain, Failure, and After "Elastic" Rebound . . . . .    | 65   |
| 38. Stress-Strain Data for Fibretex 150 in Uniaxial Testing . . . . .  | 66   |
| 39. Photographs of Fibretex 200-Warp Direction in Tension Testing at (Left to Right) Start, 10 Percent Strain, Failure, and After "Elastic" Rebound . . . . .    | 67   |
| 40. Photographs of Fibretex 200-Fill Direction in Tension Testing at (Left to Right) Start, 10 Percent Strain, Failure, and After "Elastic" Rebound . . . . .    | 68   |
| 41. Stress-Strain Data for Fibretex 200 in Uniaxial Testing . . . . .  | 69   |
| 42. Photographs of Fibretex 300-Warp Direction in Tension Testing at (Left to Right) Start, 10 Percent Strain, Failure, and After "Elastic" Rebound . . . . .    | 70   |
| 43. Photographs of Fibretex 300-Fill Direction in Tension Testing at (Left to Right) Start, 10 Percent Strain, Failure, and After "Elastic" Rebound . . . . .    | 71   |
| 44. Stress-Strain Data for Fibretex 300 in Uniaxial Testing . . . . .  | 72   |

| Figure   | Page |
|--|------|
| 45. Photographs of Fibretex 400-Warp Direction in Tension Testing at (Left to Right) Start, 10 Percent Strain, Failure, and After "Elastic" Rebound . . . . .              | 73   |
| 46. Photographs of Fibretex 400-Fill Direction in Tension Testing at (Left to Right) Start, 10 Percent Strain, Failure, and After "Elastic" Rebound . . . . .              | 74   |
| 47. Stress-Strain Data for Fibretex 400 in Uniaxial Testing . . . . .  | 75   |
| 48. Photographs of Style 5793-Warp Direction in Tension Testing at (Left to Right) Start, 10 Percent Strain, Failure, and After "Elastic" Rebound . . . . .                | 76   |
| 49. Photographs of Style 5793-Fill Direction in Tension Testing at (Left to Right) Start, 10 Percent Strain, Failure, and After "Elastic" Rebound . . . . .                | 77   |
| 50. Stress-Strain Data for Style 5793 in Uniaxial Testing . . . . .  | 78   |
| 51. Photographs of Stabilenka 200-Warp Direction in Tension Testing at (Left to Right) Start, 10 Percent, Failure, and After "Elastic Rebound . . . . .                    | 79   |
| 52. Photographs of Stabilenka 200-Fill Direction in Tension Testing at (Left to Right) Start, 10 Percent Strain, Failure, and After "Elastic" Rebound . . . . .            | 80   |
| 53. Stress-Strain Data for Stabilenka 200 in Uniaxial Testing . . . . .  | 81   |
| 54. Photographs of Mount Mills Fabric-Warp Direction in Tension Testing at (Left to Right) Start, 10 Percent Strain, Failure, and After "Elastic" Rebound . . . . .        | 82   |
| 55. Photographs of Mount Vernon Mills Fabric-Fill Direction in Tension Testing at (Left to Right) Start, 10 Percent Strain, Failure, and After "Elastic" Rebound . . . . . | 83   |
| 56. Stress-Strain Data for Mount Vernon Mills Fabric in Uniaxial Testing . . . . .   | 84   |
| 57. Photographs of Corning Fiberglass Fabric-Warp Direction in Tension Testing at (Left to Right) Start, 10 Percent Strain, Failure, and After "Elastic" Rebound . . . . . | 85   |

## CHAPTER I

### INTRODUCTION

#### Geotechnical Fabric

Geotechnical fabric is a generic term applied to a wide variety of artificial fiber textile products used in the construction industry today. Other names for geotechnical fabric include geofabric, filter cloth, and civil engineering fabric. Approximately 50 different geotechnical fabrics are commercially available in the United States. The fabrics are classified as either woven or nonwoven and can vary in weights from 3 oz per sq yd to over 26 oz per sq yd. Many of these fabrics may be characterized by relatively light weight, moderate to high tensile strength, initial semi-elastic behavior, ability to undergo large amounts of elongation without rupture, permeability equivalent to that of a medium to fine sand, and high resistance to corrosion and bacterial action. Almost all geotechnical fabric will undergo deterioration after exposure to ultraviolet radiation (sunlight) for a 30- to 60-day period unless treated. Woven geotechnical fabrics are manufactured on a weaving loom while nonwoven geotechnical fabrics are manufactured by a bonding process, therefore, heat bonded or chemically bonded. Geotechnical fabrics are currently produced in 6 ft to 60 ft widths, and in lengths up to several thousand feet on special order. Approximate fabric costs range from less than \$0.30 per sq yd for the lighter weight fabrics to over \$6.00 per sq yd for the heavier weight



fabrics. Woven fabrics are usually more expensive than nonwoven fabrics for the same weight.

For a number of years geotechnical fabrics have been used in the construction industry in roads, railway construction, earth structures and hydraulic structures but their application has been limited because there are no design procedures available for selection and use. In order to develop design parameters, laboratory investigations and field tests must be performed to understand the reactions to certain soil conditions, loads, and loading conditions.

In 1973, McGowan and Ovelton [1]<sup>1</sup> determined that geotechnical fabrics had three basic operational functions: separation, filtration, and reinforcement. In 1974, Leflaive and Puig [2] defined a fourth function applicable to some fabrics, principally nonwoven fabrics having appreciable thickness, that of drainage in the plane of the fabric. In 1977, Stewart et al. [3] defined a fifth function, lateral restraint of cohesionless soils, as a special category of the reinforcement concept applicable to low-volume roadways. Kinney and Barenberg [4], in 1978, further subdivided the reinforcement concept, in evaluation of fabric-reinforced unsurfaced roadways, to include the concept of membrane-type fabric support developed from wheelpath rutting. Only the separation function will be considered in this report.

#### Statement of Problem

This report deals with the function of geotechnical fabric as a separation medium between a layer of soft cohesive subgrade and cohesionless

---

<sup>1</sup>References are listed, in order of first citation, at the end of the report.

cover material. Many hypotheses and theories have been developed over the years but little quantitative data are available concerning geotechnical fabric as a separation medium.

In recent years, geotechnical fabric has been used in both temporary and permanent roadway construction, primarily on very soft, wet, cohesive subgrades. Its primary functions were to prevent contamination of granular base materials by underlying subgrade soils, and to provide tensile stress-carrying ability to base material, increasing its ultimate strength and load-deformation modulus. Most design procedures now are based primarily on many years of actual construction experience. Little quantitative data exist, especially with respect to what degree of improvement results from fabric separation and whether or not any large difference in separation performance occurs between various types of commercially available geotechnical fabrics.

#### Scope of Research

It is the purpose of this research to investigate the effect of geotechnical fabric as a separation medium. By placing different fabrics in between a layer of soft, wet subgrade and a layer of aggregate, it will be shown what the effect on deformation is and if there is any difference in which fabric is used.

## CHAPTER II

### LITERATURE SURVEY

#### Introduction

Current literature pertaining to the separation function of geotechnical fabrics in undocumented field tests and design procedures is abundant but at this time literature devoted to laboratory research is essentially nonexistent. While such observations allow interference of expected behavior, a lack of quantitative data exists, especially with respect to what degree of improvement results from fabric separation and whether or not any large difference in separation performance occurs between various types of commercially available geotechnical fabrics.

At this time only one article could be found with regard to laboratory research of geotechnical fabrics used as a separation media, so articles dealing with field testing were evaluated to determine which characteristics of fabric separation need to be determined in the laboratory. To avoid repetition in the presentation of various authors' opinions and in order to eliminate literature which does not contribute to the overall effectiveness of the literature survey, discussions of only three articles are presented in this report.

#### Snaith and Bell (5)

In their paper presented in Geotechnique, December, 1978, they

discussed the filtration behavior of construction fabrics under conditions of dynamic loading. In their test they compacted a typical cohesive subgrade for Northern Ireland to 95 percent relative compaction. Then they placed a layer of fabric secured tightly against the sides of the box and added aggregate also typical to Northern Ireland. Water was added to insure saturation of the subbase and the specimens were placed into the loading frame. For a period of twenty-four hours the stress normal to the plane of the fabric was varied sinusoidally between 25 and  $75 \text{ kN/m}^2$  at a rate of 5HZ.

They concluded that an explanation can be found from the behavior of the pore water pressure at the fabric interface. The pore water pressure in the subgrade increases in response to the increasing normal pressure in any given cycle of load. As the normal pressure reduces at a later stage in the cycle the excess pore water pressure will not dissipate instantaneously. Therefore the subgrade pore water pressure will remain high during testing. This will tend to reduce the interparticle contact pressures and assist the dynamically applied pressure in breaking down the soil structure, possibly freeing clay sized particles or flocs. It will be obvious that to prevent the internal filter forming below the fabric membrane, both an elevated and a fluctuating pore water pressure is required in the immediate vicinity of the fabric. Conversely it may be concluded that the fabrics which performed well are preventing one or both of these requirements.

T. A. Haliburton and Jack Fowler (6)

In their paper presented to the First Canadian Symposium on Geotextiles the authors presented the benefits of placing a layer of fabric

between a layer of soft subgrade material and a layer of cohesionless cover material. The benefits were separation of the soft subgrade and cover material, lateral restraint of the cover material under applied vehicular loadings and "membrane-type" support from the fabric carrying part of the imposed wheel loads.

When a properly selected geotechnical fabric is placed between a soft cohesive subgrade, usually at or above its plastic limit, and essentially cohesionless cover material, the fabric will prevent intrusion of fines into the cohesionless material and also prevent penetration of the granular cover material into the plastic subgrade, while allowing drainage of excess pore pressures from the subgrade. The primary function of the geotechnical fabric in a separation mode is to insure that the roadway remains as originally designed. An appropriate fabric permeability is one which would allow outflow of water and relief of excess pore pressures while retaining fine soil particles without clogging, or else undesirable excess pore pressures may be created and cause general loss of subgrade support strength. Furthermore, the fabric must resist puncture and abrasion by aggregate particles of the cover material.

#### Bender and Barenberg (7)

Bender and Barenberg (7) presented results of research conducted for the Celanese Fibers Marketing Company. They evaluated Mirafi 140 in a soil-fabric-aggregate system. The soil used was a low plasticity clay and the aggregate was crushed limestone.

The benefits of placing a geotechnical fabric between the subgrade and aggregate layers were confinement and reinforcement of aggregate layer, confinement of the subgrade soil, separation of soil and aggregate

layers, and introduction of a filter medium which permits the free flow of water from the soil into the aggregate layer while preventing the migration of fine particles from the soil into the coarse aggregate layer.

With regard to the separation mode, the authors stated that infiltration of fine grained soils into the aggregate layer is a major cause of failure in soil-aggregate systems. When the fine grained soils force into the aggregate materials, it tends to plug the voids of the aggregate, preventing free drainage of the water from the aggregates. In a saturated state, many aggregates exhibit a reduced stability and reduced load carrying capacity. Intermixing of the soil and aggregate tends to reduce the effective depth of the system, thus changing the design. Inclusion of a layer of fabric inhibits the migration, thus maintaining the separation of the soil and aggregate layers.

#### Summary

After reviewing the above literature and numerous other published and non-published articles, several important items of interest were noted. These items are:

1. The fabric should prevent intrusion of fines into the cohesionless material.
2. The fabric should prevent penetration of the granular cover material into the plastic subgrade.
3. The fabric should allow drainage of excess pore water pressure from the subgrade.
4. The fabric should resist puncture and abrasive action by the aggregate particles of the cover material.

## CHAPTER III

### MATERIAL, EQUIPMENT, AND PROCEDURES

#### Fabrics Evaluated in Testing Program

A total of 17 artificial fiber geotechnical fabrics were obtained for evaluation in the study. The 17 fabrics, identified in Table I, consisted of 7 nonwoven and 10 woven fabrics. Fiber material consisted of various combinations of polypropylene, nylon, polyamide, and polyester. Fabrics were obtained through correspondence with the geotechnical fabric manufacturers.

In Table I, the "fabric trade name" is the designation provided by the particular fabric manufacturer when supplying the fabric. Descriptive data indicated in Table I are those of the author, obtained in part from manufacture-supplied literature. Also listed in Table I is the fabric manufacturer.

#### Testing Program

Four types of tests were conducted on the fabric samples. The first of these tests was a uniaxial tension test. The purpose of this test was to determine the stress-strain characteristics of each fabric and to find two woven and two nonwoven fabrics with dissimilar characteristics. It was established at the start of the testing program that two woven fabrics, one with high tensile strength and stress-strain modulus and one with low tensile strength and stress-strain modulus would be subjected to further

TABLE I  
FABRICS USED IN INITIAL TESTING

| Fabric Trade Name         | Fabric Manufacturer or Distributor  | Fabric Description  |
|---------------------------|-------------------------------------|---|
| Mount Vernon Mills Fabric | Advance Construction Specialties    | Woven Nylon Monofilament                                      |
| Celanese 500X/Mirafi 500X | Celanese Corporation                | Woven Polypropylene Monofilament                              |
| Celanese 600X/Mirafi 600X | Celanese Corporation                | Woven Polypropylene Monofilament                              |
| Diamond 8                 | Collins & Aikman Corporation        | Woven Nylon Monofilament                                      |
| Special 400               | Collins & Aikman Corporation        | Woven Nylon Monofilament                                      |
| Retain 72                 | Collins & Aikman Corporation        | Woven Nylon Monofilament                                      |
| Stitchbond 1375           | Collins & Aikman Corporation        | Nonwoven Stitchbonded Polyester Monofilament                  |
| Fibretex 150              | Crown Zellerbach                    | Nonwoven Needle-Punched Spunbonded Polypropylene Monofilament |
| Fibretex 200              | Crown Zellerbach                    | Nonwoven Needle-Punched Spunbonded Polypropylene Monofilament |
| Fibretex 300              | Crown Zellerbach                    | Nonwoven Needle-Punched Spunbonded Polypropylene Monofilament |
| Fibretex 400              | Crown Zellerbach                    | Nonwoven Needle-Punched Spunbonded Polypropylene Monofilament |
| Corning Fiberglass Fabric | Dow-Corning Corporation             | Woven Fiberglass Monofilament                                 |
| Tyapr 3401                | E. I. DuPont De Nemours & Co., Inc. | Nonwoven Spunbonded Polypropylene Monofilament                |



TABLE I (Continued)

| Fabric Trade Name          | Fabric Manufacturer or Distributor | Fabric Description  |
|----------------------------|------------------------------------|---|
| Bidim C-34                 | Monsanto Textiles Co.              | Nonwoven Mechanically Entangled Continuous Polyester Filament |
| Nicolon 66475/Geolon 66475 | Nicolon Corporation                | Woven Polypropylene Multifilament Strands                     |
| Stabilenka 200             | Nicolon Corporation                | Woven Fiberglass Monofilament                                 |
| Style 5793                 | Westpoint Pepperell                | Woven Polyester Multifilament Strands                         |

testing. Similarly, two nonwoven fabrics were selected and subjected to further testing. Other testing consisted of creep measurement, which provides time-dependent elongation under applied static load, measurement of soil-fabric frictional resistance by direct shear testing and separation testing. The primary test of this report, the separation test, consisted of inserting a sample of fabric in between a layer of soft clay and a layer of aggregate, applying an alternating static load with two air cylinders and measuring the displacement of the loading foot directly under the loaded area.

#### Details of Uniaxial Tension Testing

All 17 fabrics obtained from manufacturers were subjected to uniaxial tension testing. Six-inch wide fabric specimens were chosen for use and tests were conducted with an initial twelve-inch length of sample between grip points. A typical tension test can be seen in Figure 1. The tension tests were conducted at a rate of one percent strain per minute (0.12 in./min). The strain rate and the specimen's dimensions were based upon results obtained by earlier testing by Haliburton, Anglin, and Lawmaster [8].

#### Details of Creep Testing

The fabric was placed in the creep testing grips and lapped completely around each grip to prevent fabric pullout. The top grip was then suspended from a steel frame and a weight hanger attached to the bottom grip. Each fabric was subjected to a static load sufficient to induce tensile stress equal to that developed at two percent, six percent, and ten percent elongation during the uniaxial tension testing. The static load

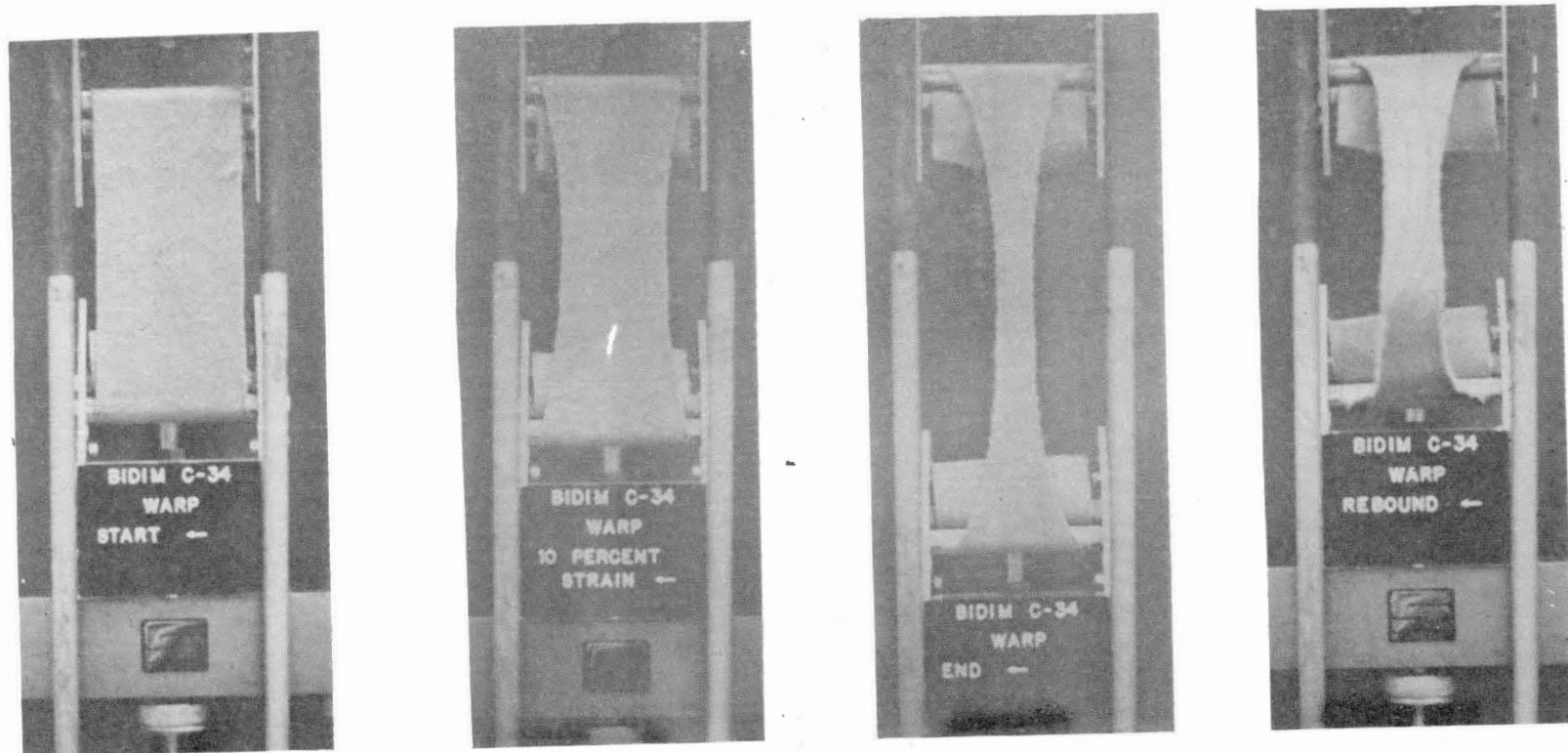


Figure 1. Photographs of Bidim C-34-Warp Direction in Tension Testing of (Left to Right) Start, 10 Percent Strain, Failure, and Rebound

### Details of Separation Testing

The separation experiment was designed to simulate a subgrade-fabric-aggregate system, subjected to a "rocking type" load which might approximate the effects of wheel load passage. A schematic of the test setup is shown in Figure 2. Several boxes were constructed of 13 in. x 6.5 in. dimension, 13 in. high to hold the subgrade-fabric-aggregate system. The subgrade material consisted of a white Georgia kaolinite clay which had a liquid limit of 70 and a plastic limit of 33. With a plasticity index of 37, the kaolinite clay was classified CH by the Unified Soil Classification System.

The subgrade material was mixed at a water content of 45 percent (dry-weight basis) and compacted to nine inches depth inside each test box in three consecutive three-inch lifts by static compaction. After compaction with a hydraulic compression testing machine the soil had a dry unit weight of approximately 76 pounds per cubic foot. At this water content and density the clay had a cohesion of approximately 200 pounds per square foot.

After the subgrade had been compacted, the fabric was cut into 8.0 in. x 15 in. strips, with the 15.0 in. dimension in the warp direction or finished edge. The edges of the fabric were fastened to the perimeter of the test box by bolt clamping. This provided fabric anchorage and restriction to fabric slippage under the "rocking type" load during the test.

Aggregate cover was then placed on the fabric. The aggregate was simulated by half inch steel ball bearings placed to a depth of two inches. The steel ball bearings were used to provide uniform aggregate properties during the test such that changes in effective particle size would not occur from

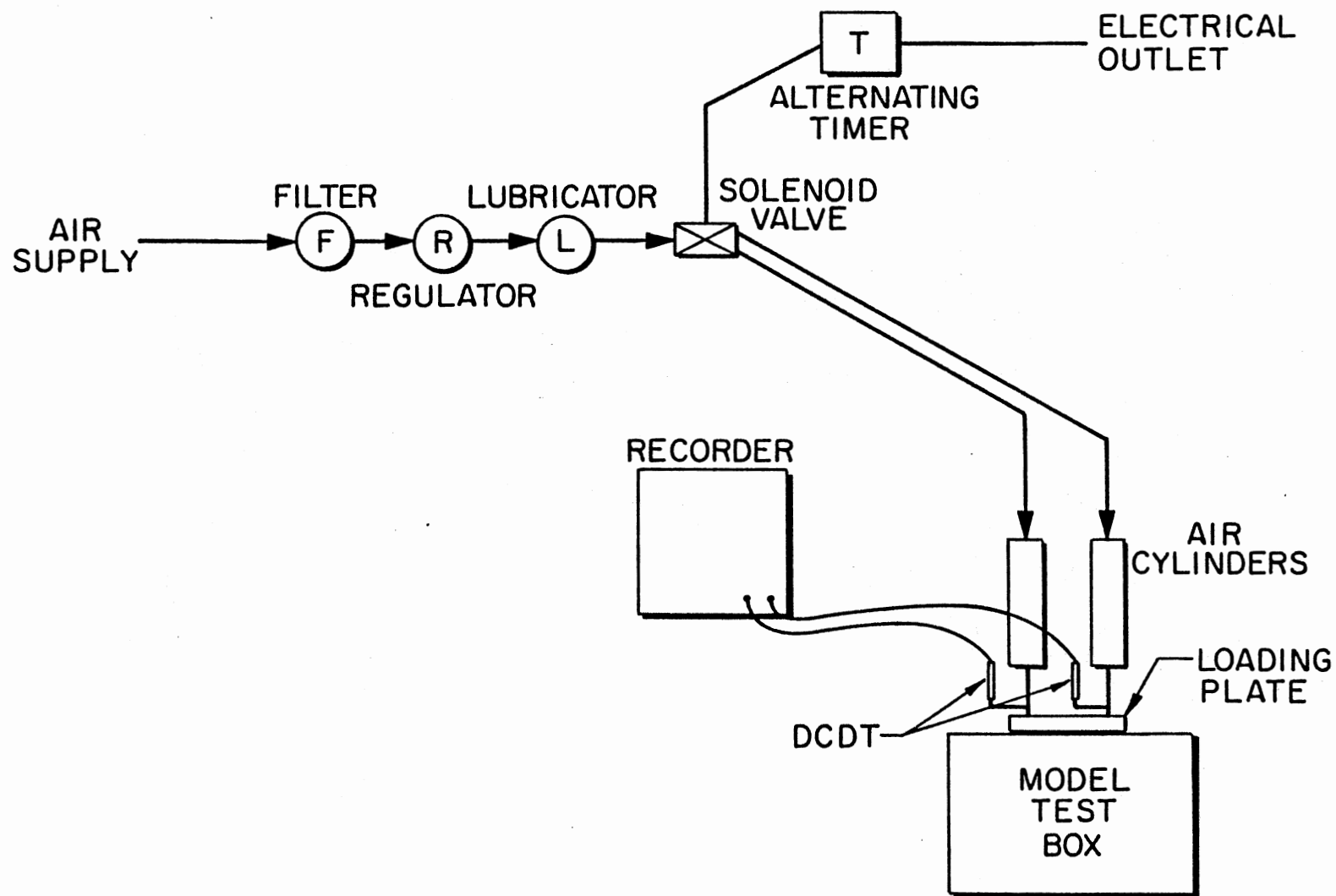


Figure 2. Schematic Diagram of Separation Testing Equipment

necessary to produce tensile stress developed in the material at two percent was applied and deformations were monitored with time until they had (essentially) ceased. Additional weight was then added to increase the fabric stress to the value developed at six percent elongation and the procedure repeated. The procedure was then repeated to produce a fabric tensile stress equivalent to that developed at ten percent elongation. The test setup and procedure was based upon earlier work by Haliburton, Anglin, and Lawmaster [8].

#### Details of Direct Shear Testing

The coefficient of friction between soil and fabric was determined by producing shear at the soil-fabric interface, under various values of applied normal stress. A motorized direct shear machine was used with a deformation rate of 0.025 inch per minute. A conventional Karolo-Warner two-inch square shear box was modified by inserting a metal insert to fill the lower half of the shear box, and fabric was then clamped to the flat surface. The shear box was then placed in the shear machine and the top half of the shear box was filled with standard Ottawa testing sand. Prior to conducting the soil-fabric friction studies, a standard direct shear test was performed on the Ottawa sand to determine the angle of internal friction,  $\phi$ , in loose and dense states. Shear test data for each fabric tested were used to determine the coefficient of sand-fabric friction and resulting angle of internal friction,  $\phi$ , for comparison with the sand-sand internal friction angle. The testing procedure was based upon earlier work by Haliburton, Anglin, and Lawmaster [8].

aggregate edge crushing. The ball bearings also had a uniformity coefficient  $C_u$  of one; thus aggregate density would not change during the loading process and use of the ball bearings tended to minimize soil-fabric friction at the "aggregate"-fabric interface, and thus eliminate the effect of aggregate lateral restraint. After the ball bearings had been placed, a plate of 3/4-inch plywood, with a rectangular cutout for the loading foot was placed on the ball bearings and clamped to the box. This plate was used to keep the ball bearings from being displaced upward during the test, thus simulating the restrictive action of the pavement. A detailed drawing of the test box can be seen in Figure 3.

The subgrade-fabric-aggregate-cover plate system is now placed into the loading frame. Load was applied to the surface of the aggregate by a 6-in.-long by 3-in.-wide loading plate. The loading plate was connected to two side-by-side mounted, two and one-half inch diameter double-acting hydraulic cylinders. Compressed air was used as the hydraulic fluid, with air supply controlled by a standard pressure regulator. The loading plate was placed through the cutout hole in the plywood plate and a seating load of 20 pounds per square inch in both cylinders was applied to the surface of the aggregate, and then 40 pounds per square inch pressure was cycled back and forth between cylinders on five second intervals, using a mechanical timer and a solenoid valve, to produce a "rocking type" load.

Measurement of the vertical displacement of the loading plate at the point of load application from each cylinder was obtained by two Hewlett-Packard direct current displacement transducers (DCDT). The dual DCDT output was monitored by a Sergeant-Welch Model DRSG dual pen strip chart recorder. Figure 4 shows the test box with fabric placed on the subgrade

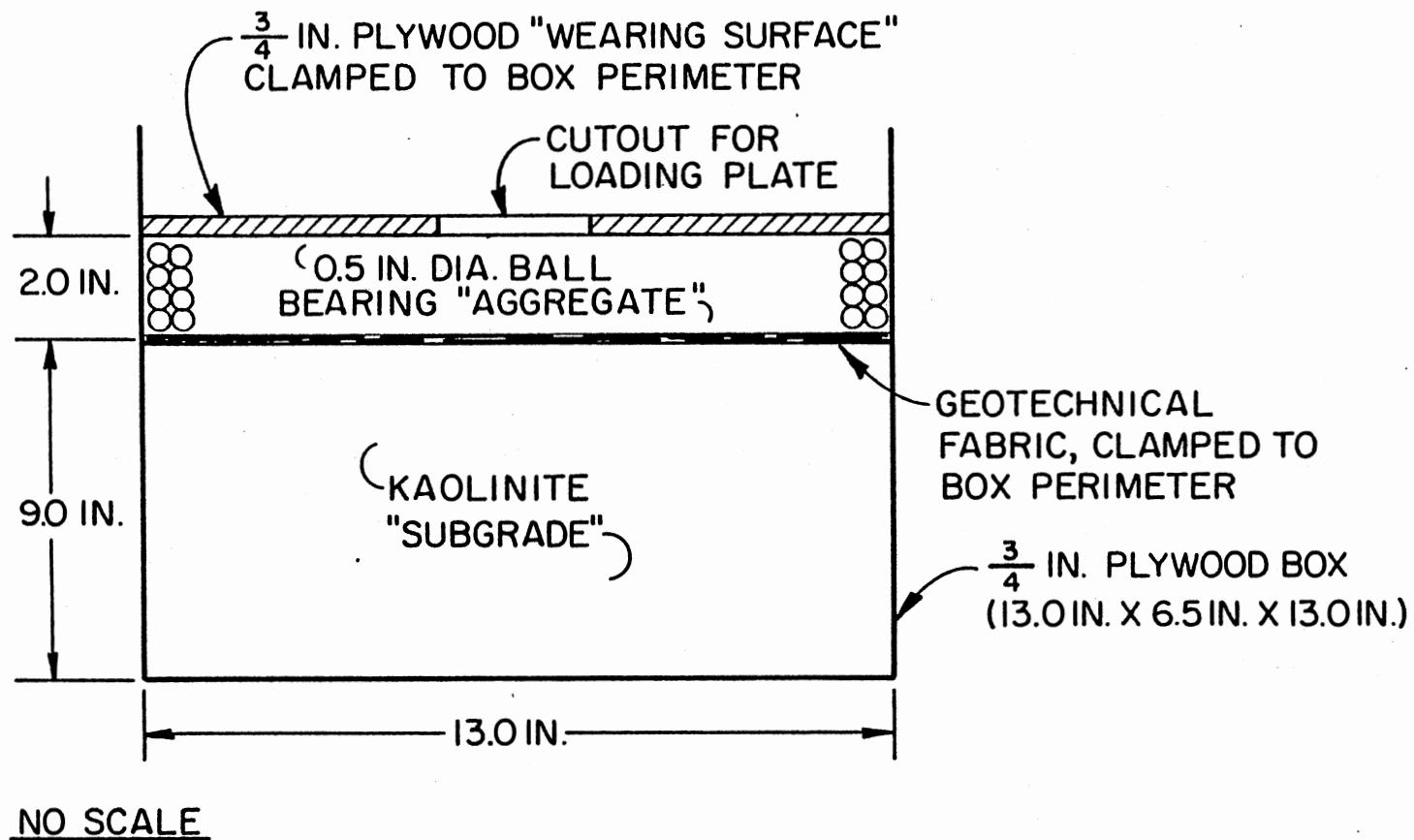


Figure 3. Schematic Diagram of Separation Model Test Box



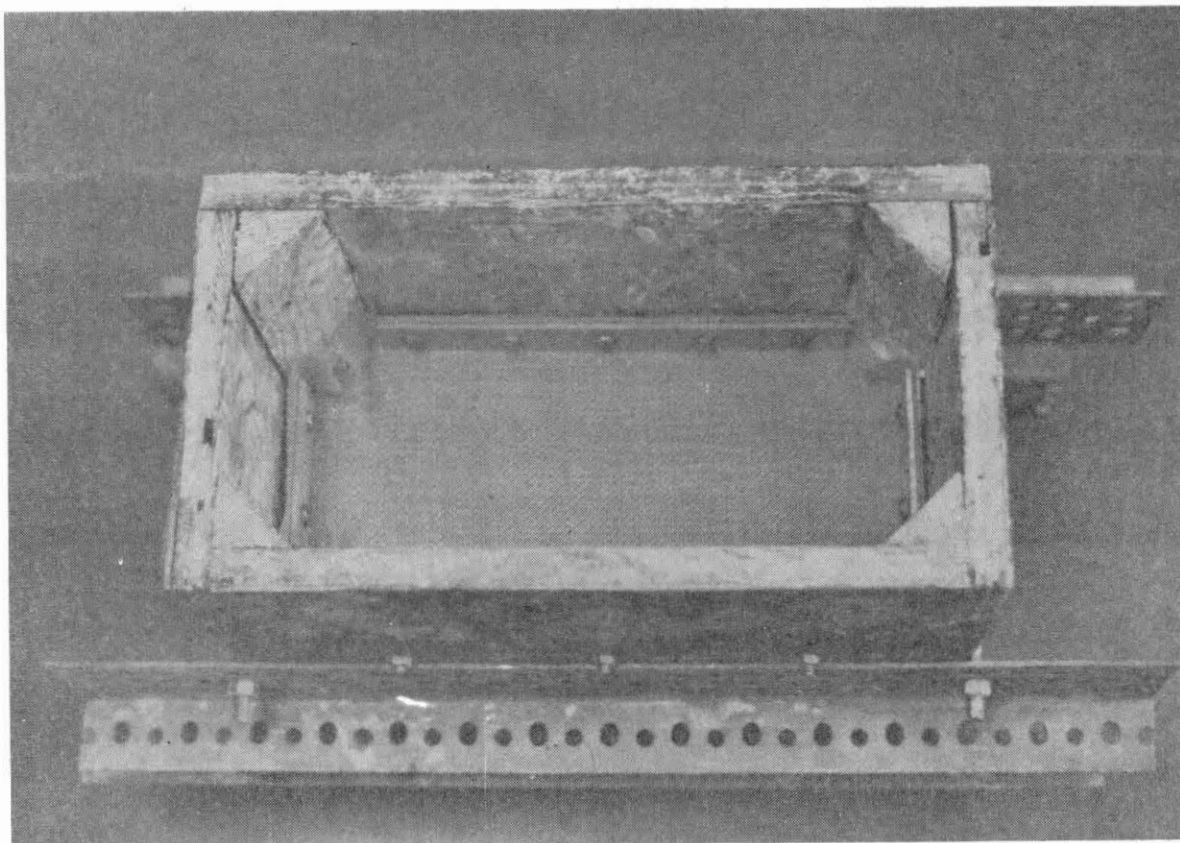


Figure 4. Separation Experiment Test Box Containing Kaolinite Subgrade, with Geotechnical Fabric Anchored in Place

while Figure 5 shows the aggregate cover. A photograph of the complete apparatus, ready for testing, is shown in Figure 6.

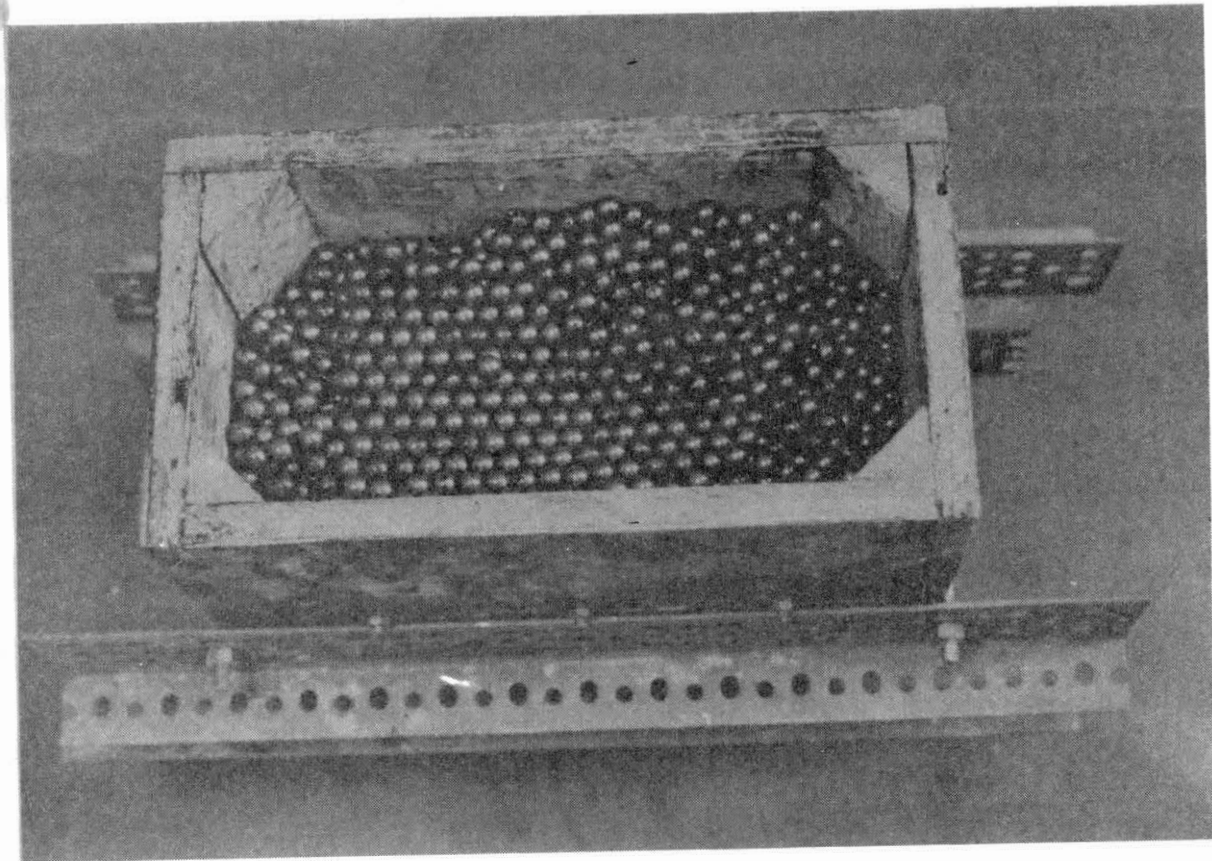


Figure 5. Separation Experiment Test Box with 0.5-in.dia Ball  
Bearing Aggregate Placed Over Geotechnical Fabric

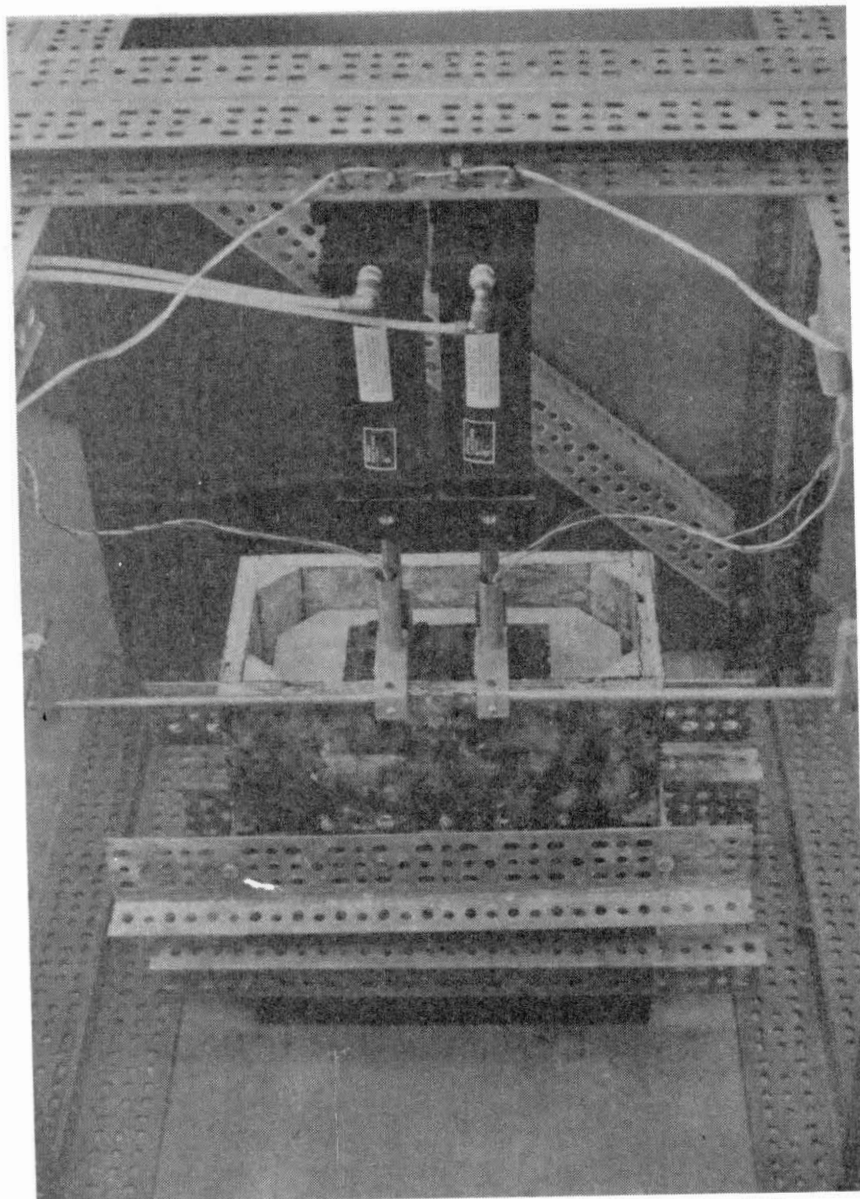


Figure 6. Separation Experiment Test Setup, Ready for Conduct of Testing

## CHAPTER IV

### RESULTS AND DISCUSSION

All 17 geotechnical fabrics were initially tested in uniaxial tension and direct shear. Four geotechnical fabrics were then selected for further testing as separation medium. Creep tests were also run on the four fabrics to determine the time-dependent elongation characteristic of the fabric.

#### Selection of Geotechnical Fabrics

Preliminary tests to determine the fabrics' physical characteristics were conducted. These tests included uniaxial tension testing, sand-fabric direct shear testing, and creep testing. From these preliminary tests, four geotechnical fabrics were selected to be tested as a separation medium. The four fabrics selected were:

1. Bidim C-34--a nonwoven, needle punched polyester fabric manufactured by the Monsanto Company.
2. Typar 3401--a nonwoven, heat bonded polypropylene fabric manufactured by E. I. DuPont Nemours & Company.
3. Mirafi 500X--a woven, split tape polypropylene fabric manufactured by Celanese Corporation.
4. Geolon 66475--a woven, multi-filament polypropylene fabric produced by the Nicolon Corporation.

The tension testing consisted of at least three uniaxial tension

tests in the warp and fill directions. The warp direction is defined as the direction parallel to the finished edge, or parallel to the direction the fabric was extruded from the loom or other manufacturing device. The fill direction is defined as the direction 90 degrees to the warp direction. Wovens and nonwovens show appreciably large differences in strength of the fabric in the two directions. The Appendix contains photographs of all 17 fabrics as they were tested. Specific test results for the fabric are also presented in the Appendix immediately following the photograph of that test.

Direct shear testing was conducted to determine the soil-fabric frictional angle  $\phi_{SF}$ . Soil-fabric direct shear testing was conducted only in the warp direction, as this is the direction in which maximum stresses should be transmitted in a construction project. Tests were conducted with Ottawa 20-30 testing sand compacted to a dense state. Test results for each of the 17 fabrics tested can be found in Table II.

Creep tests were conducted on just the four fabrics selected to use as the separation medium. It should be noted the Bidim C-34 and Geolon 66475 experienced large initial creep when initial load was applied but quickly leveled off in magnitude. It should also be noted that some slippage did occur in the clamps but the effects were taken into account in the results. Bidim C-34 and Geolon 66475 reached approximately 15 percent strain, Mirafi-500X reached approximately 35 percent strain, and Typar 3401 reached 50 percent strain by the test's end.

A summary of the results of the preliminary testing on the four fabrics selected can be found in Table III. A relatively large variation can be seen in the tensile modulus and ultimate tensile strength among the four fabrics. However, soil-fabric frictional resistance was approximately

TABLE II  
SOIL-FABRIC FRICTION VALUES  
FABRIC WARP DIRECTION

| Fabric Trade Name         | Average $\phi_{SF}^1$ (Degrees) |
|---------------------------|---------------------------------|
| Celanese 500X             | 22                              |
| Celanese 600X             | 36                              |
| Diamond 8                 | 40                              |
| Special 400               | 36                              |
| Retain 72                 | 42                              |
| Stitchbond 1375           | 41                              |
| Fibretex 150              | 30                              |
| Fibretex 200              | 36                              |
| Fibretex 300              | 34                              |
| Fibretex 400              | 39                              |
| Typar 3401                | 32                              |
| Bidim C-34                | 31                              |
| Nicolon 66475             | 40                              |
| Style 5793                | 40                              |
| Corning Fiberglass Fabric | 30                              |
| Stabilenla 200            | 40                              |
| Mount Vernon Mills Fabric | 41                              |

<sup>1</sup> $\phi$  for soil alone was found to equal 54°, which includes interlock effects.

TABLE III  
WARP DIRECTION PHYSICAL PROPERTIES OF GEOTECHNICAL FABRICS  
USED IN SEPARATION TESTING PROGRAM

| Fabric Name  | Ultimate Tensile Strength (lb/in.) | Elongation at Failure (%) | Secant Tensile Modulus @ 10% Strain (lb/in.) | Ottawa Sand-Fabric Friction Angle (deg) | Creep Potential |
|--------------|------------------------------------|---------------------------|--|---|-----------------|
| Bidim C-34   | 88                                 | 50 <sup>1</sup>           | 70   | 31                                      | nil             |
| Typar 3401   | 45                                 | 50 <sup>1</sup>           | 525 <sup>2</sup>                             | 32                                      | high            |
| Mirafi 500X  | 104                                | 35                        | 480  | 29                                      | moderate        |
| Geolon 66475 | 1060                               | 21                        | 3620   | 40                                      | nil             |

<sup>1</sup>Test Terminated

<sup>2</sup>Initial Tangent Modulus--Secant modulus at 10 percent Strain 225 lb/in. Only this fabric had a higher initial tangent modulus than 10 percent secant modulus.



the same for all four fabrics. Creep tendency ranged from nil for Geolon 66475 and Bidim C-34, to moderate for Mirafi-500X; to extreme for Typar 3401. The four fabrics selected for separation testing are also fairly representative of the various kinds of geotechnical fabrics available, which are needle punched nonwoven, heat bended nonwoven, split tape woven, and multi-filament woven. Bidim C-34, Typar 3401, and Mirafi-500X are all advertised as separation materials by their respective manufacturers while Geolon 66475 is advertised as primarily a fabric to be used in reinforced embankments and placed under heavy riprap in erosion control projects. It was selected to test because of its high tensile strength and high modulus.

#### Separation Tests

After preliminary preparation of the subgrade-fabric-aggregate system and application of the seating load the apparatus was activated and displacement-time data recorded. An arbitrary performance criterion of either 500 rocking cycles or 0.5 inch total loading head displacement was established. However, after initial observations that all systems containing fabric essentially stabilized after 100 cycles, the cycling limit criterion was reduced to 200 rocking cycles. The 0.5 inch displacement depth was arbitrary, but based on the concept that after the diameter of the steel spheres had been exceeded, aggregate rearrangement under the cover plate could occur and subsequent displacement data might not reflect the true fabric-subgrade deformation.

Each of the four fabrics were tested three times as was the control (subgrade-aggregate-cover plate without fabric) test. Excellent consistency was obtained between individual tests with the same type of fabric

and average displacement versus number of rocking cycle curves for the four fabrics and control (no fabric) case can be seen in Figure 7. The control test displaced at an essentially linear rate, reaching the 0.5 inch arbitrary displacement depth at approximately 110 rocking cycles. Embedment of one layer of ball bearings in the soft kaolinite subgrade, with some extrusion of displaced kaolinite into the ball bearings immediately above the embedded layer was the net result of the control test.

After initial displacements required to "set the fabric" under the loading plate, a linear rate of increase in displacement with number of rocking cycles was achieved for all fabrics at approximately 100 cycles. Behavior for all four fabrics was remarkably similar. Conducting the test past the 200 cycle limit shown in Figure 7 indicated a continuation of the linear relationship.

After test completion and disassembly, examination of all fabric test kaolinite subgrades indicated that some lateral displacement had occurred in the plastic clay, with the displacement approximately equal to the total deformation measured during the test. It may be reasonably assumed that the linear vertical displacement number of rocking cycles relationship achieved by all fabrics after about 100 cycles was related to plastic displacement of underlying "subgrade." Despite their dissimilar physical properties, no significant elongation or torsion was noted in any fabric after removal of aggregate during test box disassembly, which further substantiates the essentially similar displacement number of rocking cycle relationships obtained for all fabrics.

Water was extruded and pumped from the subgrade in all instances and kaolinite was found on the surface of all fabrics except the thicker Bidim C-34, where it was found in the fabric itself. Kaolinite was extruded to

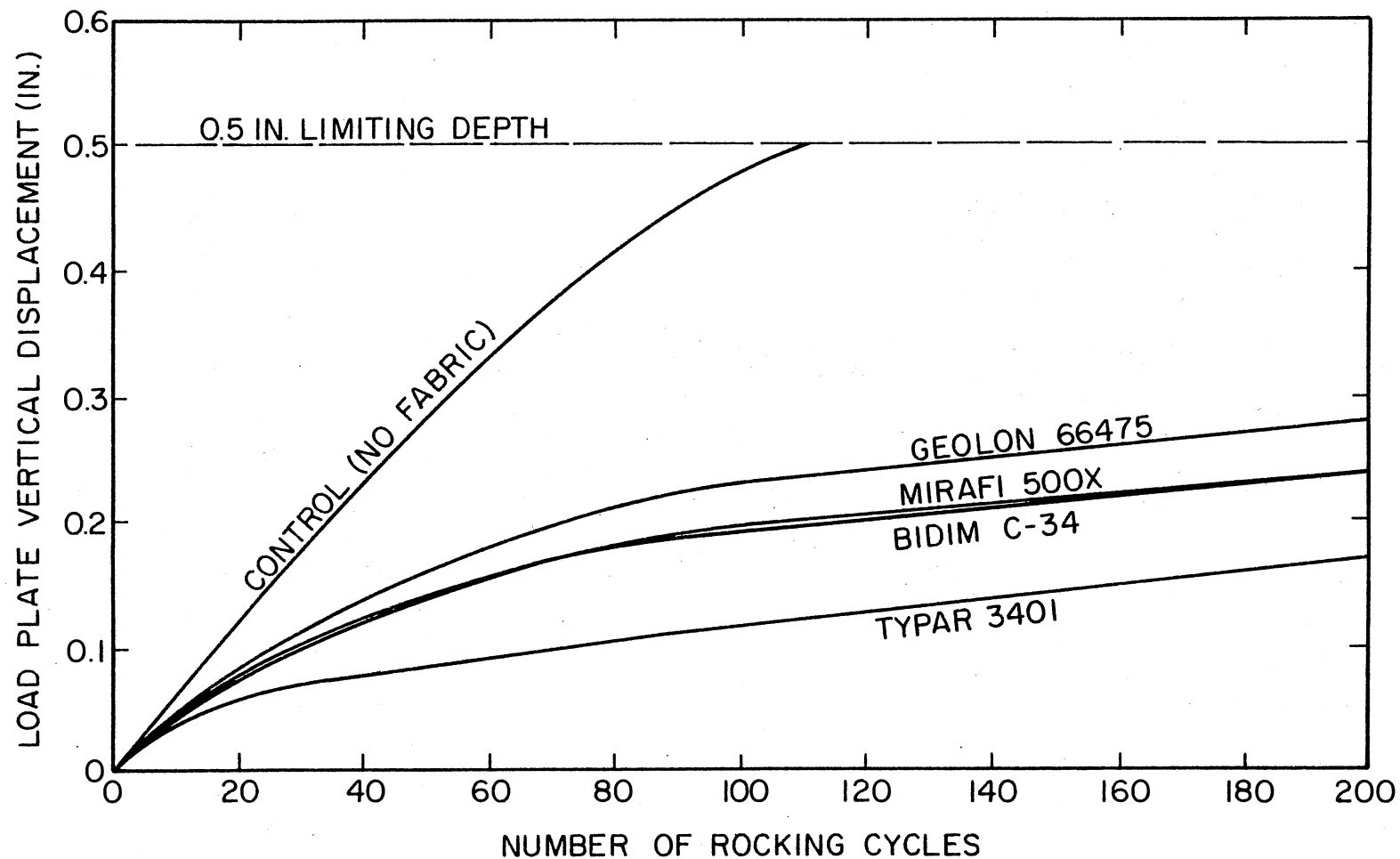


Figure 7. Displacement vs. Number of loading Cycle Relationships for the Four Test Fabrics Used in Separation Experiment

and slightly through Mirafi-500X and Geolon 66475 and was extruded into the Bidim C-34 to approximately one-half the thickness of the fabric. A definite coating of kaolinite was seen on the underside of Typar 3401 but no noticeable extrusion through the fabric pores was observed. The underside of Geolon 66475 after testing is shown in Figure 8.

No significant extrusion of kaolinite through any fabric occurred during 200 rocking cycles. All fabrics were obviously clogged to some extent by the kaolinite subgrade filling some of the fabric pores, but the exact extent of the clogging and/or permeability reduction was not determined. No significant deterioration to the fabric surface exposed to the aggregate during the short term test. The Typar 3401 fabric had noticeable aggregate indentations in its surface, and the upper surface of Bidim C-34 had some of the surface and near surface fibers pulled apart, apparently unlocking the needle-punch mechanical interlock. Obviously though these slight abrasions and indentations did not affect the performance of either fabric. If angular aggregate or longer term cycling was employed, different results might be obtained. Geolon 66475 and Mirafi-500X showed no obvious signs of aggregate indentation or abrasion.

While all fabrics achieved essentially a linear displacement-time relationship after approximately 100 rocking cycles (apparently related to displacement of underlying "subgrade"), different amounts of load plate and thus fabric deformation were required to achieve linearity. The displacements required to obtain linearity are not related to the ultimate tensile strength or 10 percent strain secant tensile modulus of the fabrics, as given in Table II. If we review each fabric's construction and their actual tensile stress-strain curves (Appendix), it gives some insight into the observed behavior. Typar 3401 is a heat bonded

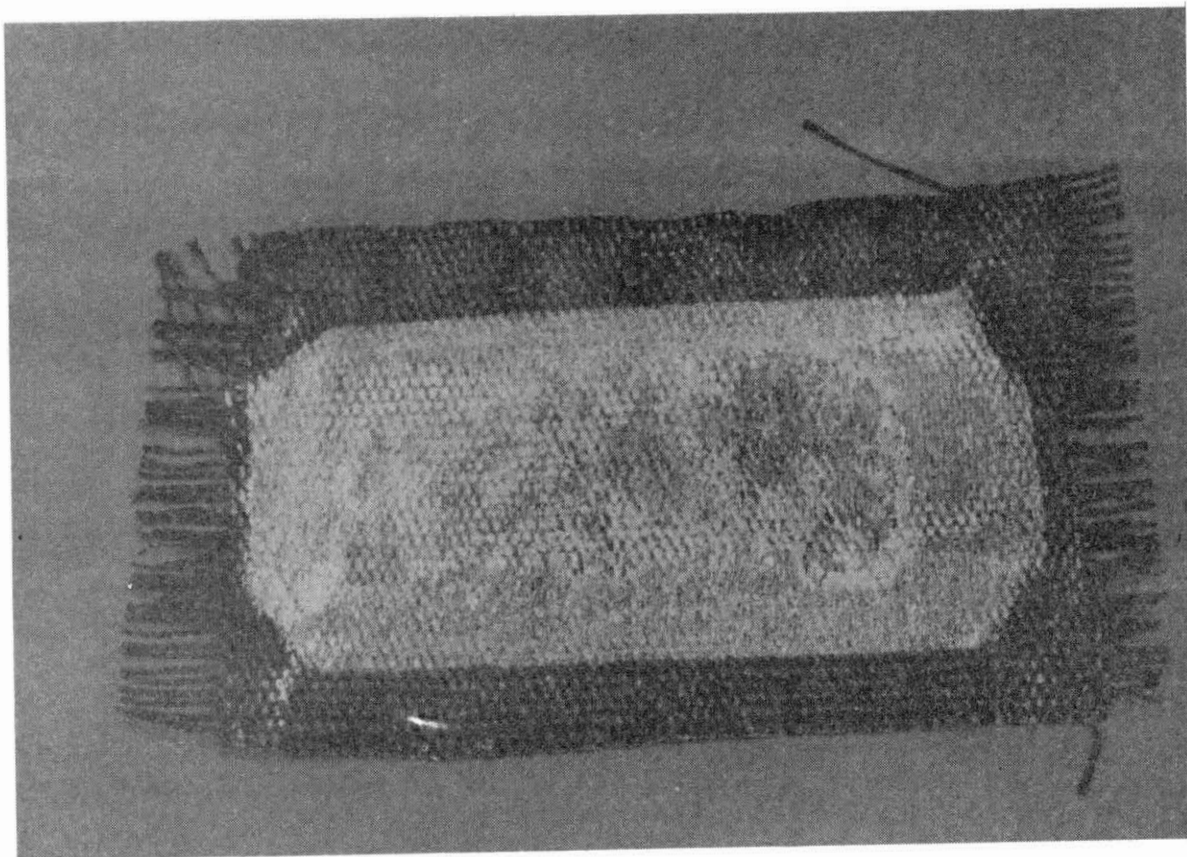


Figure 8. Underside of Geolon 66475 Fabric After Separation Testing,  
Showing Kaolinite Subgrade Smeared on the Fabric

nonwoven fabric and the heat bonding produced a fairly high initial modulus, as the nonwoven fibers need not be pulled into the direction of load application to provide deformation resistance. The needle-punched Bidim C-34 fabric develops mechanical interlock of nonwoven fibers over extremely short intervals (between needle-punches). Thus only a very short length of fiber is initially strained, despite the absence of physical bond between individual fibers. The Mirafi-500X fabric is a woven, essentially flat, split tape fabric and, though the material has more ultimate strength than either Bidim C-34 or Tyvar 3401, initially the woven fibers must be pulled flat before they can develop any resistance. Similar behavior would occur for Geolon 66475, which was the strongest fabric, both in ultimate strength and tensile deformation modulus. However, this fabric is woven of fairly large diameter strands and each strand must be pulled flat before any fabric resistance can be mobilized.

## CHAPTER V

### CONCLUSIONS AND RECOMMENDATIONS

#### Conclusions

##### Literature Survey

From the literature survey it can be seen that the majority of the understanding about geotechnical fabrics used as a separation media is from field testing. Using the results of the field testing plus the test performed by Bell and Smith, a quantitative laboratory experiment was conducted with the same important parts closely monitored. Those points were:

1. A soft cohesive clay at its plastic limit was used.
2. Prevention of intrusion of fines into the cohesionless cover material.
3. Prevention of penetration of granular cover material into the plastic subgrade.
4. Drainage of excess pore pressure from the subgrade.
5. Resist puncture and abrasion by aggregate particles in the fabric.

##### Preliminary Testing

From the preliminary testing the most important points of interest have already been noted in previous reports. The majority of the

research project and thus the results and discussions deal with the separation testing. One major point that was indicated from the creep test was that no estimates of fabric creep tendencies can be assumed, based upon manufacturing process or chemical composition.

### Separation Testing

Results of the experiment indicated a marked increase in deformation resistance of the model subgrade-fabric-aggregate-wearing surface system, as compared to the no fabric case. Behavior of the system was essentially changed from that of aggregate embedment and subgrade intrusion without fabric to a linear, but fairly small rate of plastic subgrade displacement, for all fabrics used in the test program. Results of the test program showed that all four fabrics performed essentially alike, despite some initial differences in the amount of displacement required to "set the fabric"; therefore all fabrics should give similar short-term separation performance.

During all tests, water was pumped from the kaolinite subgrade through or into the test fabrics and clay was pushed into fabric pores and smeared along the bottom surface of the fabrics. The effect of this behavior on long-term fabric clogging was not evaluated, but could be significant. Though it did not affect their performance in the short-term tests, aggregate indentation marks were noticed on the surface of the Tygar 3401 and the upper surface of the Bidim C-34. Such behavior, if continued for extended periods of time or accelerated by angular aggregate, might cause a degradation in performance.

Because of the relatively small displacements involved, it may be reasonably assumed that membrane-type support was not developed by any



fabric. Also, use of the ball-bearing aggregate, with extremely low coefficient of aggregate-fabric friction, appears to have eliminated effects of lateral restraint from the system.

For short-term separation potential, it may be concluded, based on results of the simplistic experiments conducted, that essentially all types of available geotechnical fabric will provide adequate separation of cohesive subgrade and cohesionless aggregate. As long as the fabric is not punctured, torn, or abraded by the aggregate or clogged by the subgrade, no noticeable difference in separation performance will occur.

#### Recommendations for Further Research

Investigations should be carried out, initially in the laboratory and later under controlled field conditions, to determine the long-term separation ability of geotechnical fabrics considering both separation to resist cohesive subgrade intrusion and cohesionless fines pumping. Both laboratory and field investigations should attempt to measure the long-term clogging resistance and subgrade retention of various types of geotechnical fabric, as well as the quantitative fabric properties desirable for long-term performance.

## BIBLIOGRAPHY

1. McGowan, A. and M. W. Ovelton, "Fabric Membranes in Flexible Pavement Construction over Soils of Low Bearing Capacity," Civil Engineering Publication-Weeks Review, 1973, pp. 25-29.
2. Leflaive, E. and J. Puig, Description Property de basic et Proprieties Particulieues des textiles pour les Applications Geotechniques," Proceedings, International Conference on the Use of Fabrics in Geotechniques, Paris, 1977.
3. Steward, J., R. Williamson, and J. Mohny, "Guidelines for Use of Fabrics in Construction and Maintenance of Low Volume Roads," Report No. FHWA-B-78-205, Pacific Northwest Region Forest Service, U.S. Department of Agriculture, Washington, D.C., June, 1977.
4. Kinney, T. C. and E. J. Barenbert, Mechanisms by Which Fabric Stabilizes Aggregate Layers on Soft Subgrades," Miscellaneous Paper, Geotechnical Laboratory, U.S. Army Engineer Waterways Experiment Station, Vicksburg, Mississippi, February, 1978.
5. Snaith, M. S. and A. L. Bell, "The Filtration Behavior of Construction Fabrics Under Conditions of Dyanmic Loading," *Geotechnique*, Vol. 28, December, 1978.
6. Haliburton, T. A. and Jack Fowler, "Design and Construction of Fabric Reinforced Roads and Embankments on Soft Foundation," Preprint of paper presented at First Canadian Symposium on Geotextiles, Galgary, Alberta, September, 1980.
7. Bender, David A. and Ernest J. Barenberg, "Design and Behavior of Soil-Fabric-Aggregate Systems," Preprint of paper presented at 57th Annual Meeting of Transportation Research Board, Washington, D.C., January, 1978.
8. Haliburton, T. A., C. C. Anglin, and Jack D. Lawmaster, "Selections of Geotechnical Fabrics for Embankment Reinforcement." School of Civil Engineering, Oklahoma State University, Stillwater, Oklahoma, May, 1978.

## APPENDIX

### FIGURES AND TEST RESULTS

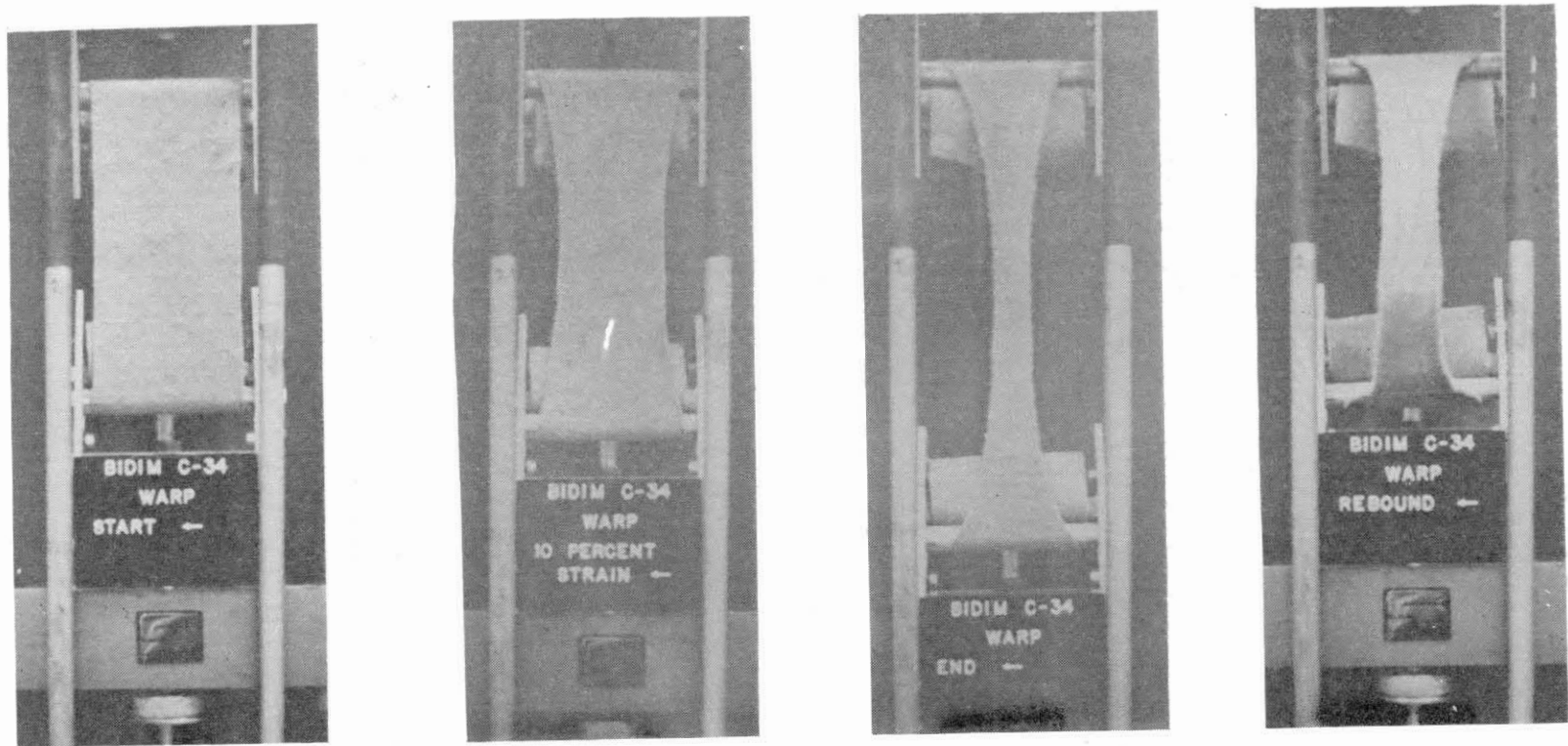


Figure 9. Photographs of Bidim C-34-Warp Direction in Tension Testing at (Left to Right) Start, 10 Percent Strain, Failure, and Rebound

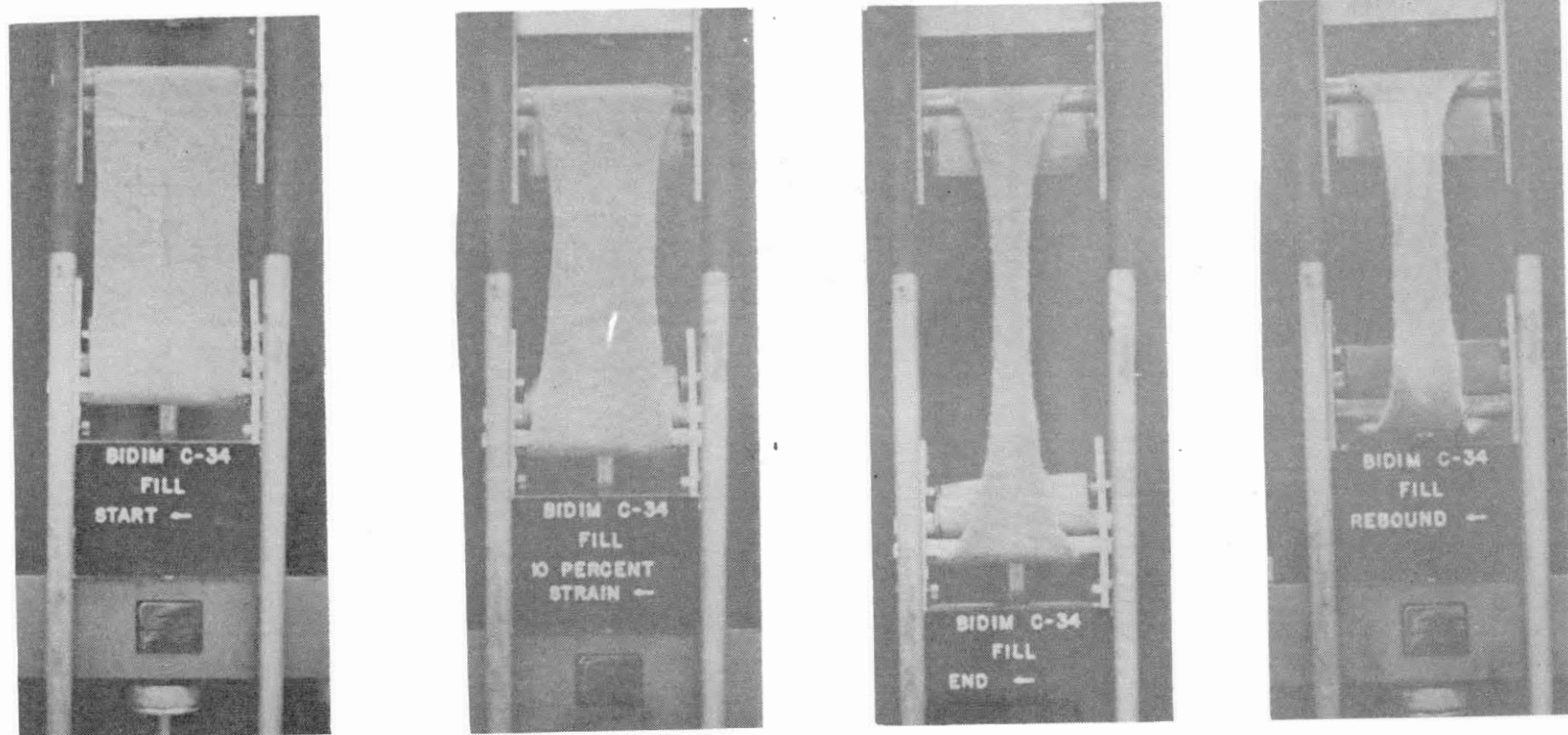


Figure 10. Photographs of Bidim C-34-Fill Direction in Tension Testing at (Left to Right) Start, 10 Percent Strain, Failure, and After "Elastic" Rebound

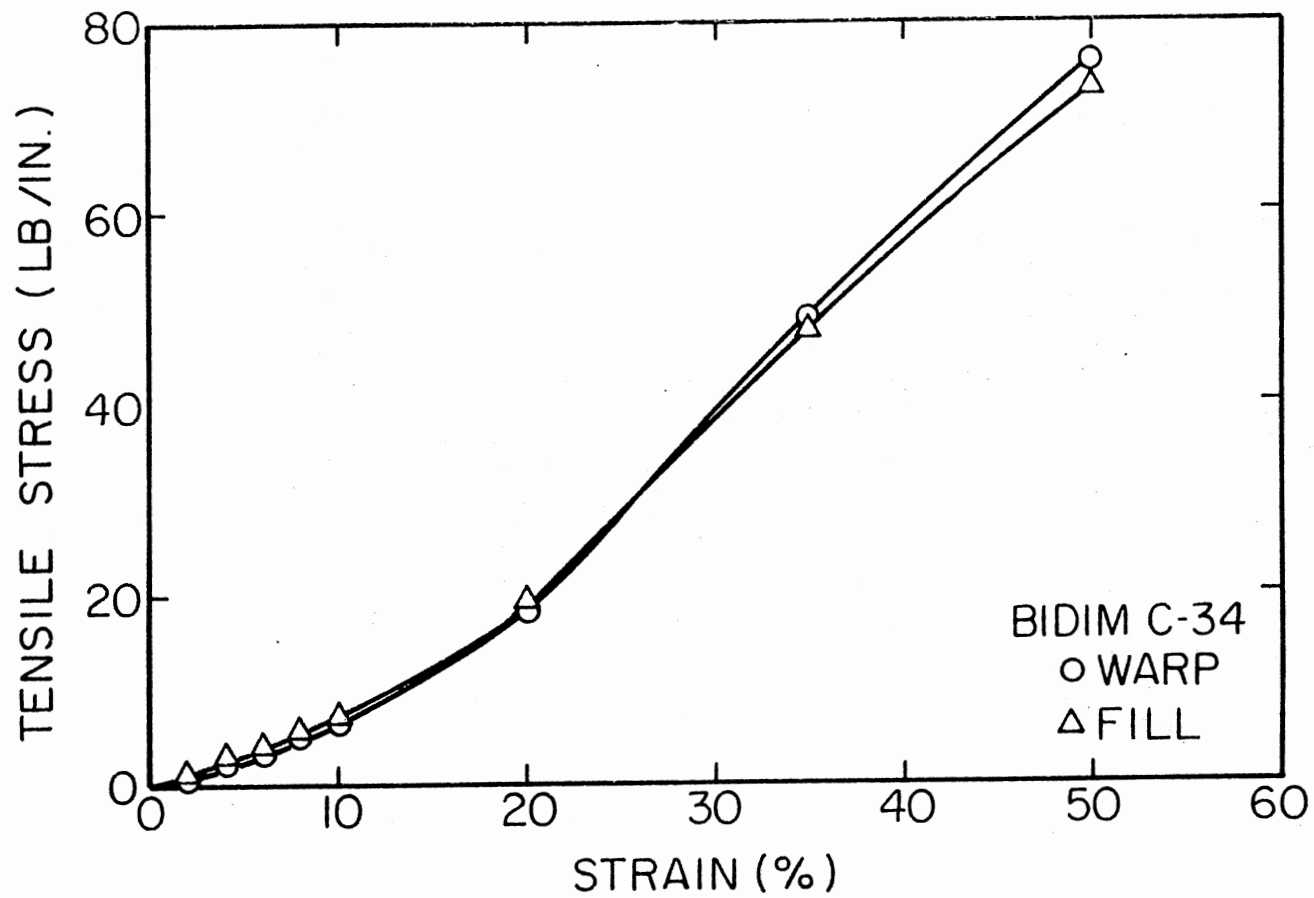


Figure 11. Stress-Strain Data for Bidim C-34 in Uniaxial Testing

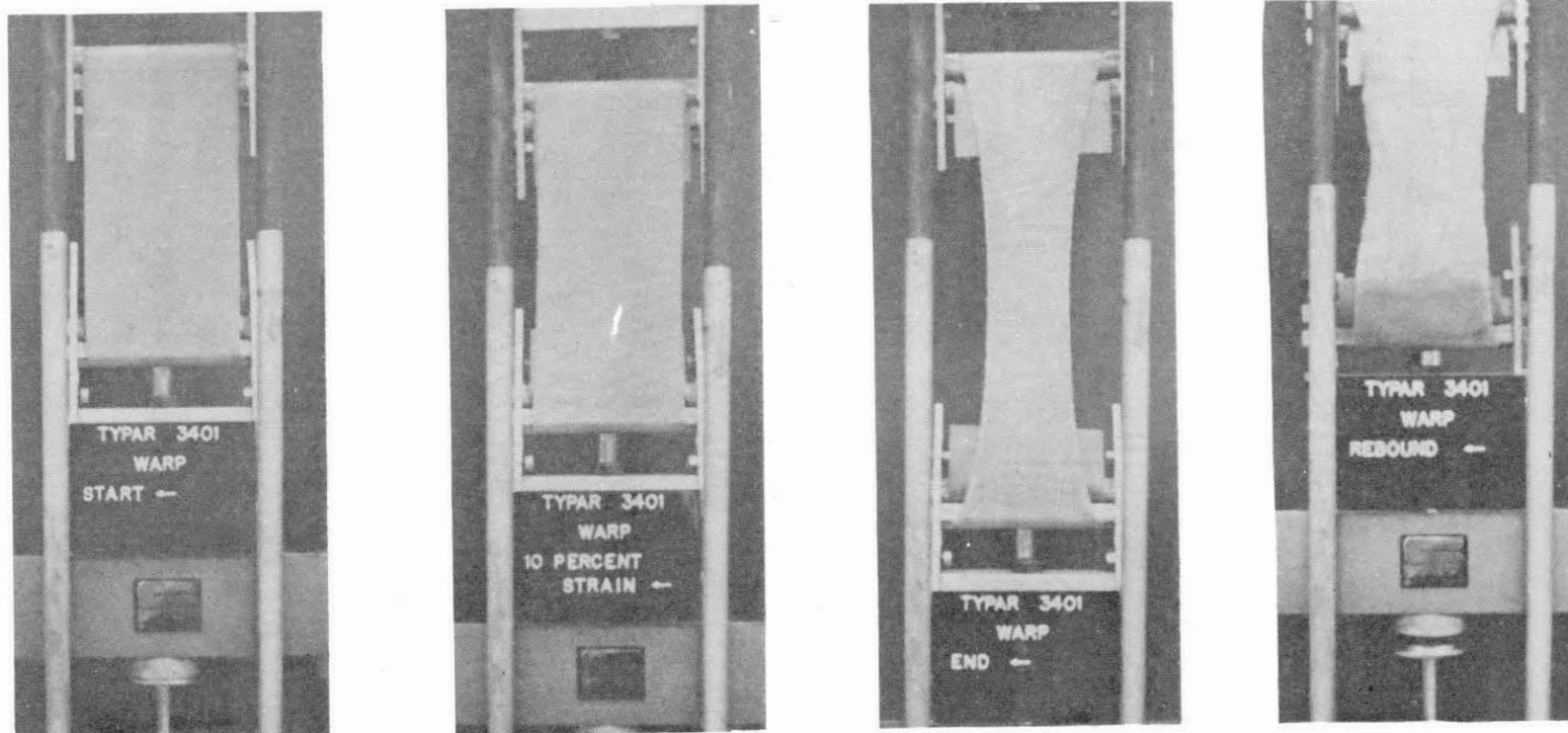


Figure 12. Photographs of Typar 3401-Warp Direction in Tension Testing at (Left to Right) Start, 10 Percent Strain, Failure, and After "Elastic" Rebound

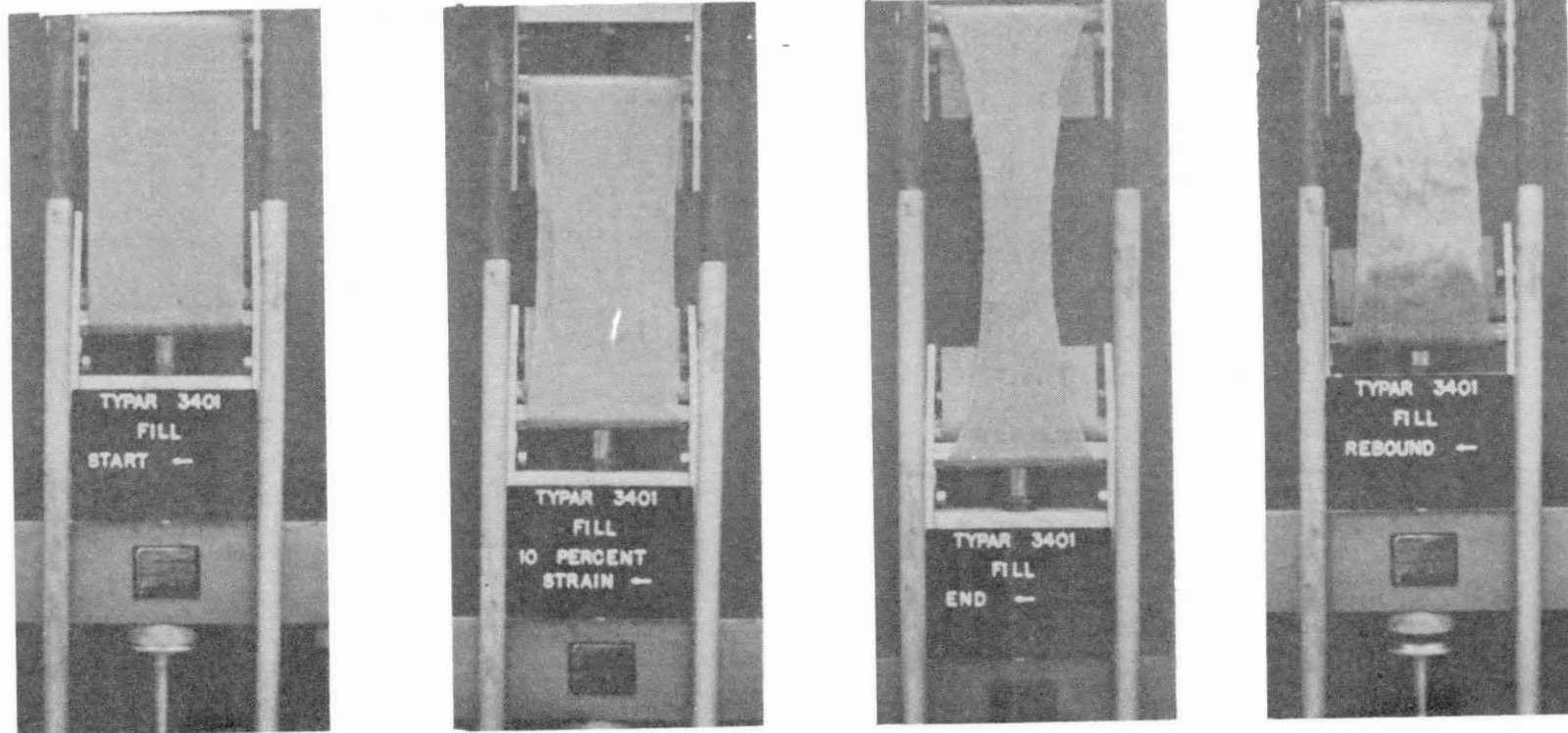


Figure 13. Photographs of Typar 3401-Fill Direction in Tension Testing at (Left to Right) Start, 10 Percent Strain, Failure, and After "Elastic" Rebound



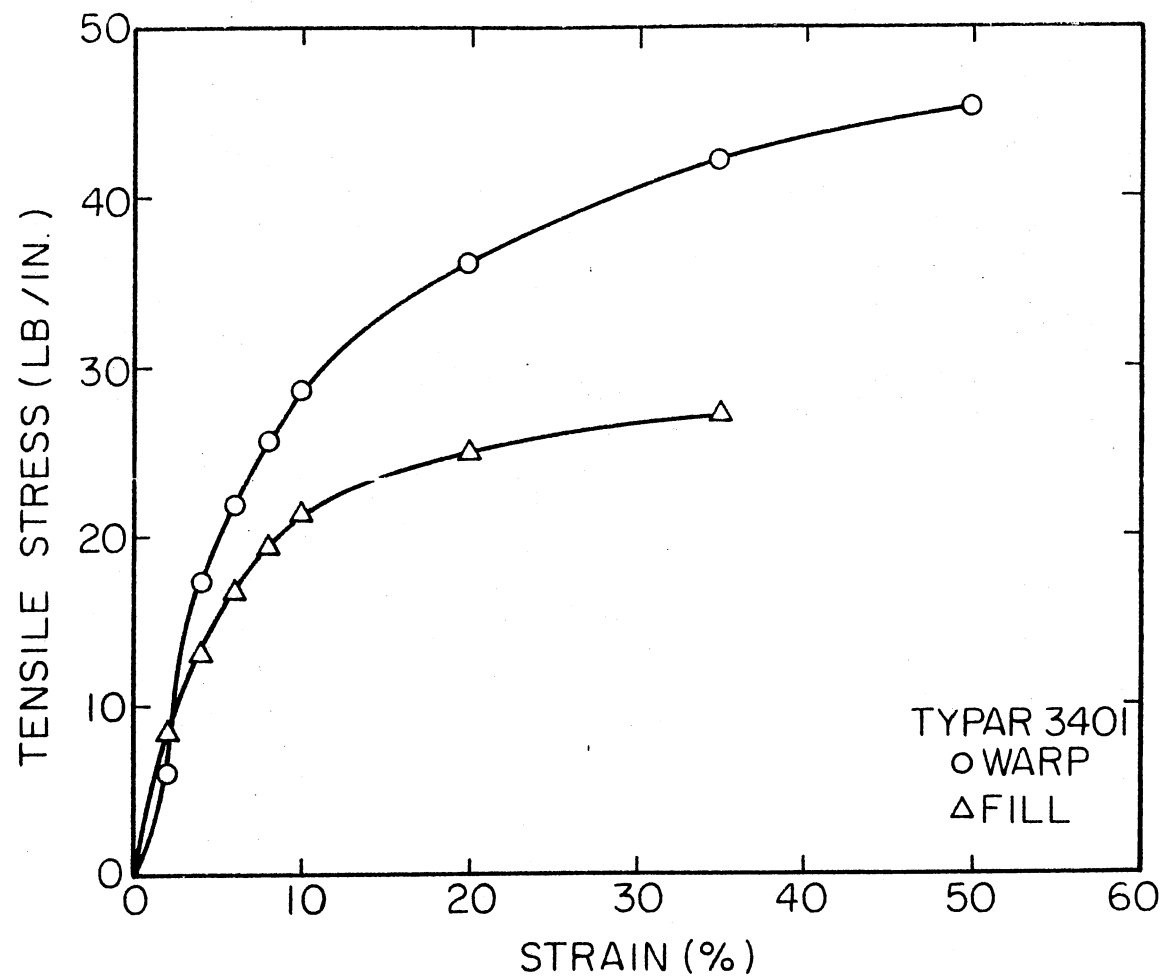


Figure 14. Stress-Strain Data for Typar 3401 in Uniaxial Testing

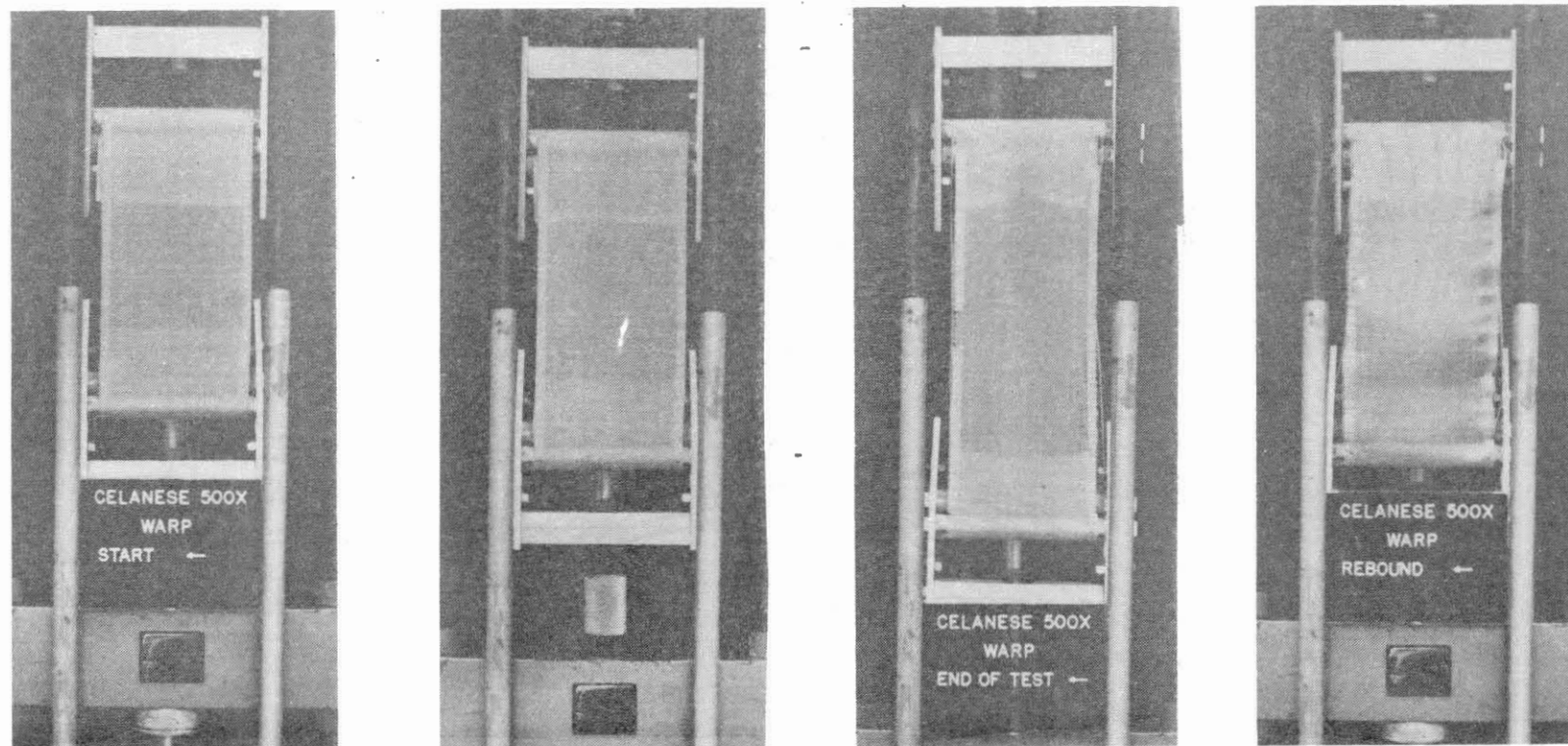


Figure 15. Photographs of Celanese 500-Warp Direction in Tension Testing at (Left to Right) Start, 10 Percent Strain, Failure, and After "Elastic" Rebound

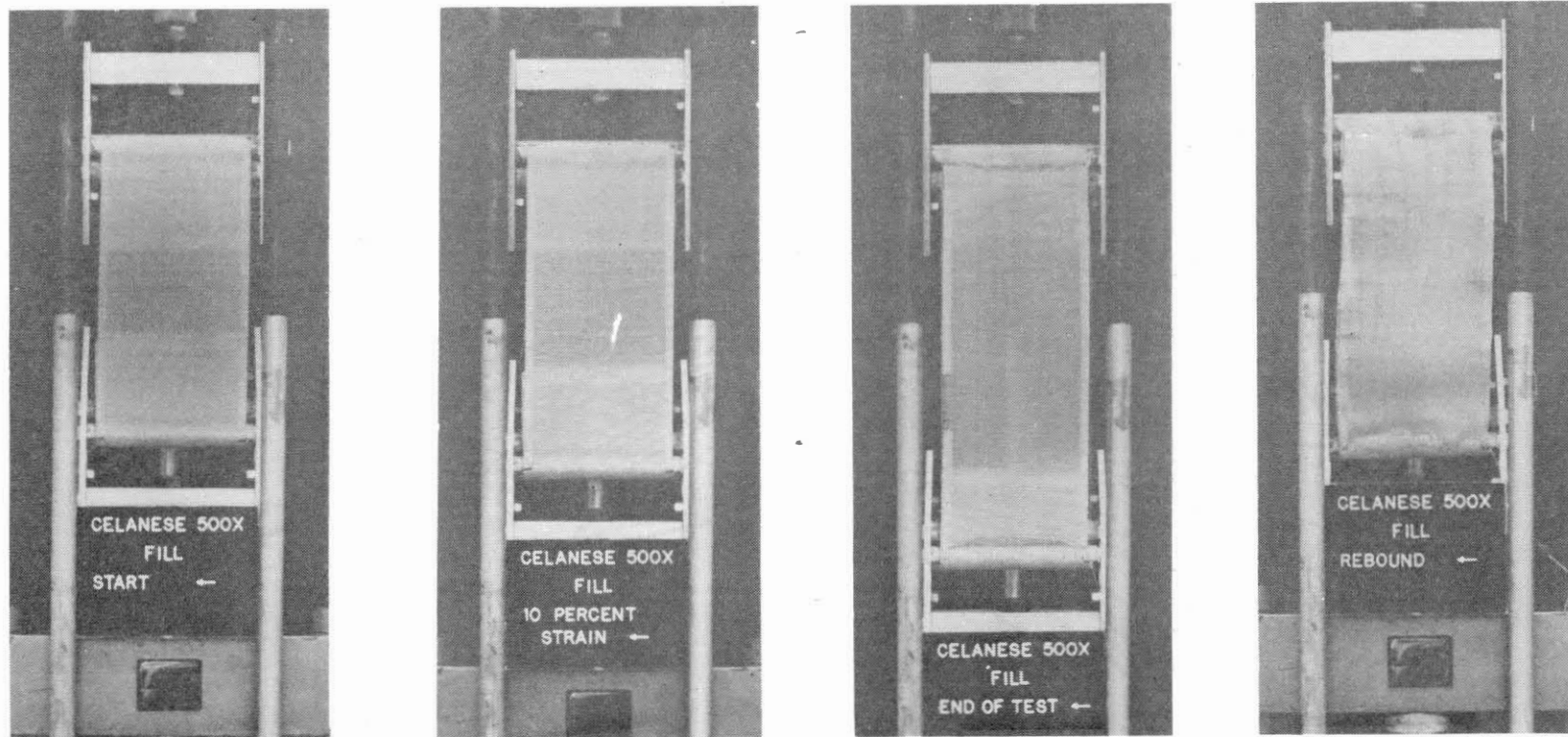


Figure 16. Photographs of Celanese 500-Fill Direction in Tension Testing at (Left to Right) Start, 10 Percent Strain, Failure, and After "Elastic" Rebound

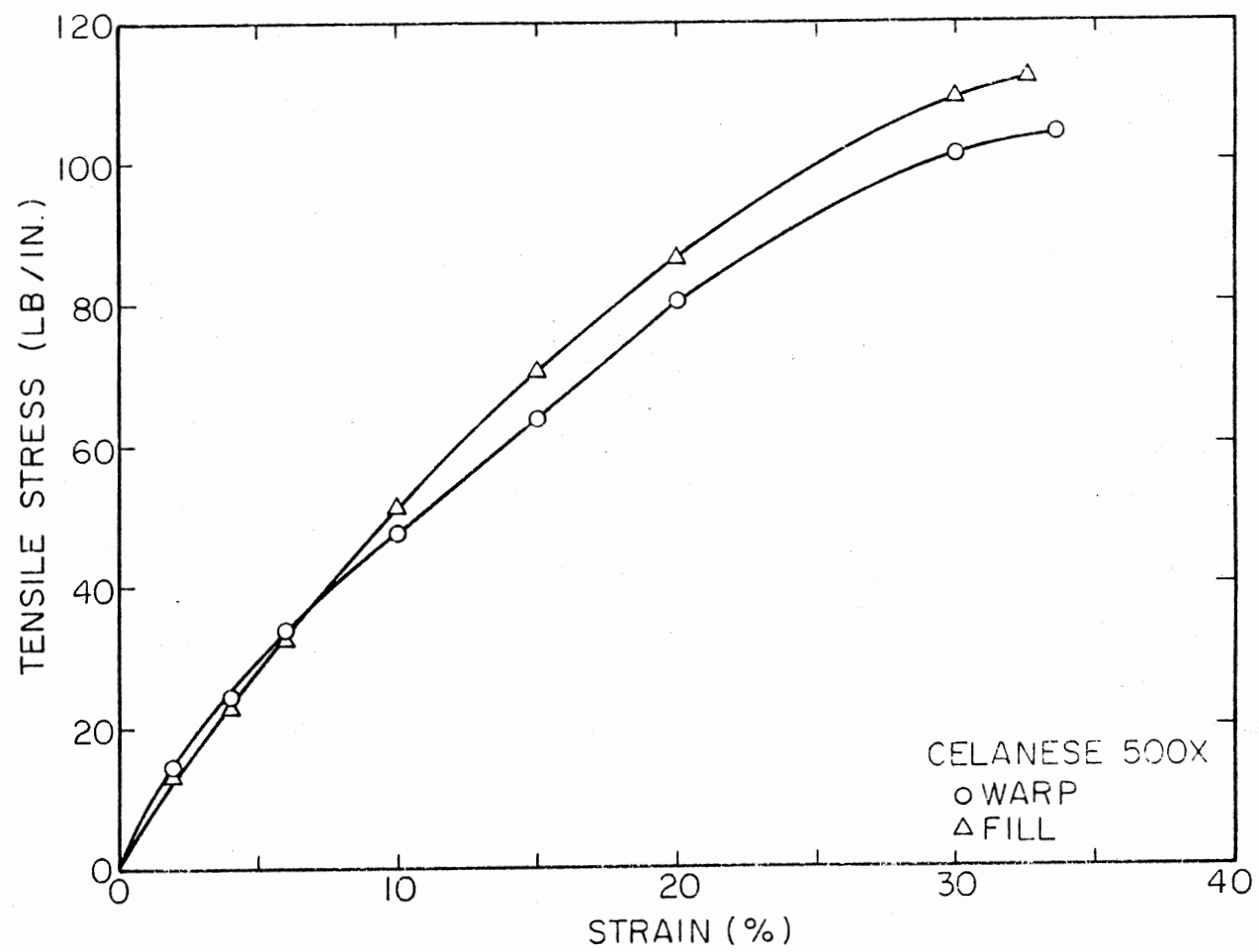


Figure 17. Stress-Strain Data for Celanese 500X in Uniaxial Testing

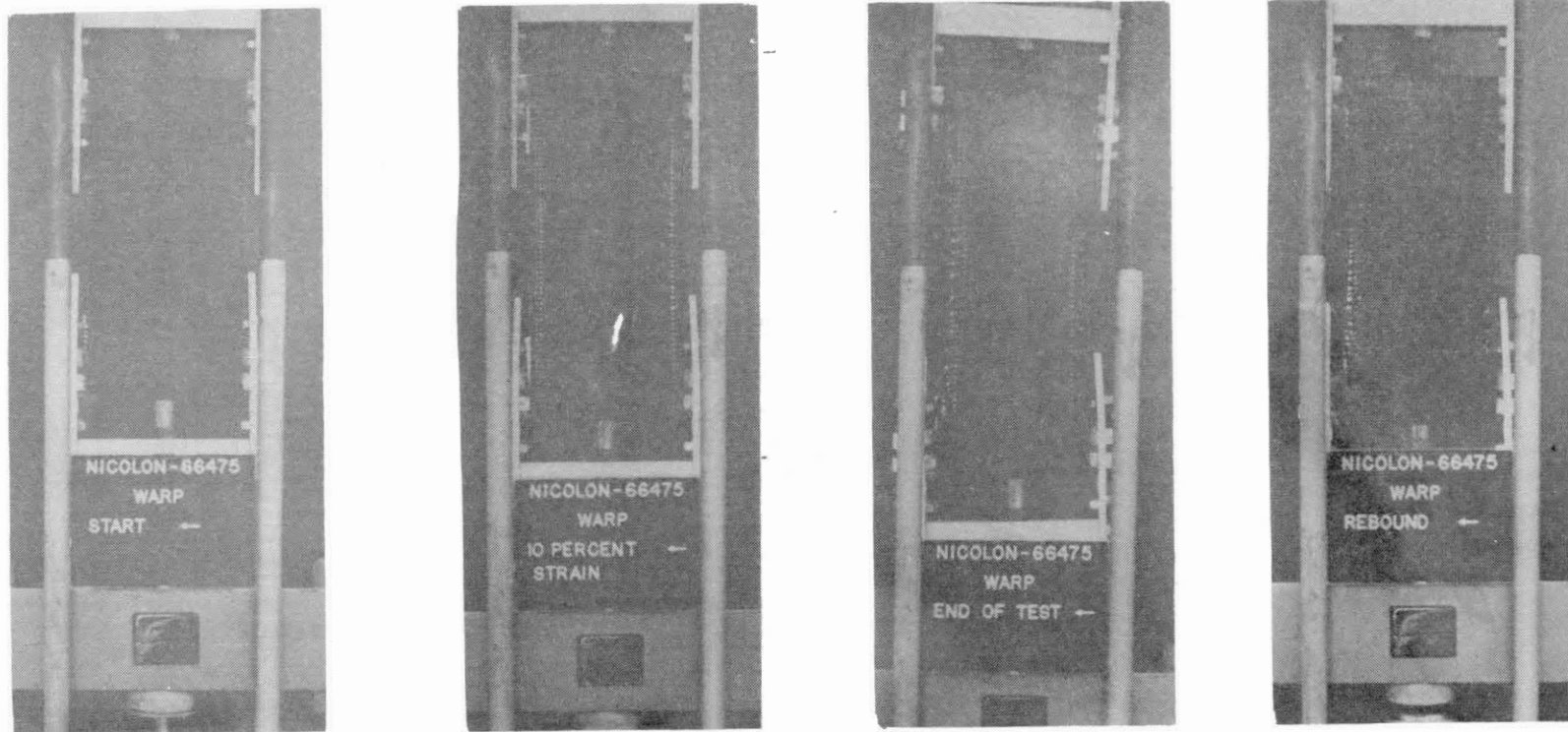


Figure 18. Photographs of Nicolon 66475-Warp Direction in Tension Testing at (Left to Right) Start, 10 Percent Strain, Failure, and After "Elastic" Rebound

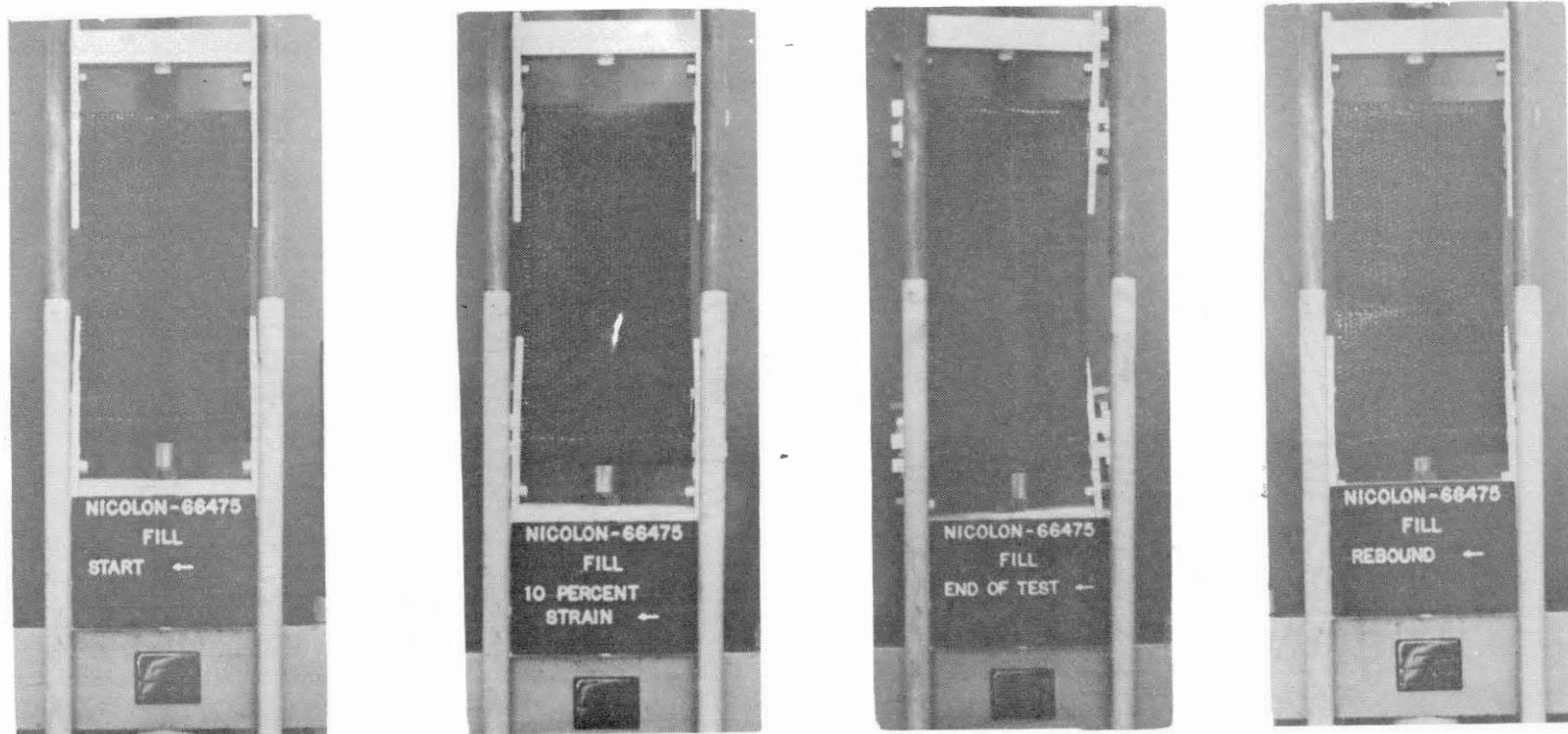


Figure 19. Photographs of Nicolon 66475-Fill Direction in Tension Testing at (Left to Right) Start, 10 Percent Strain, Failure, and After "Elastic" Rebound

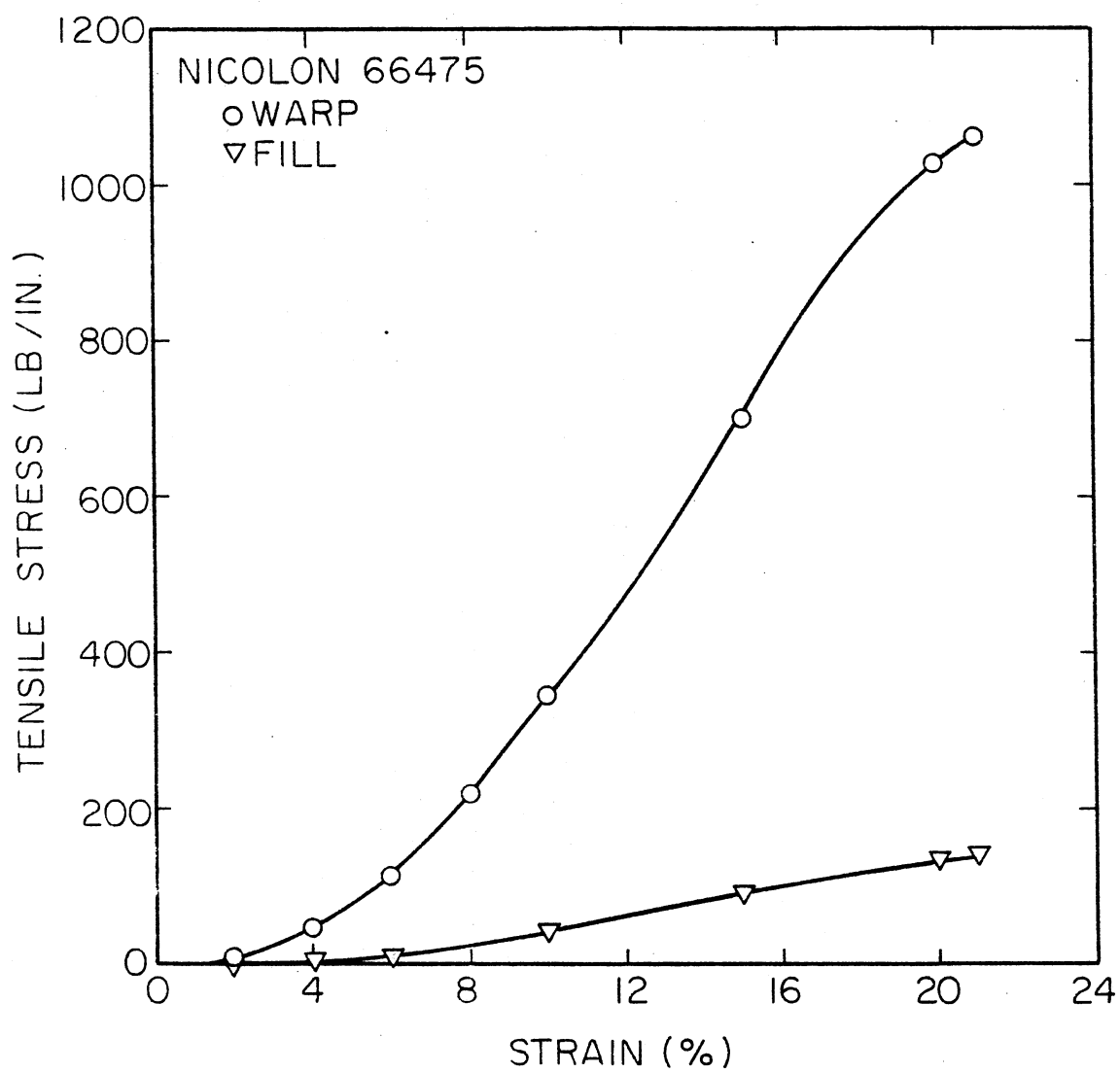


Figure 20. Stress-Strain Data for Nicolon 66475 in Uniaxial Testing

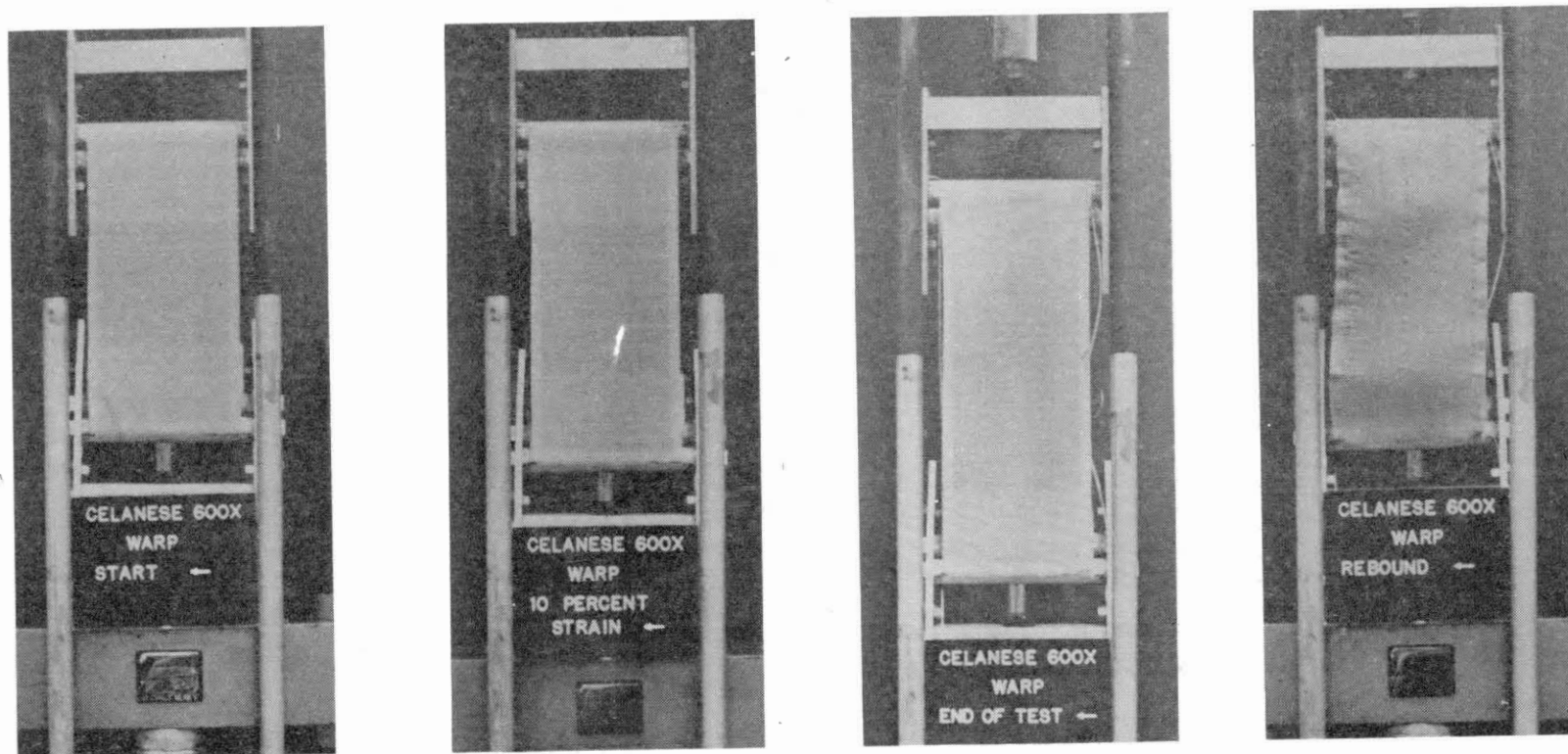


Figure 21. Photographs of Celanese 600X-Warp Direction in Tension Testing at (Left to Right) Start, 10 Percent Strain, Failure, and After "Elastic" Rebound



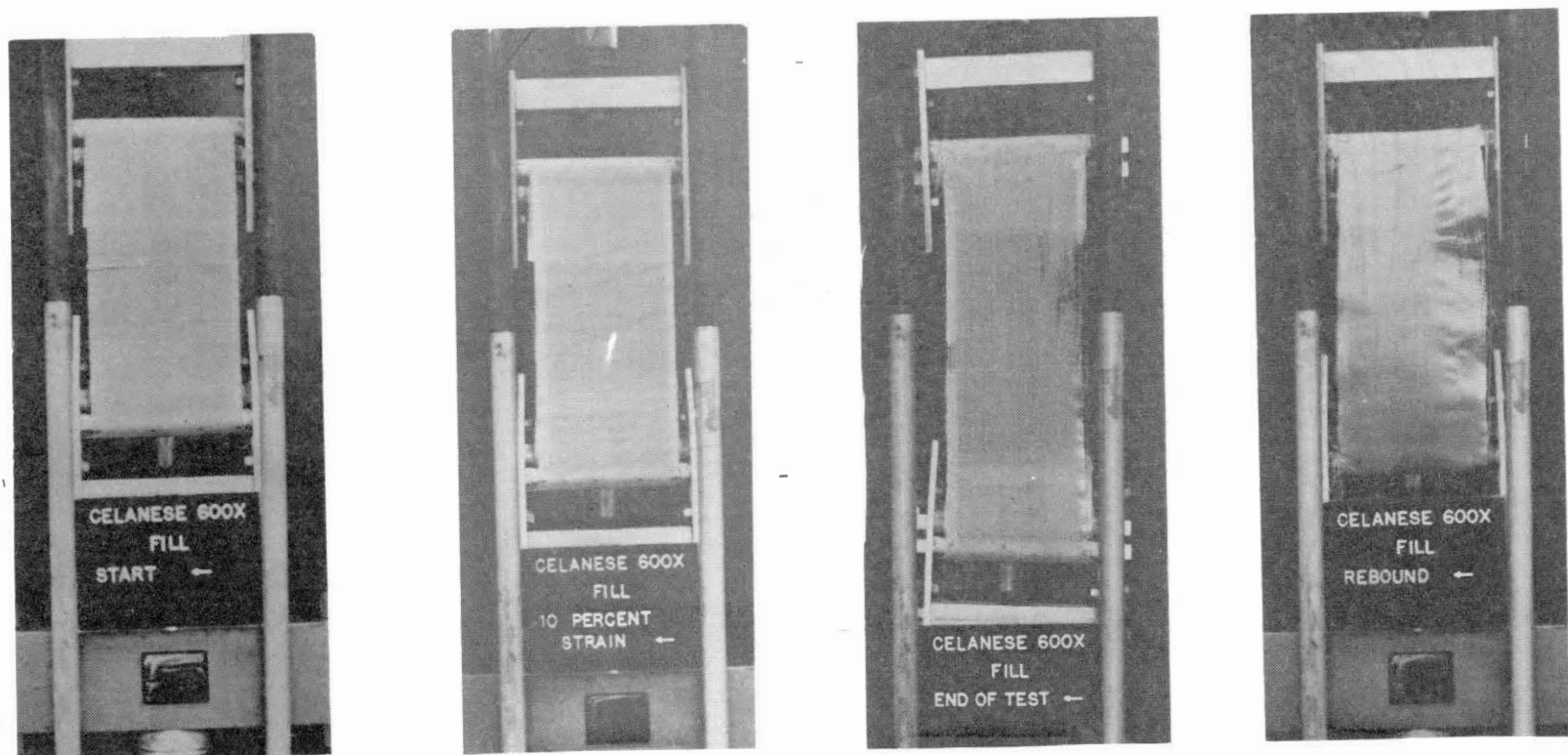


Figure 22. Photographs of Celanese 600X-Fill Direction in Tension Testing at (Left to Right) Start, 10 Percent Strain, Failure, and After "Elastic" Rebound

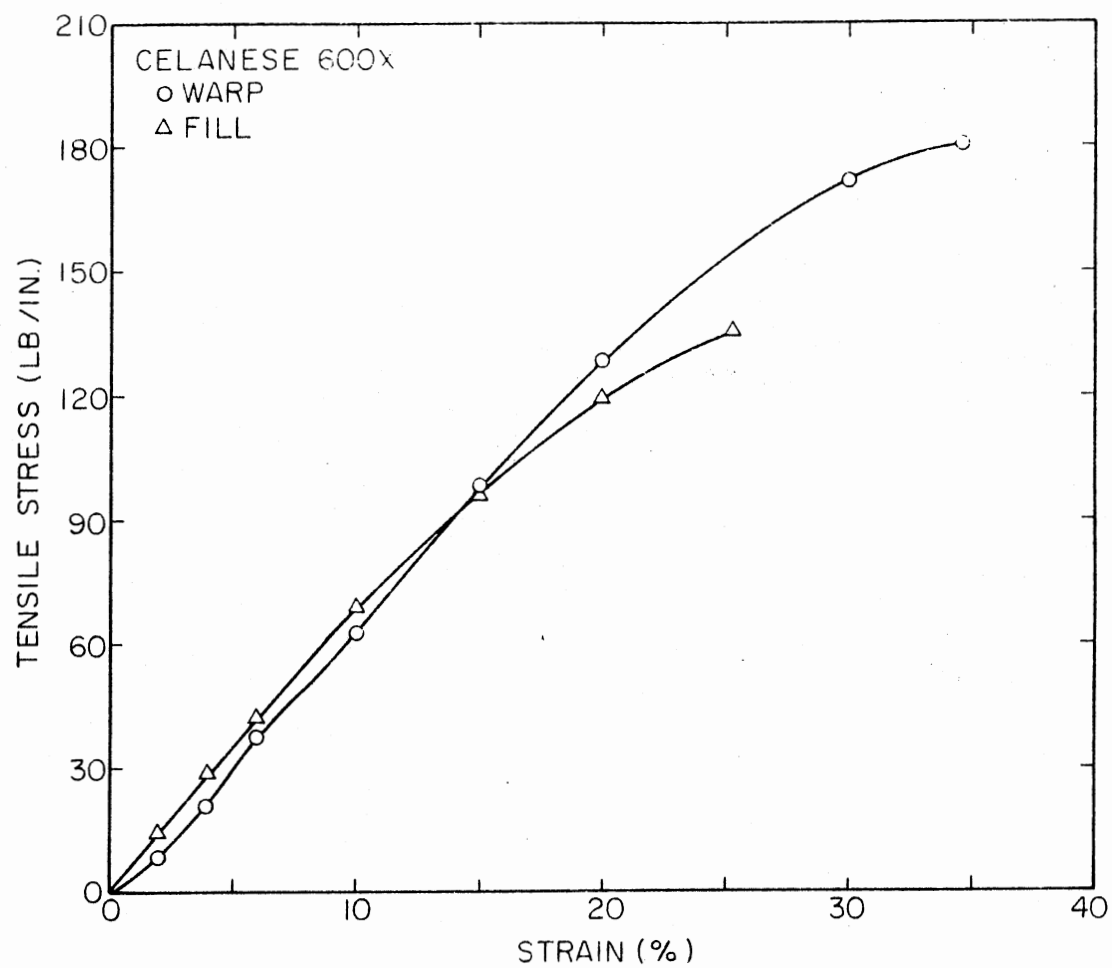


Figure 23. Stress-Strain Data for Celanese 600X in Uniaxial Testing

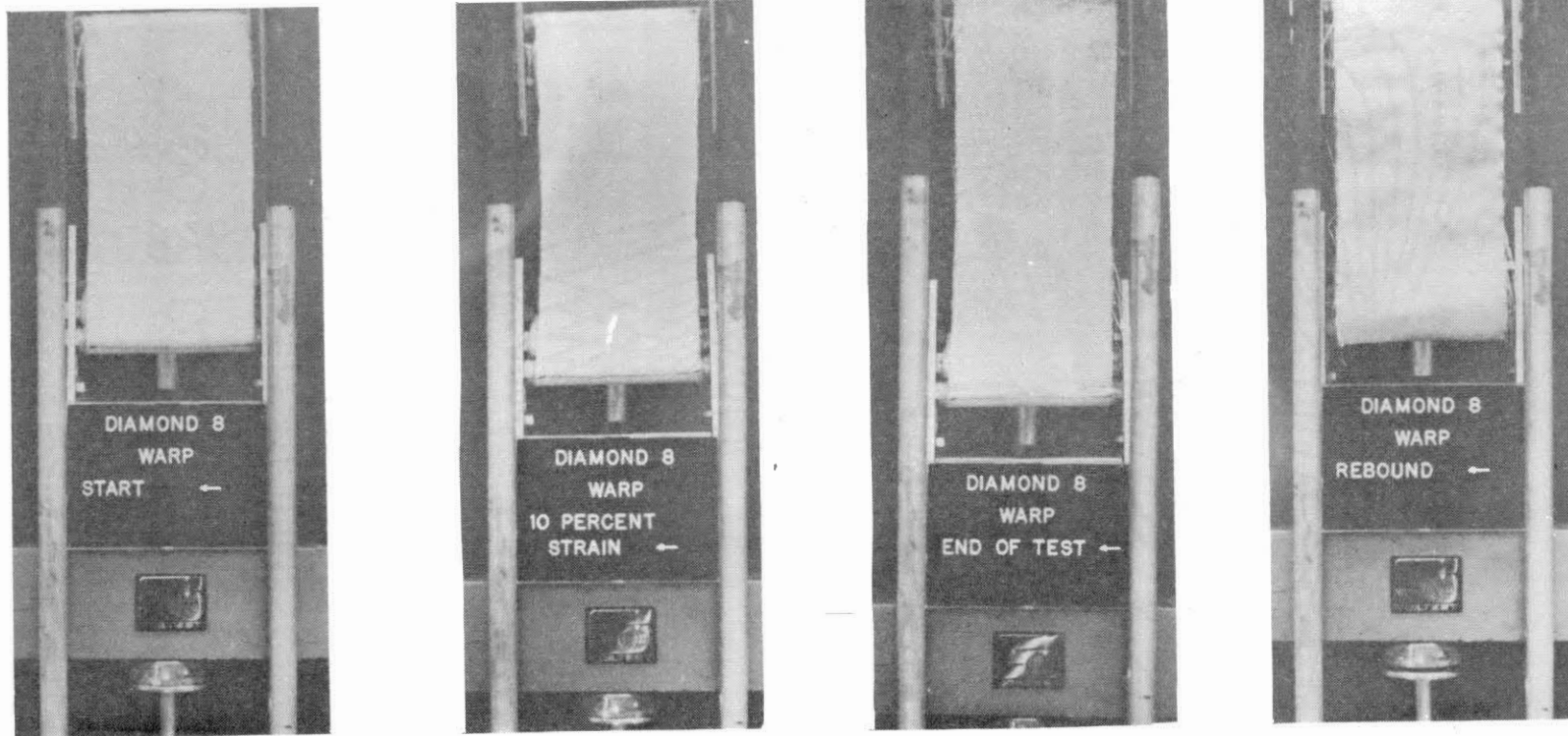


Figure 24. Photographs of Diamond 8-Warp Direction in Tension Testing at (Left to Right) Start, 10 Percent Strain, Failure, and After "Elastic" Rebound

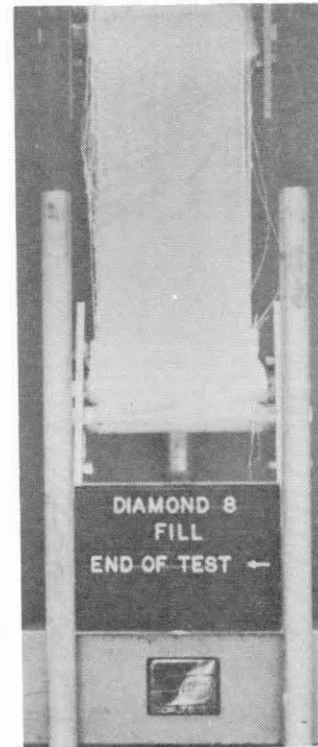
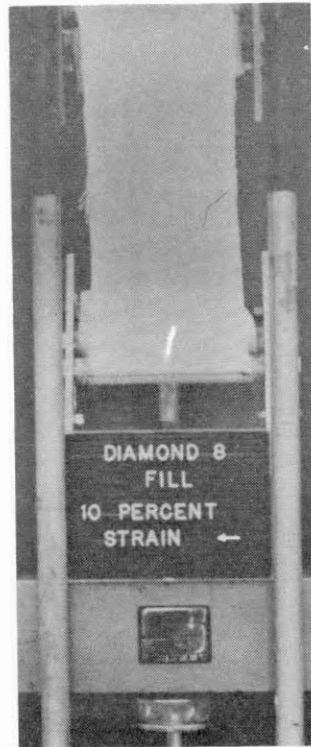


Figure 25. Photographs of Diamond 8-Fill Direction in Tension Testing at (Left to Right) Start, 10 Percent Strain, Failure, and After "Elastic" Rebound

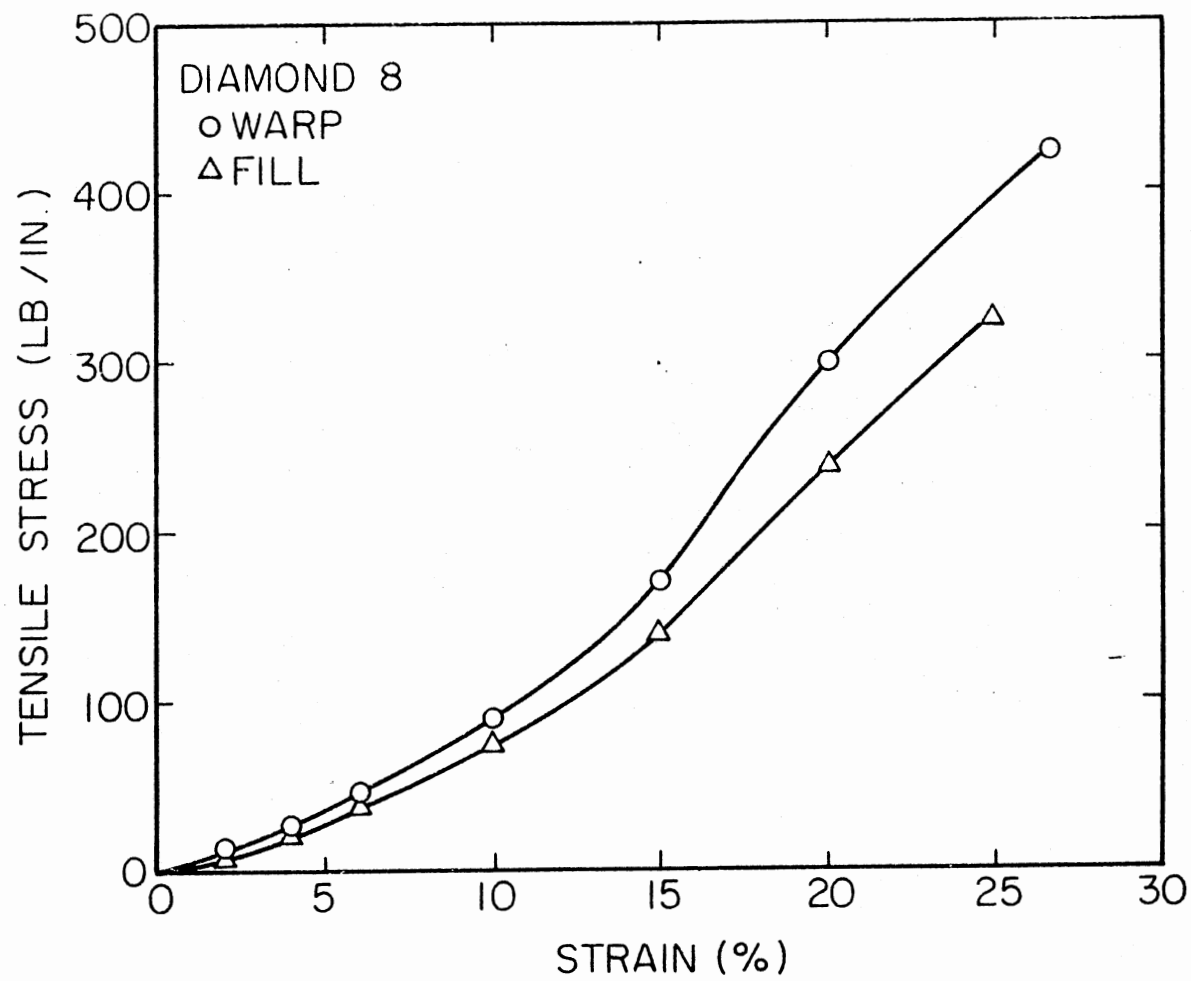


Figure 26. Stress-Strain Data for Diamond 8 in Uniaxial Testing

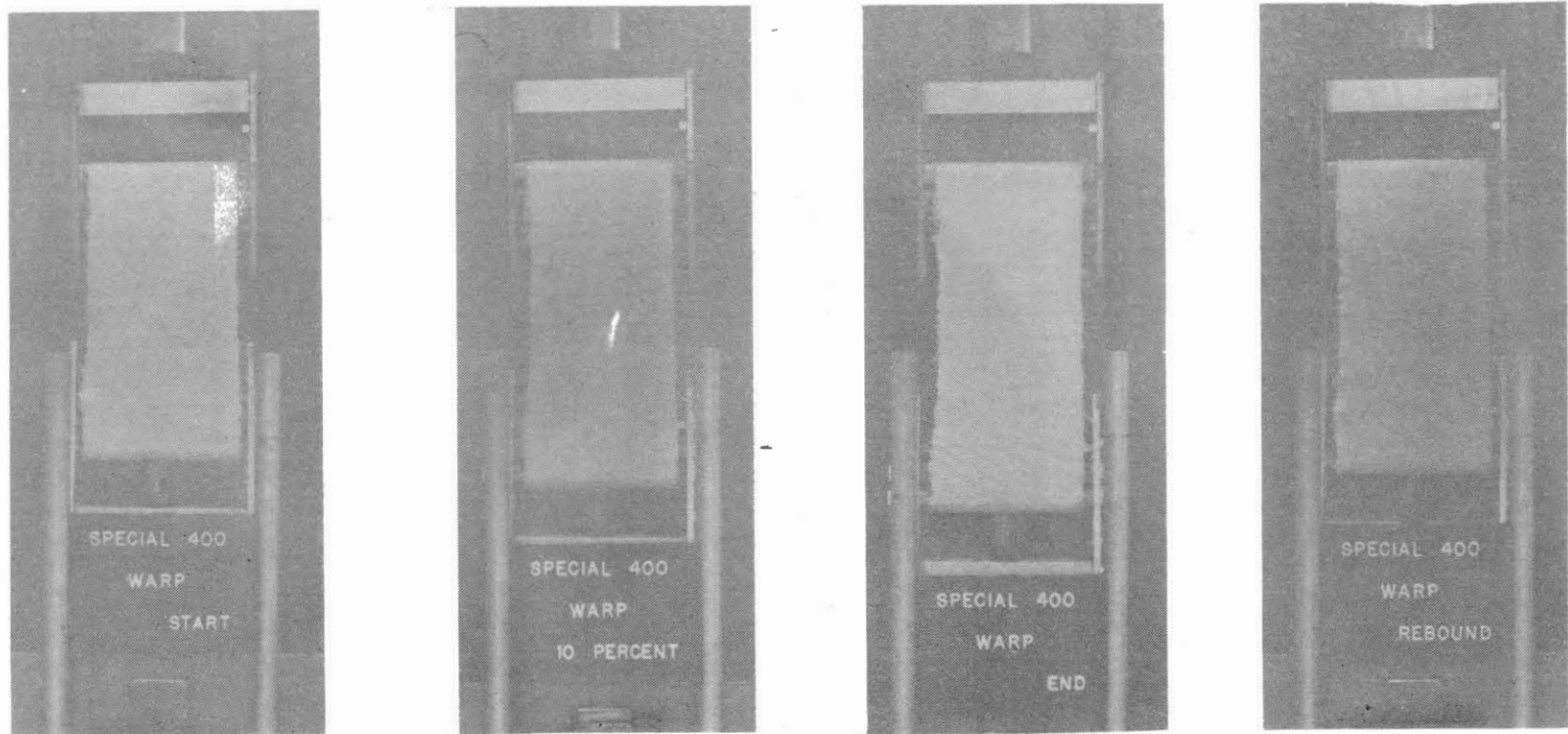


Figure 27. Photographs of Special 400-Warp Direction in Tension Testing at (Left to Right) Start, 10 Percent Strain, Failure, and After "Elastic" Rebound

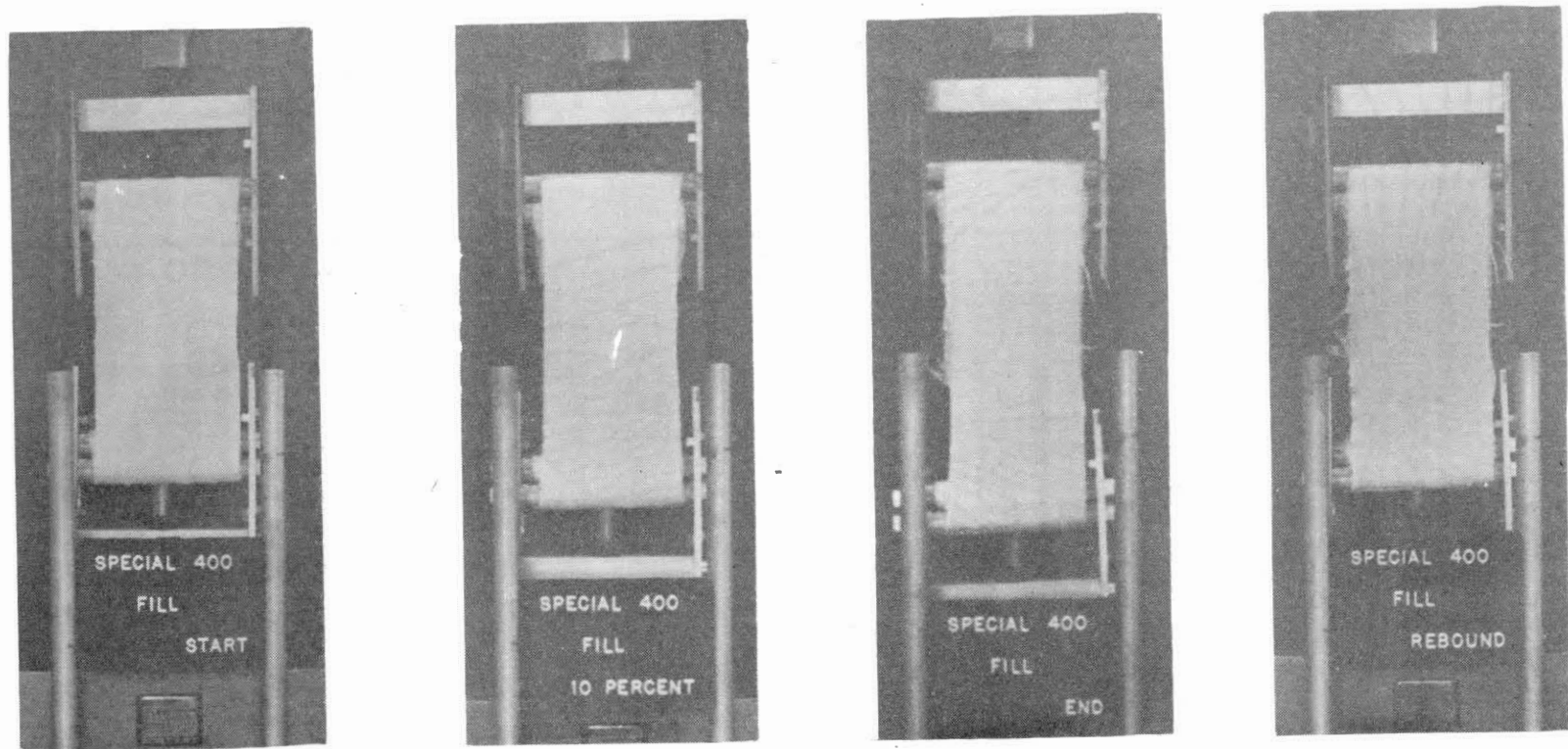


Figure 28. Photographs of Special 400-Fill Direction in Tension Testing at (Left to Right) Start, 10 Percent Strain, Failure, and After "Elastic" Rebound

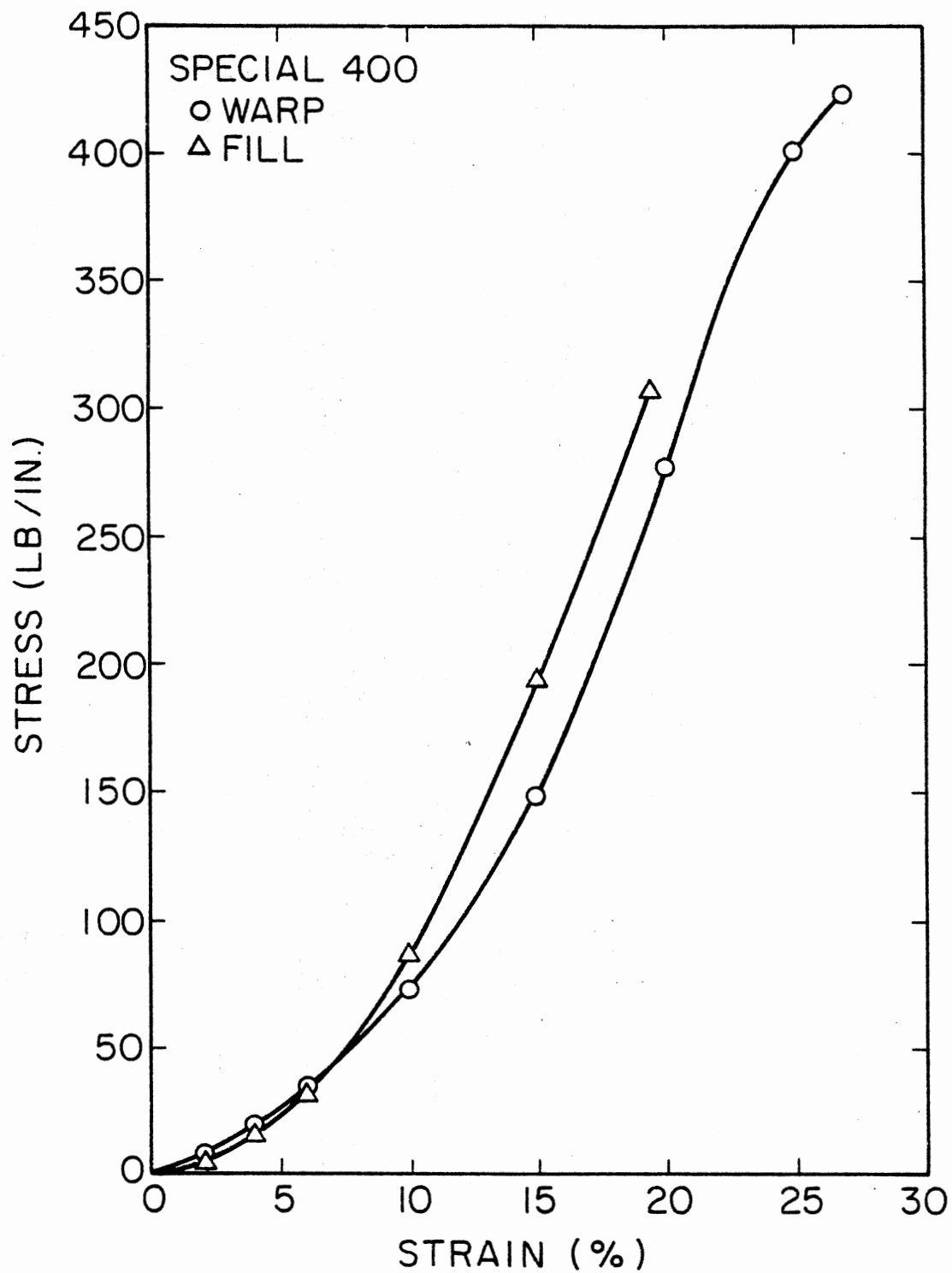


Figure 29. Stress-Strain Data for Special 400 in Uniaxial Testing



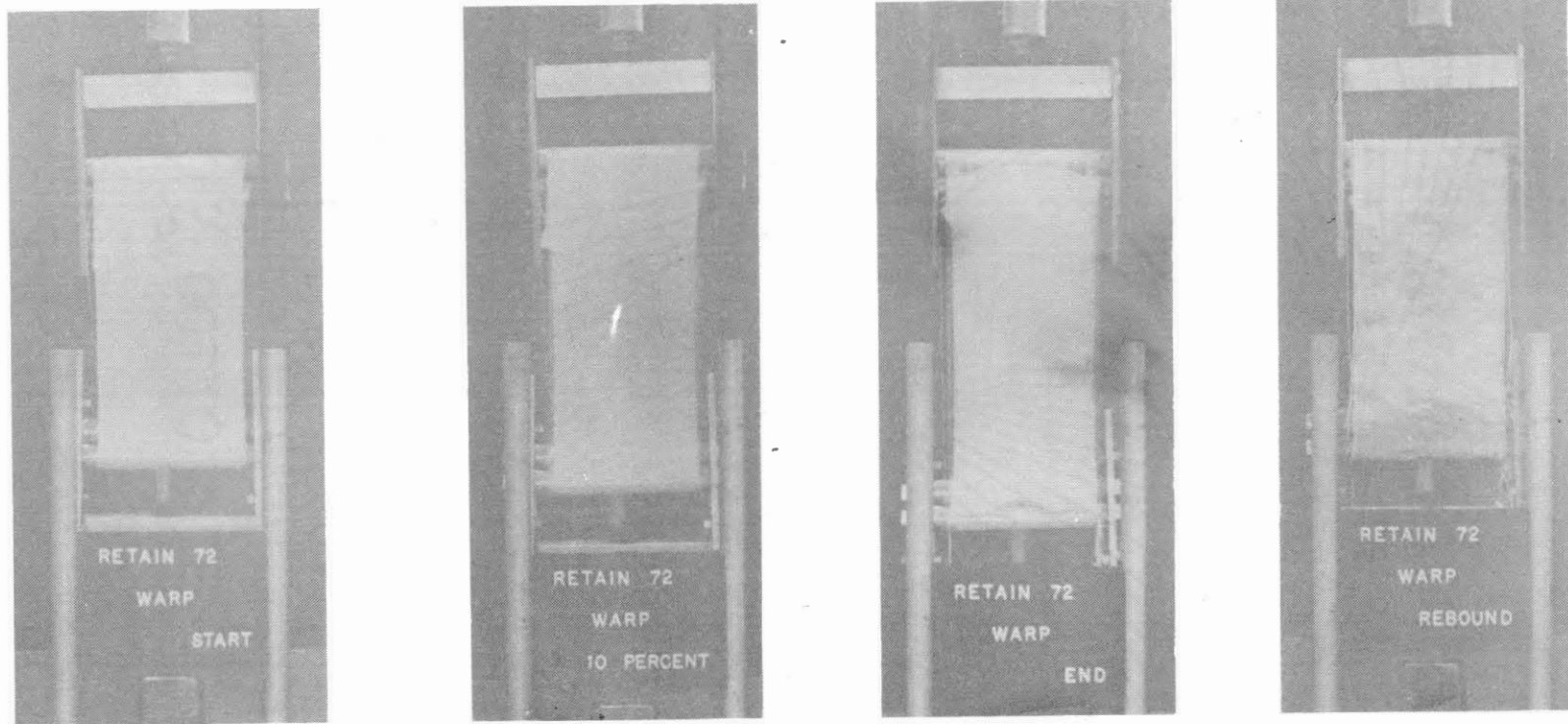


Figure 30. Photographs of Retain 72-Warp Direction in Tension Testing at (Left to Right) Start, 10 Percent Strain, Failure, and After "Elastic" Rebound

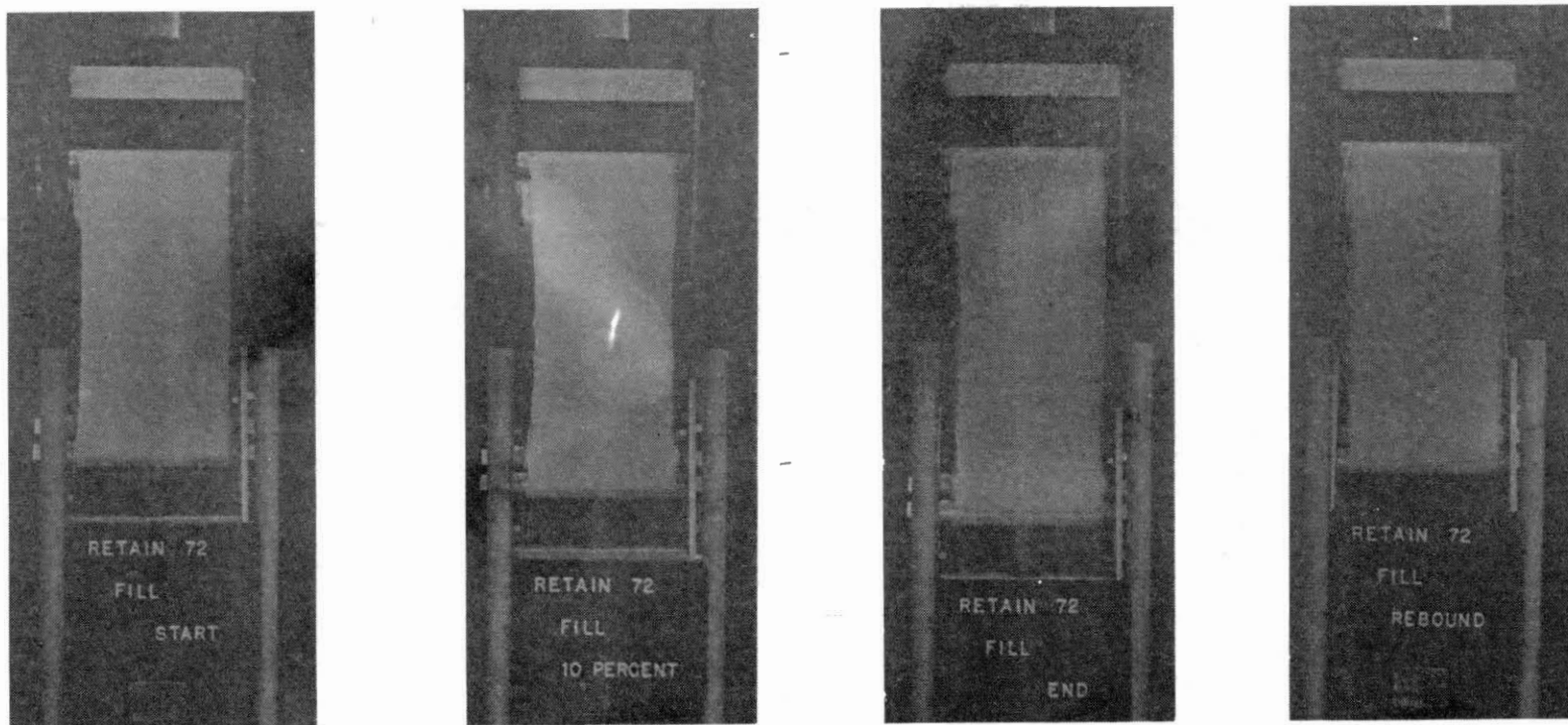


Figure 31. Photographs of Retain 72-Fill Direction in Tension Testing at (Left to Right) Start, 10 Percent Strain, Failure, and After "Elastic" Rebound

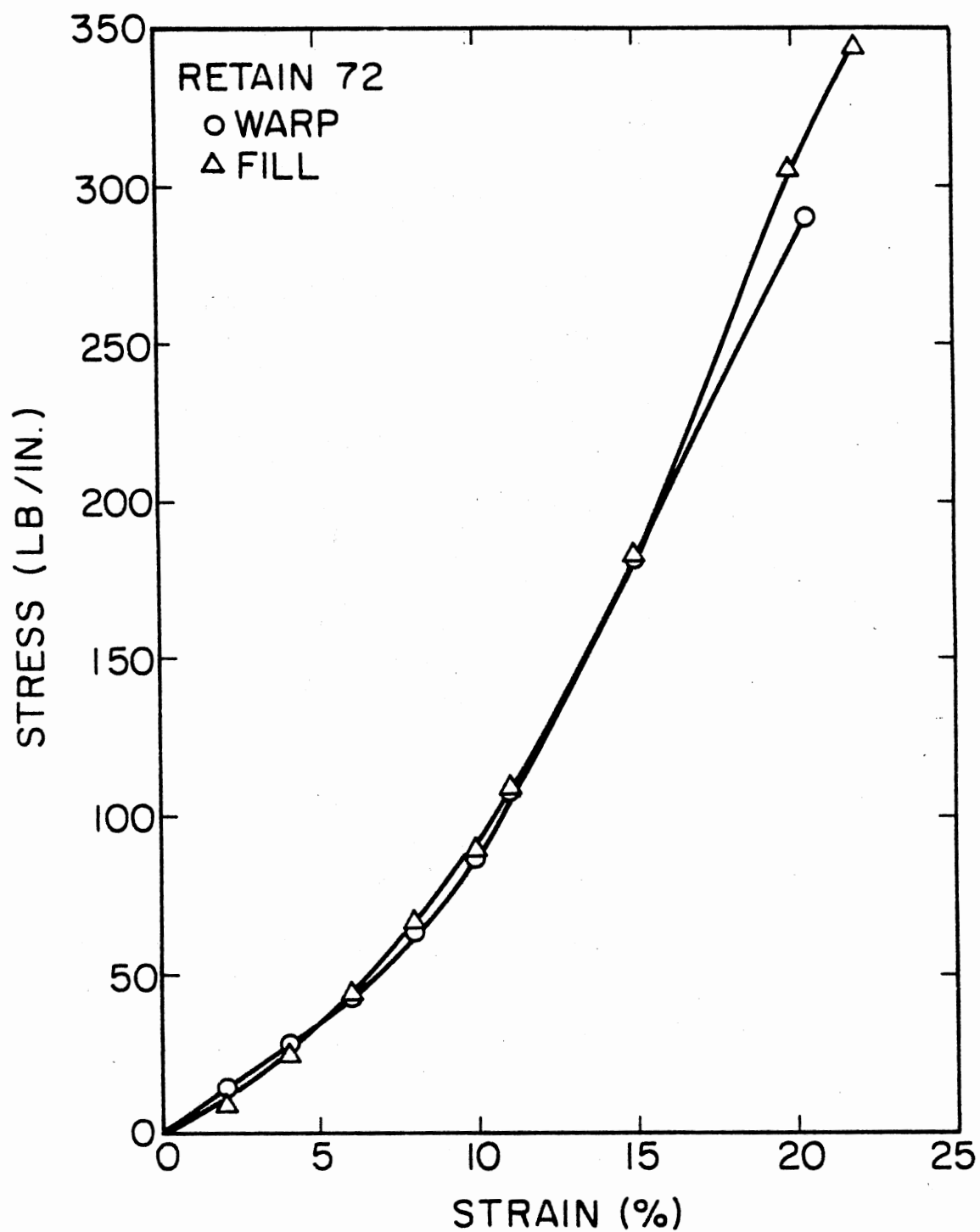


Figure 32. Stress-Strain Data for Retain 72 in Uniaxial Testing

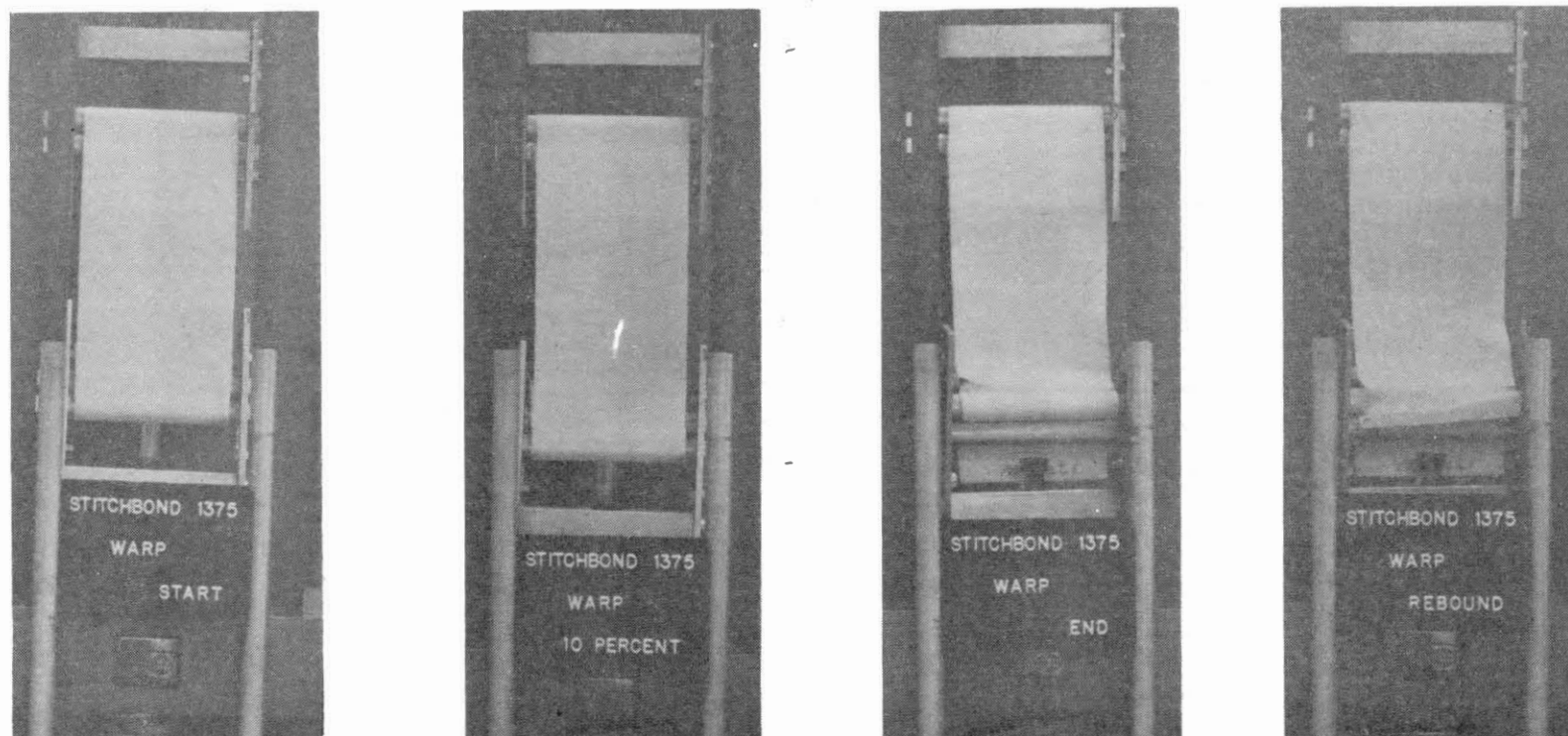


Figure 33. Photographs of Stitchbond 1375-Warp Direction in Tension Testing at (Left to Right) Start, 10 Percent Strain, Failure, and After "Elastic" Rebound

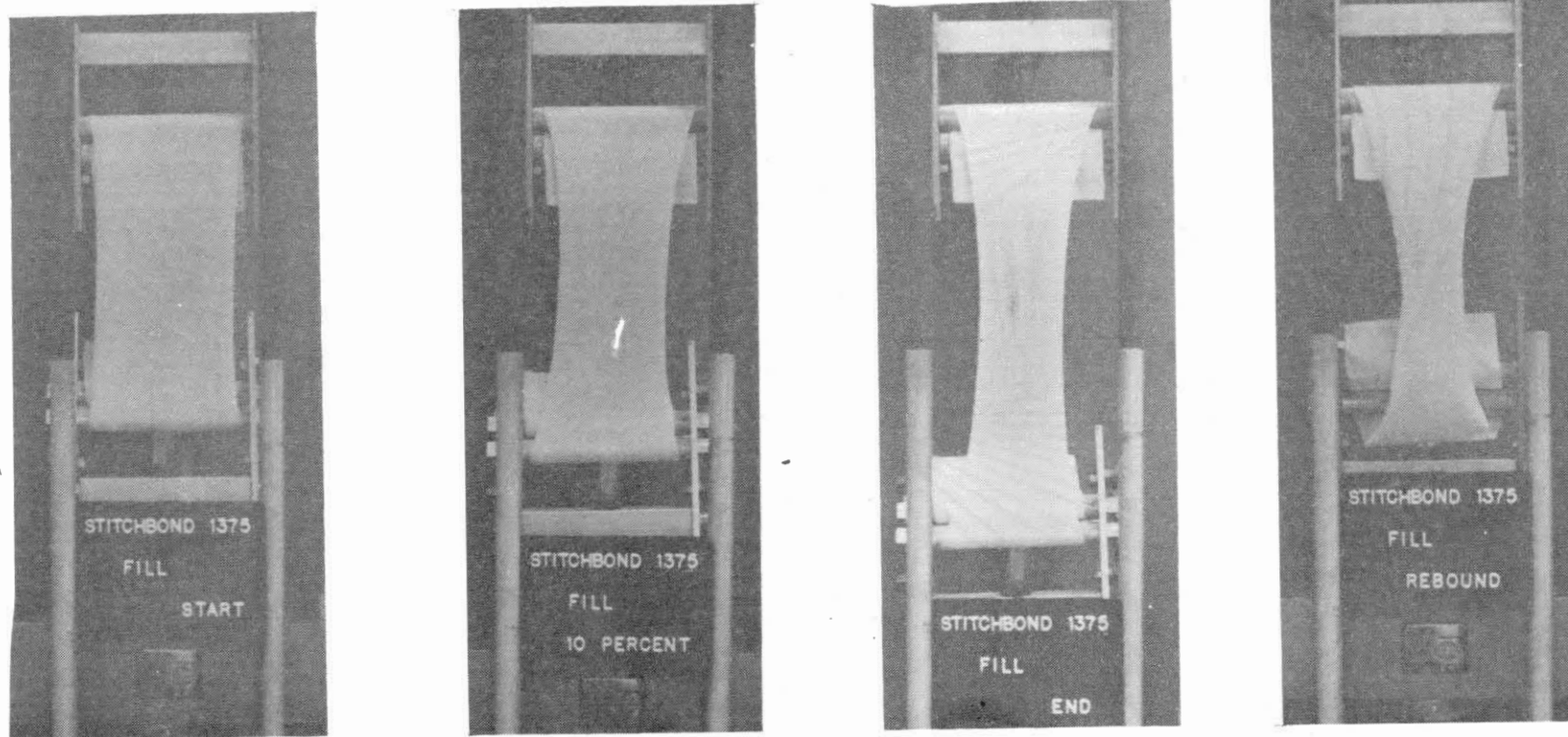


Figure 34. Photographs of Stitchbond 1375-Fill Direction in Tension Testing at (Left to Right) Start, 10 Percent Strain, Failure, and After "Elastic" Rebound

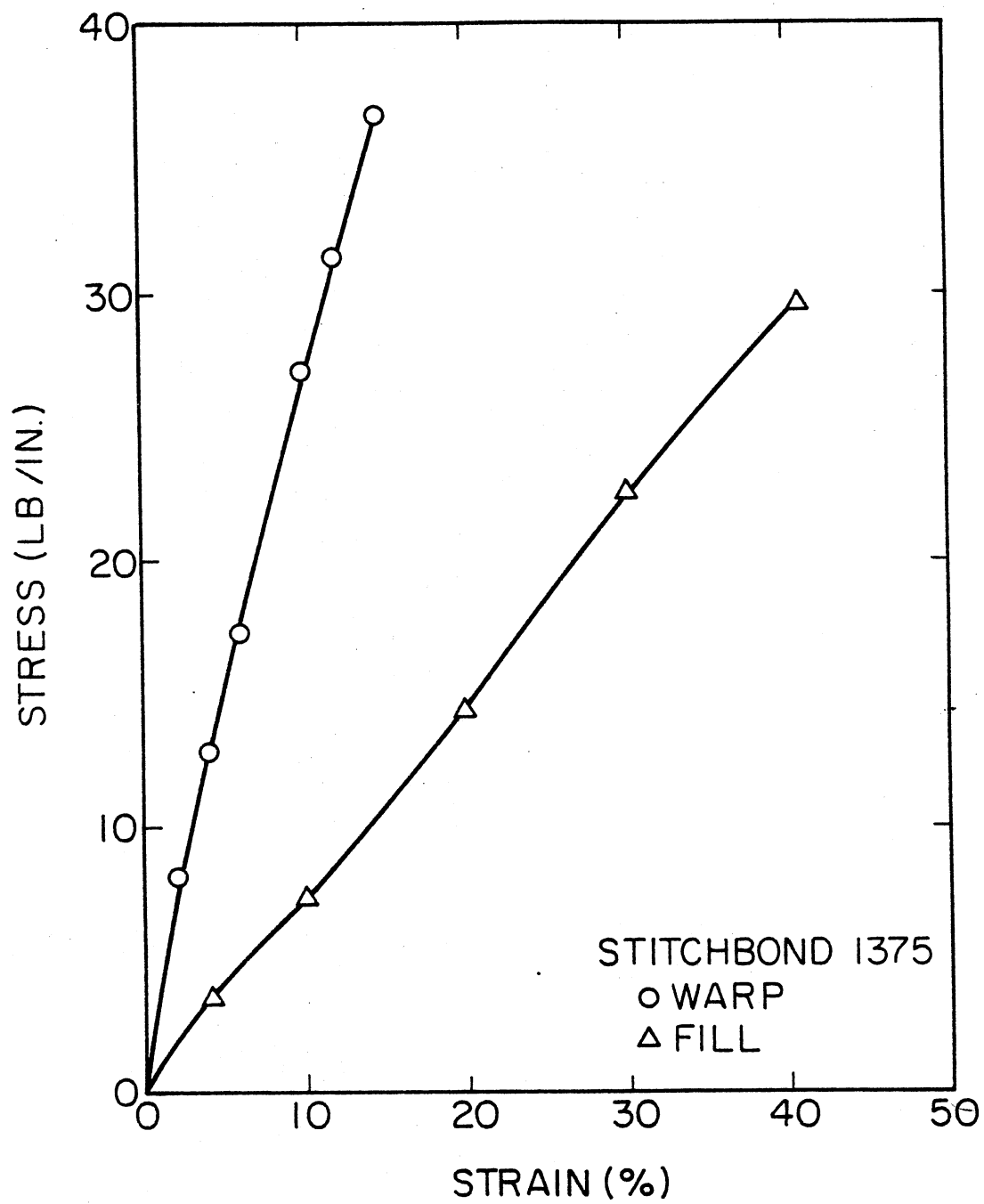


Figure 35. Stress-Strain Data for Stitchbond 1375 in Uniaxial Testing

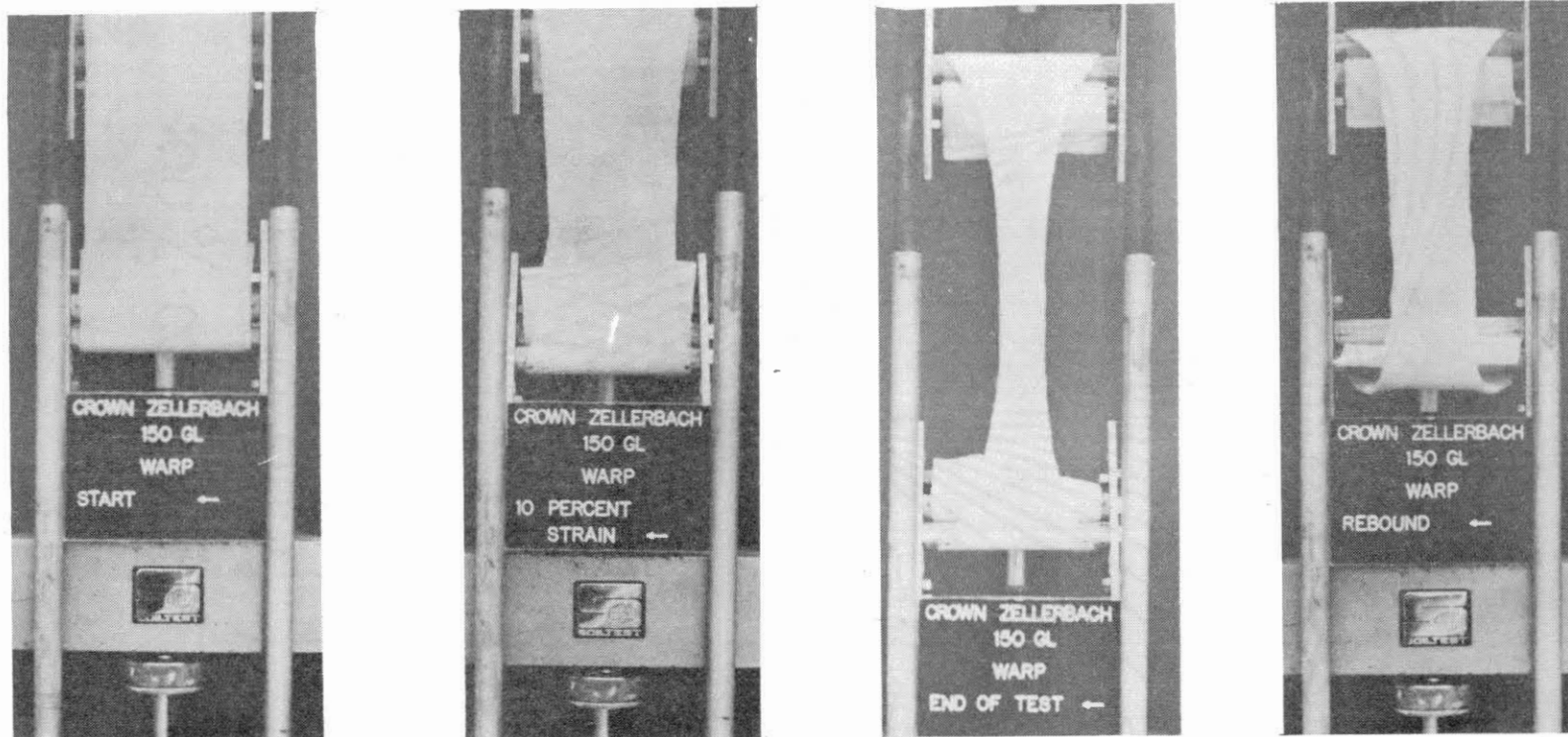


Figure 36. Photographs of Fibretex 150-Warp Direction in Tension Testing at (Left to Right) Start, 10 Percent Strain, Failure, and After "Elastic" Rebound

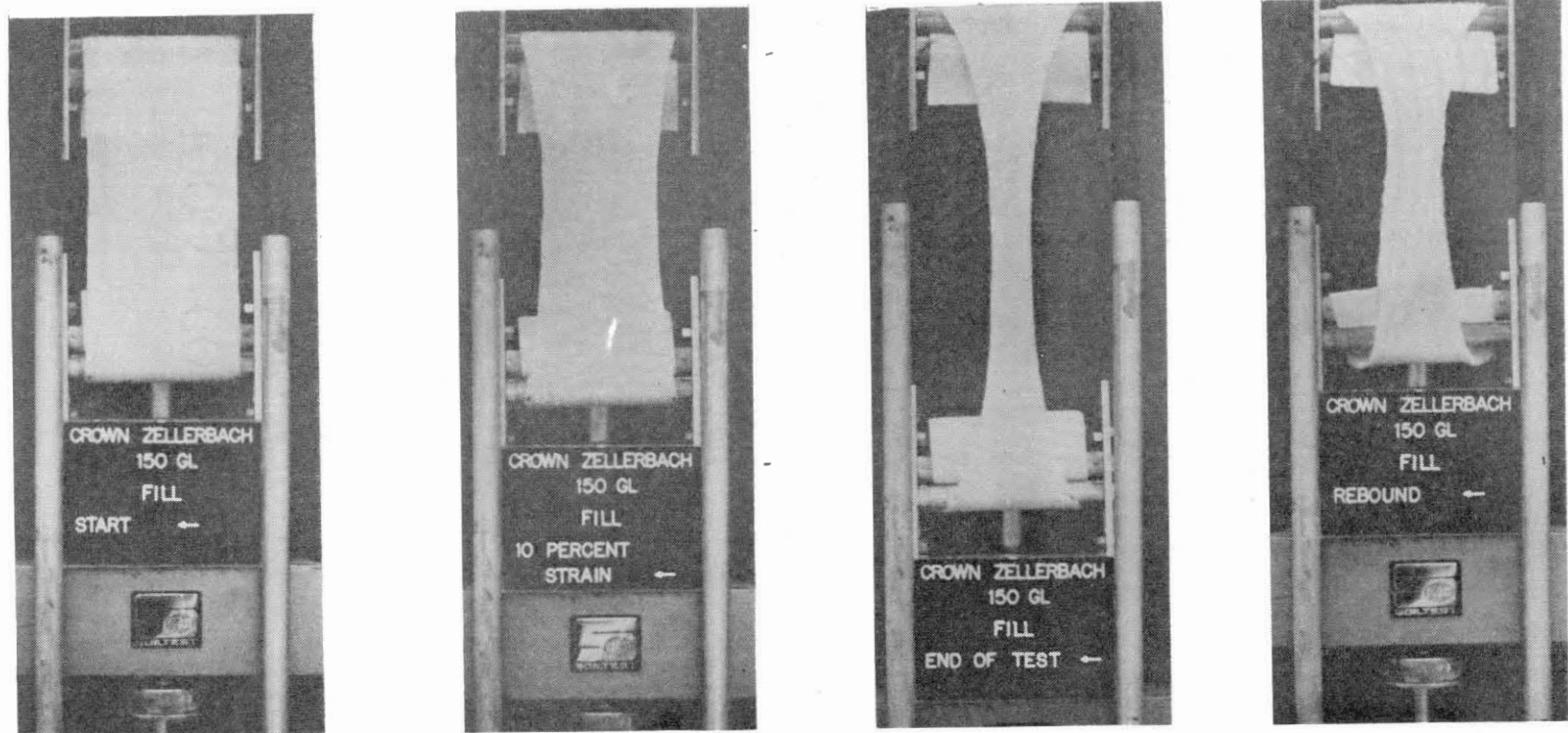


Figure 37. Photographs of Fibretex 150-Fill Direction in Tension Testing at (Left to Right) Start, 10 Percent Strain, Failure, and After "Elastic" Rebound



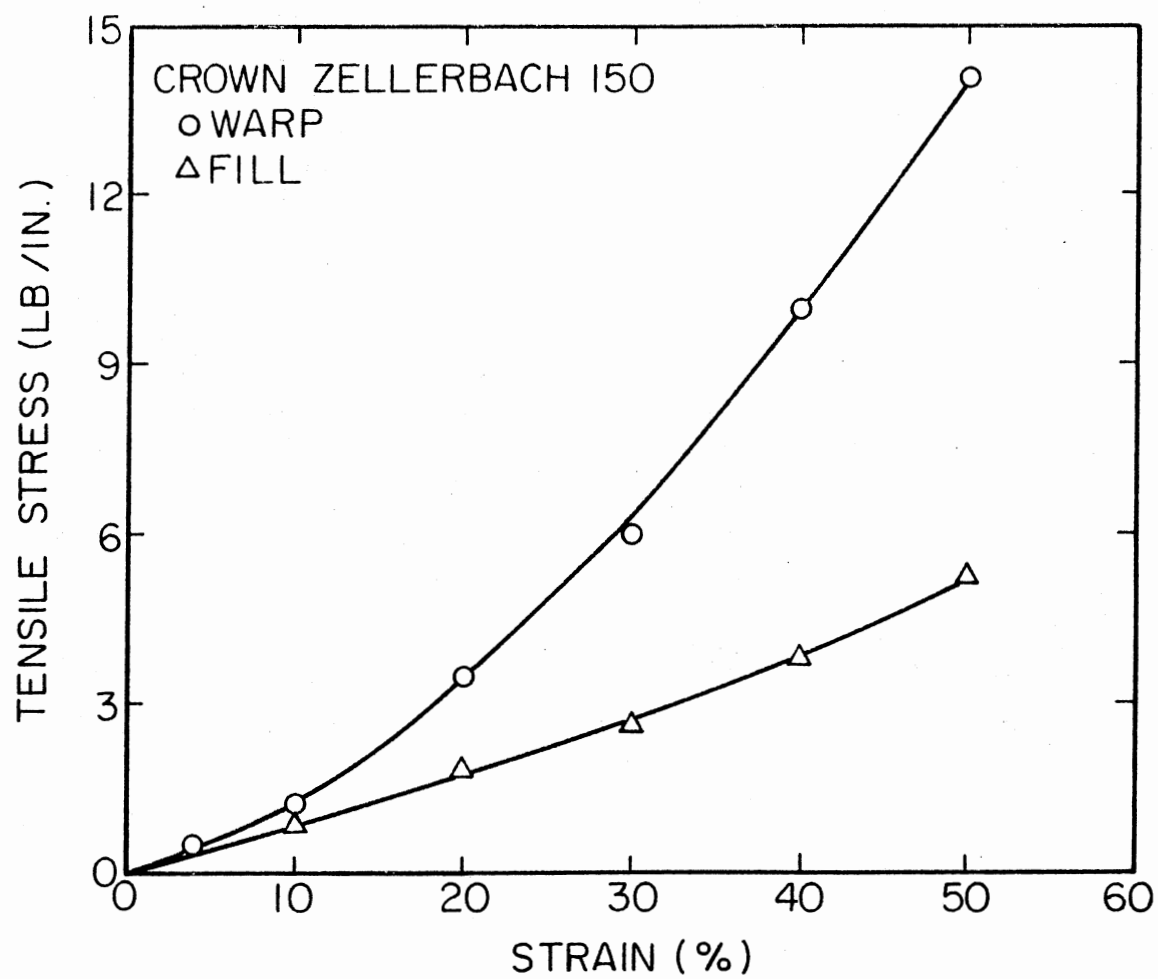


Figure 38. Stress-Strain Data for Fibretex 150 in Uniaxial Testing

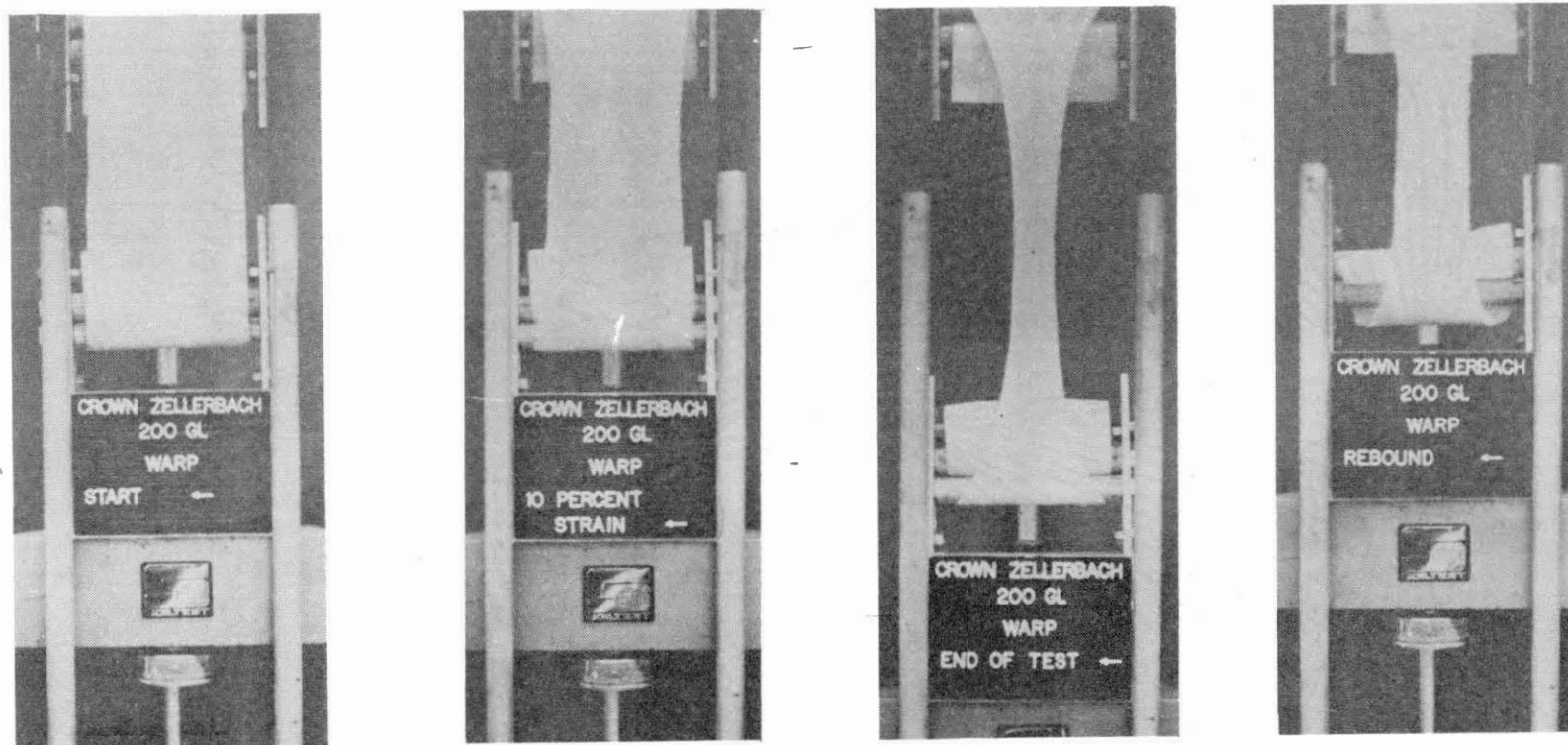


Figure 39. Photographs of Fibretex 200-Warp Direction in Tension Testing at (Left to Right) Start, 10 Percent Strain, Failure, and After "Elastic" Rebound

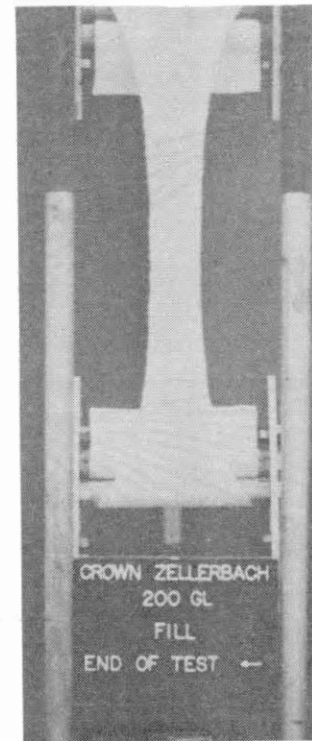


Figure 40. Photographs of Fibretex 200-Fill Direction in Tension Testing at (Left to Right) Start, 10 Percent Strain, Failure, and After "Elastic" Rebound

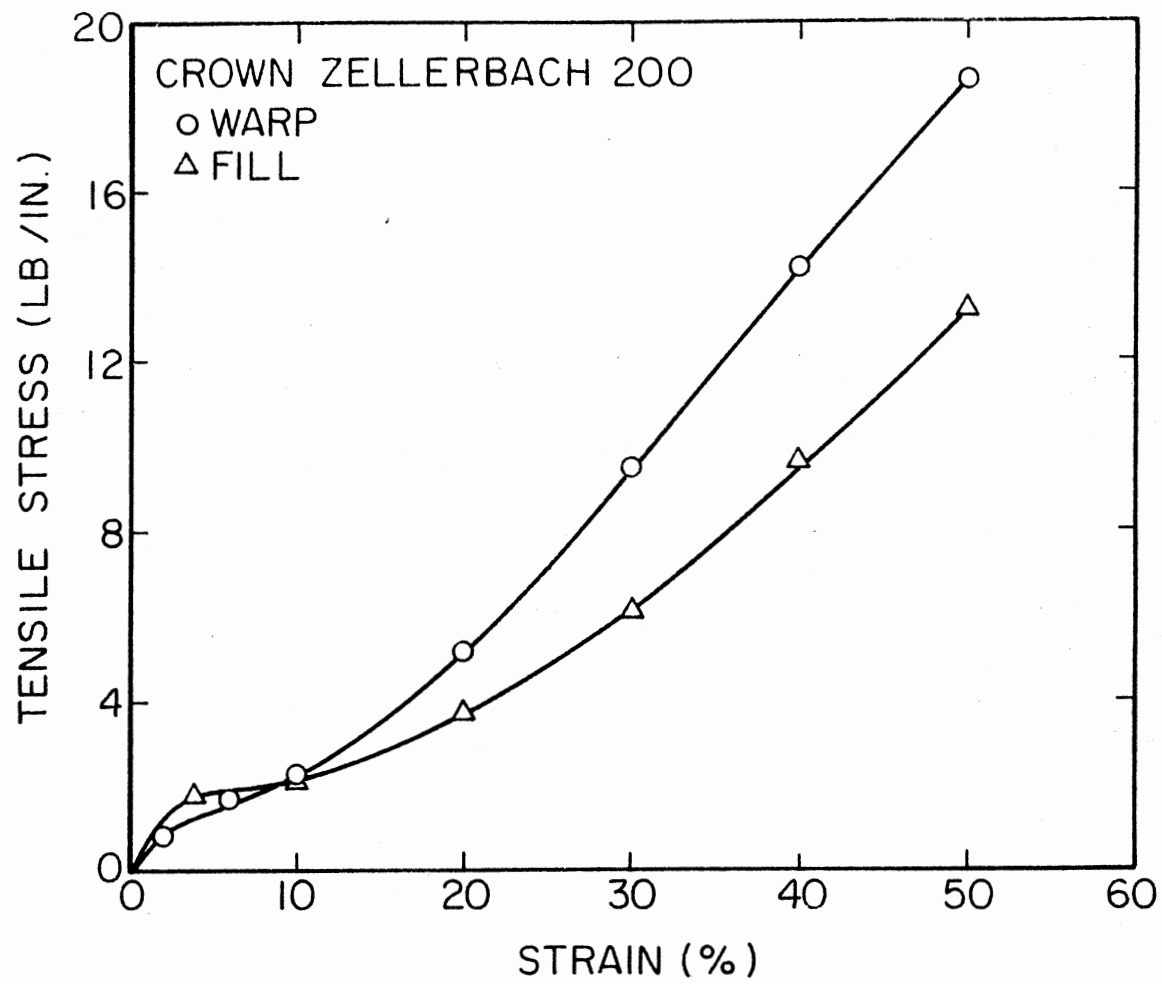


Figure 41. Stress-Strain Data for Fibretex 200 in Uniaxial Testing

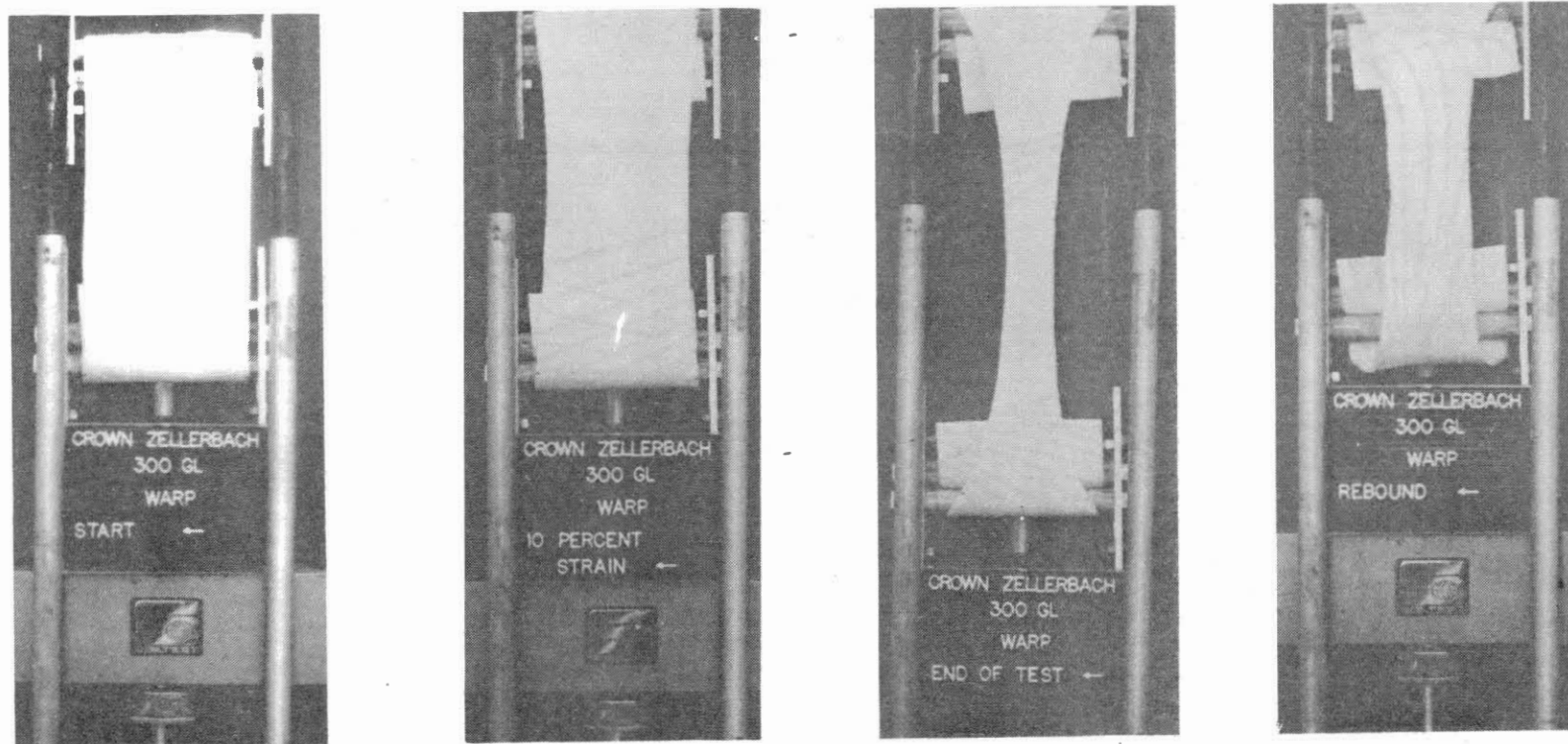


Figure 42. Photograph of Fibretex 300-Warp Direction in Tension Testing at (Left to Right) Start, 10 Percent Strain, Failure, and After "Elastic" Rebound

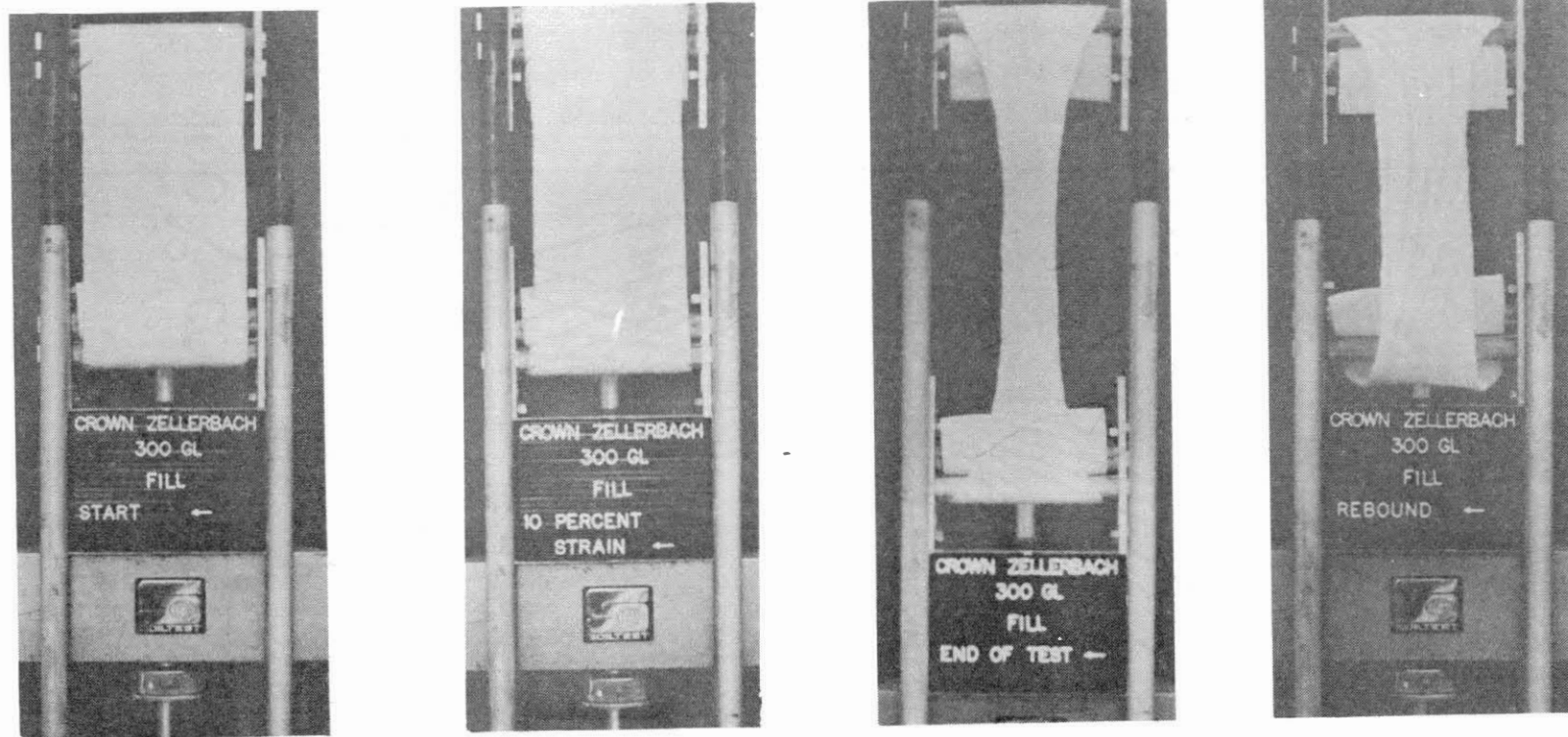


Figure 43. Photographs of Fibretex 300-Fill Direction in Tension Testing at (Left to Right) Start, 10 Percent Strain, Failure, and After "Elastic" Rebound

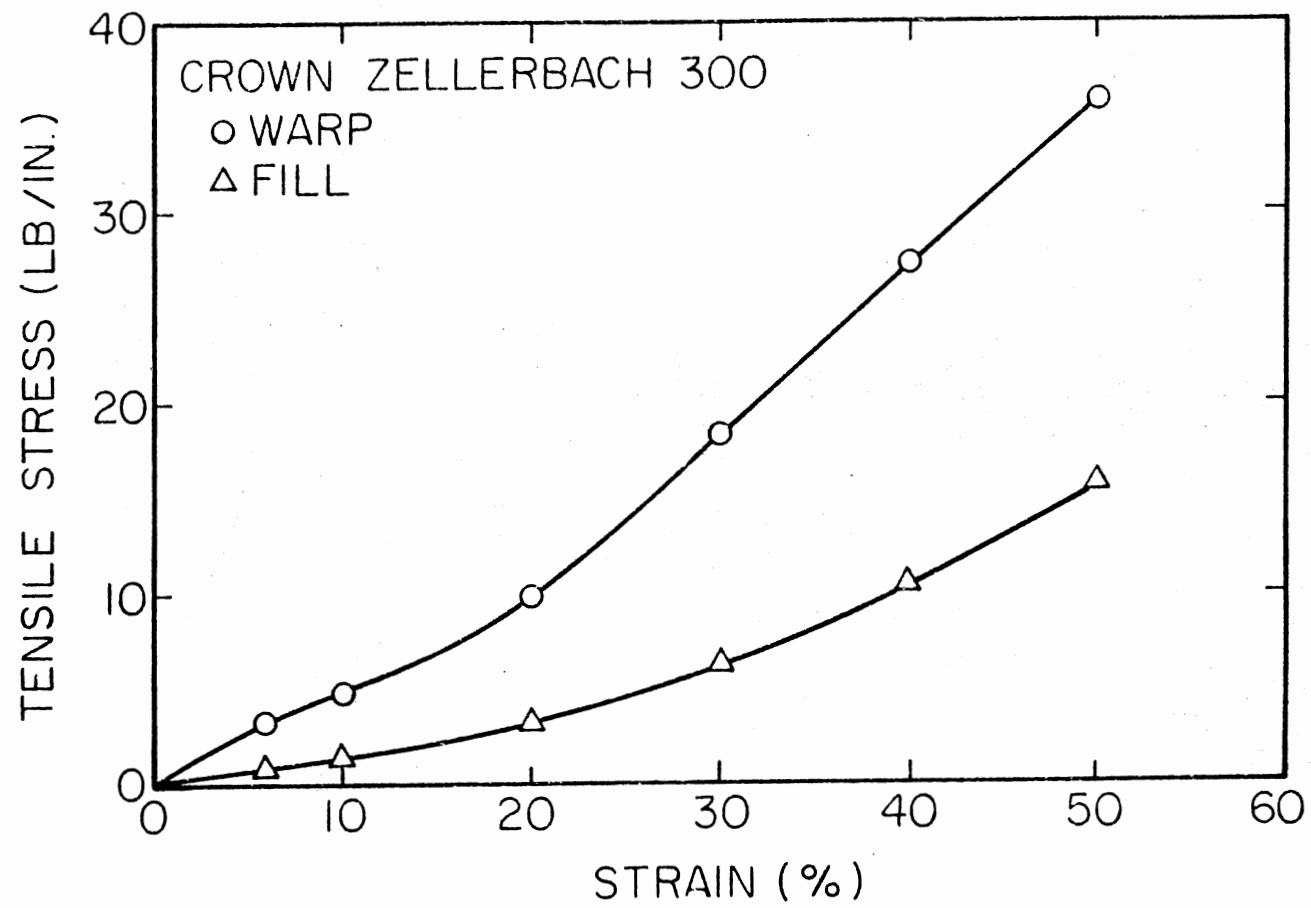


Figure 44. Stress-Strain Data for Fibretex 300 in Uniaxial Testing

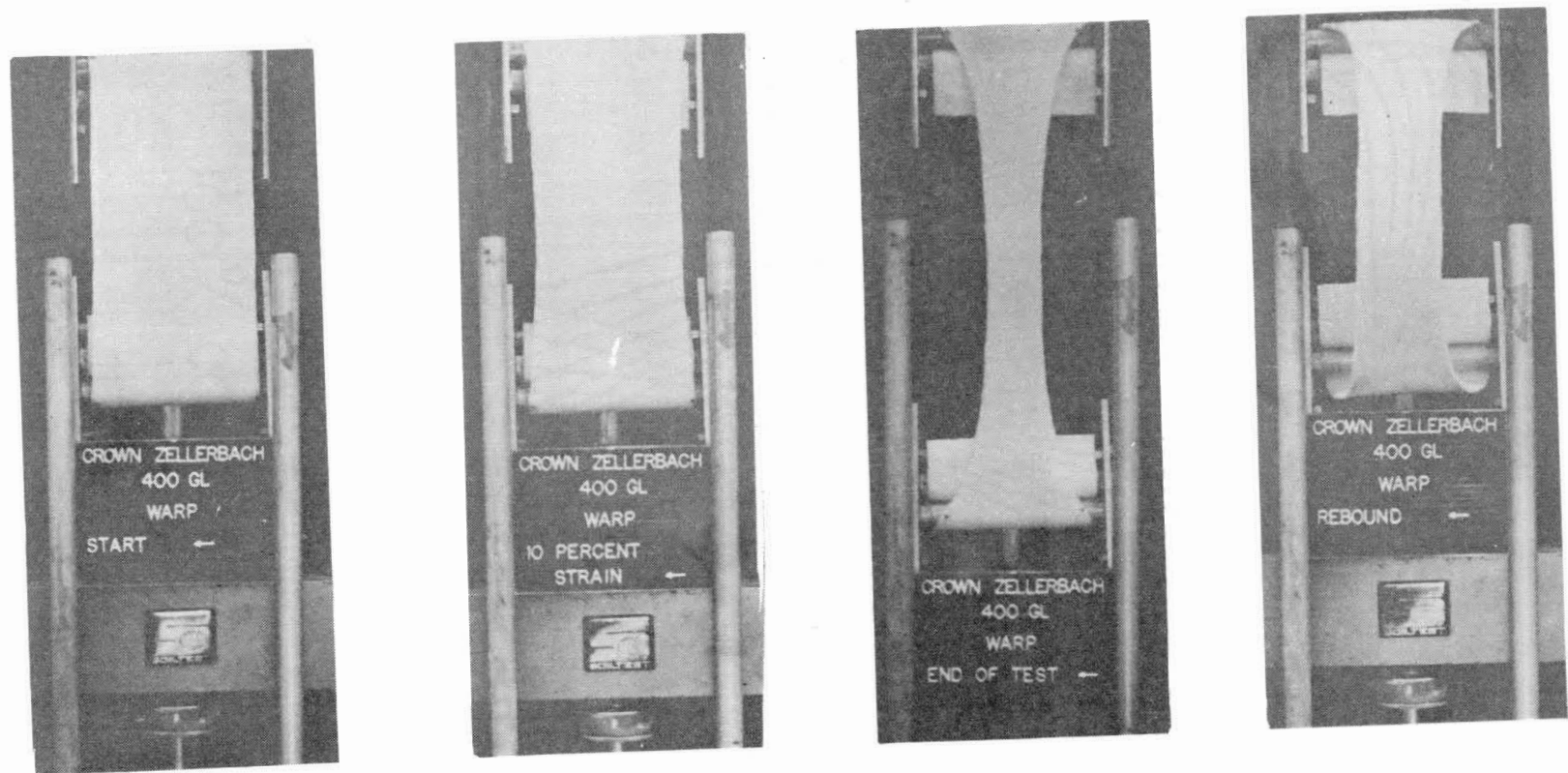


Figure 45. Photographs of Fibretex 400-Warp Direction in Tension Testing at (Left to Right) Start, 10 Percent Strain, Failure, and After "Elastic" Rebound



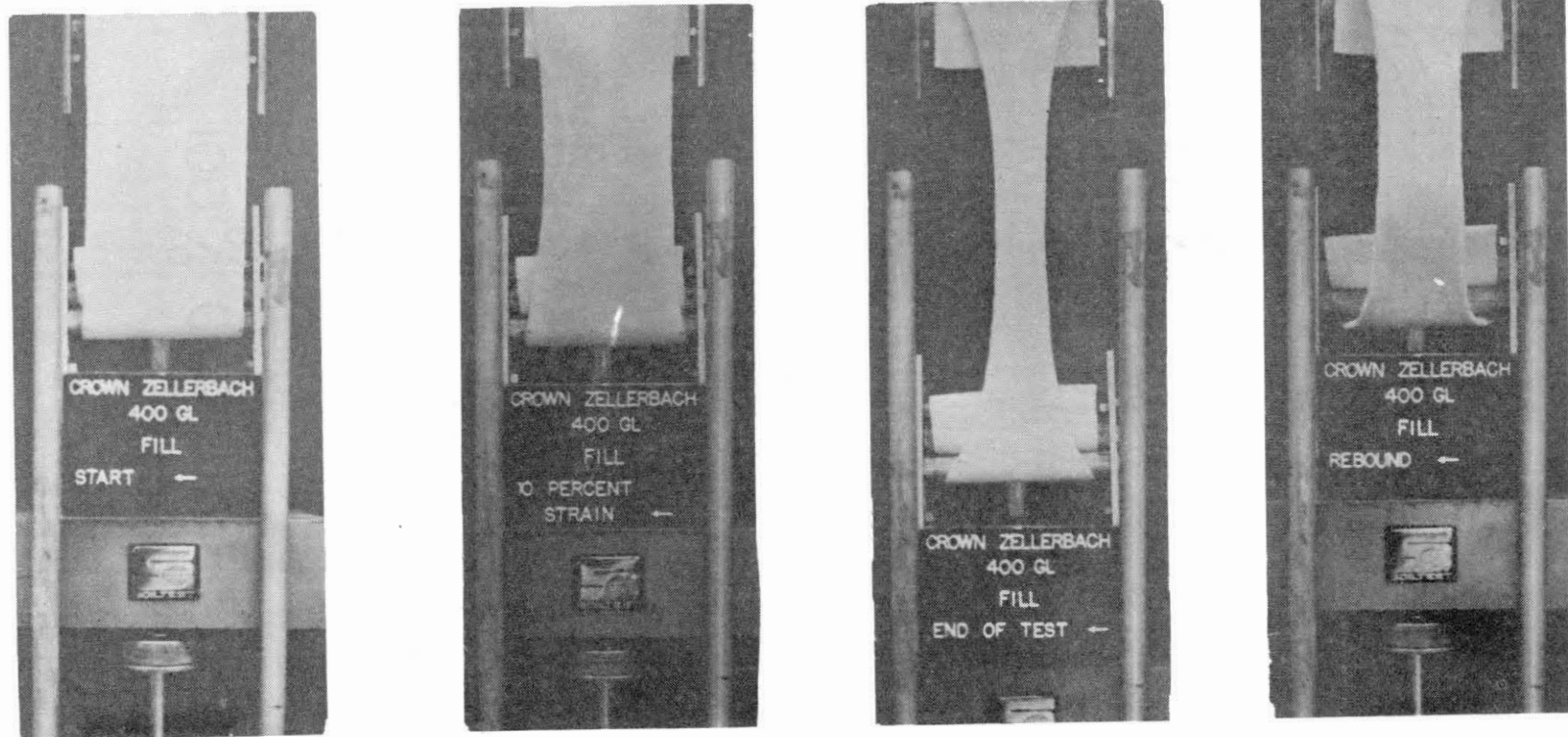


Figure 46. Photographs of Fibretex 400-Fill Direction in Tension Testing at (Left to Right) Start, 10 Percent Strain, Failure, and After "Elastic" Rebound

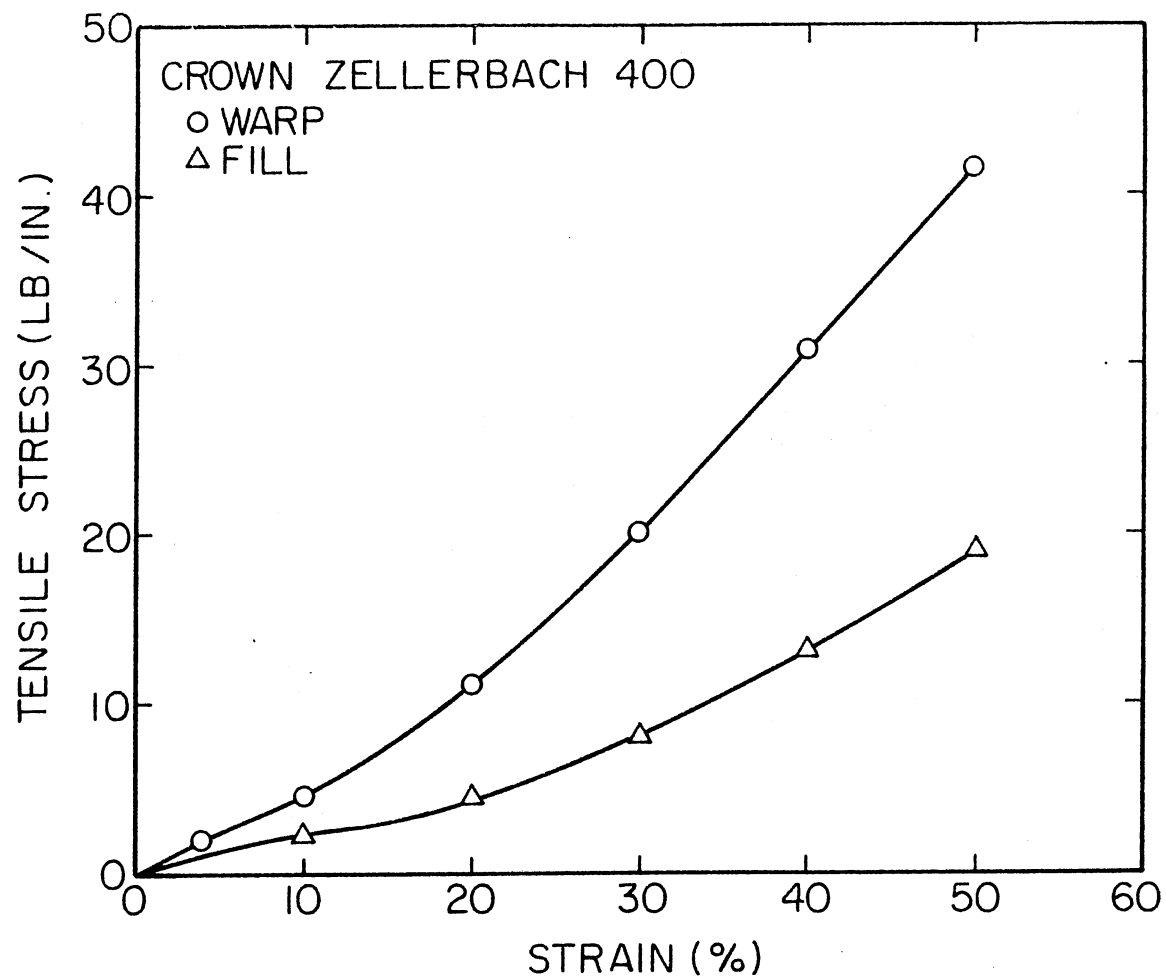


Figure 47. Stress-Strain Data for Fibretex 400 in Uniaxial Testing

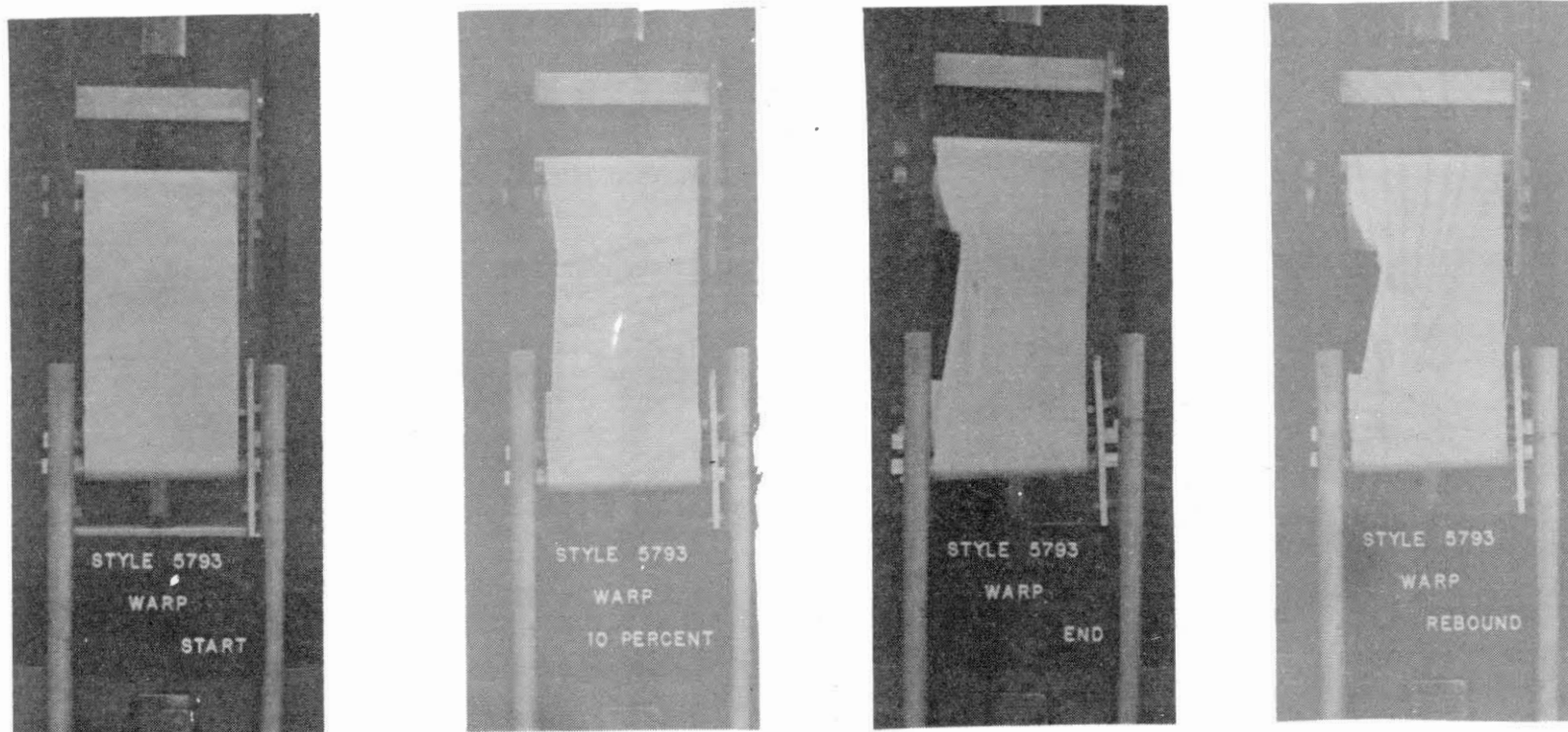


Figure 48. Photographs of Style 5793-Warp Direction in Tension Testing at (Left to Right) Start, 10 Percent Strain, Failure, and After "Elastic" Rebound

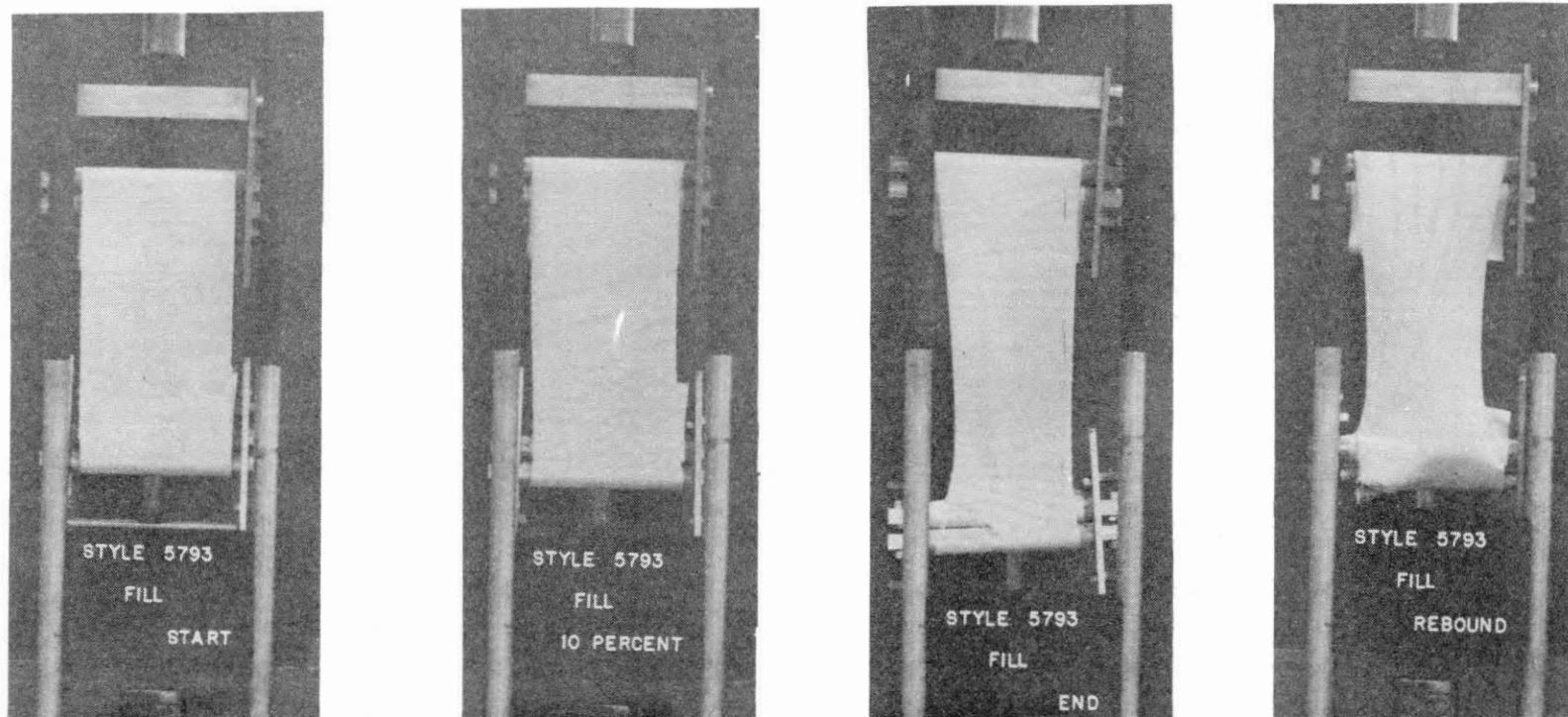


Figure 49. Photographs of Style 5793-Fill Direction in Tension Testing at (Left to Right) Start, 10 Percent Strain, Failure, and After "Elastic" Rebound

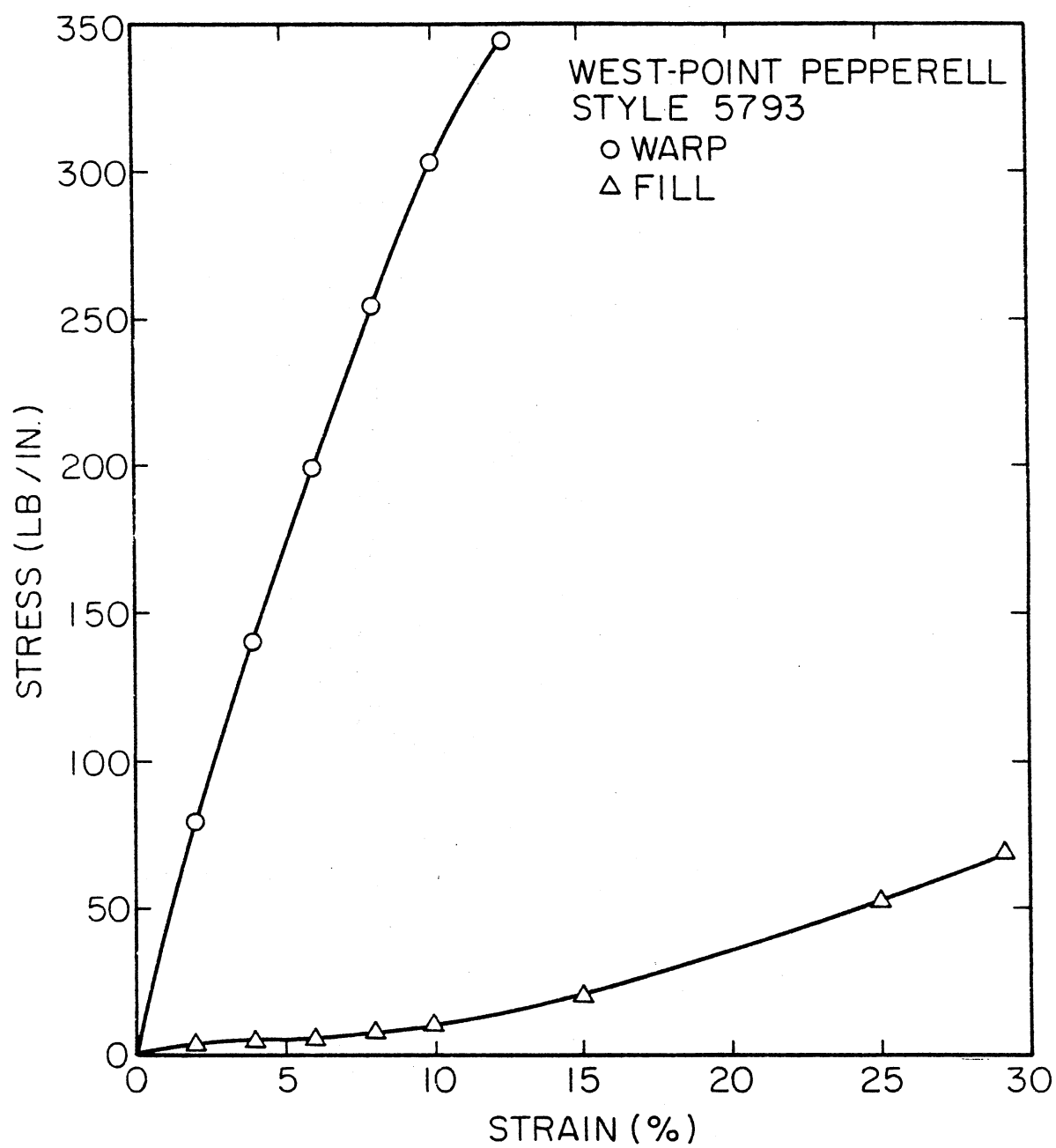


Figure 50. Stress-Strain Data for Style 5793 in Uniaxial Testing

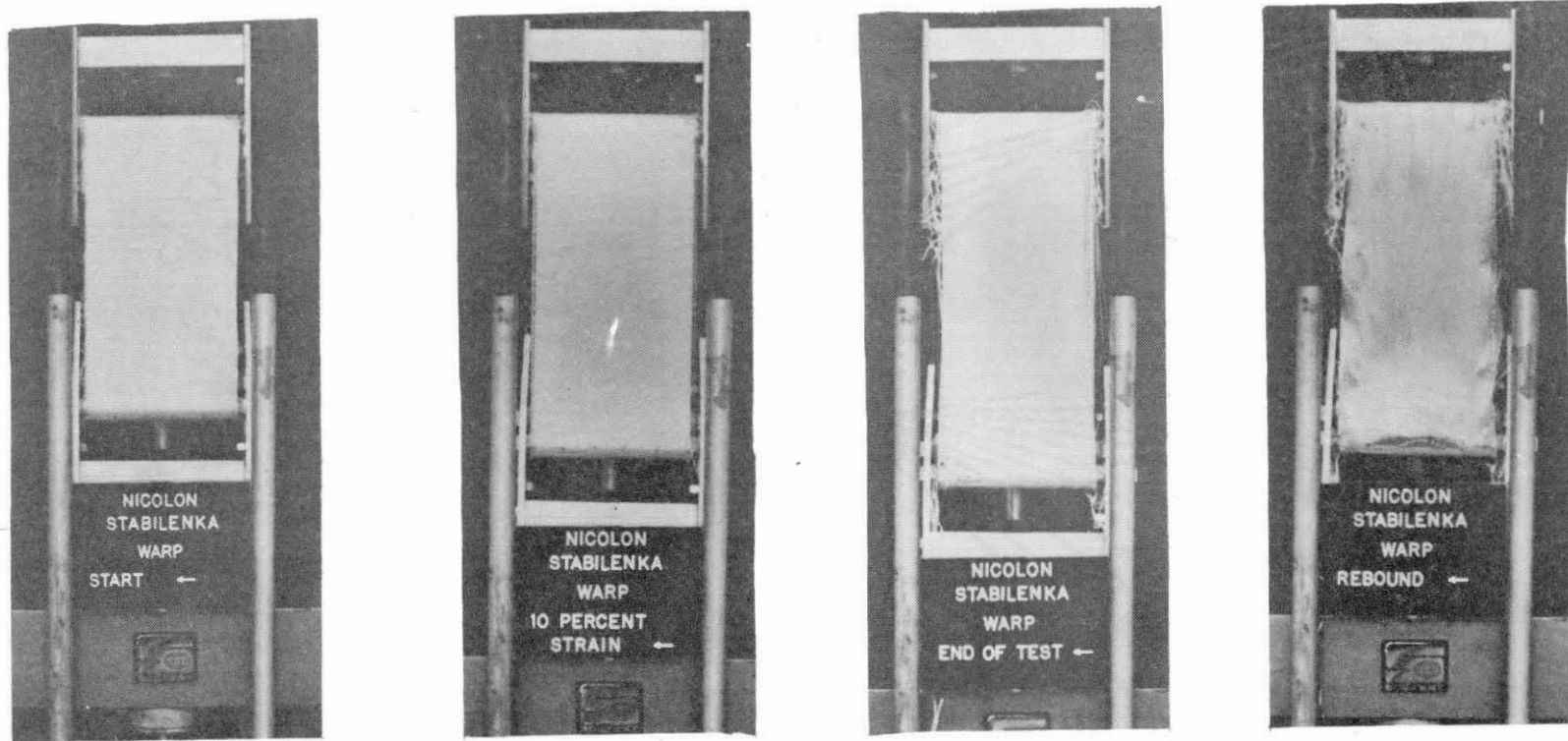


Figure 51. Photographs of Stabile nka 200-Warp Direction in Tension Testing at (Left to Right) Start, 10 Percent Strain, Failure, and After "Elastic" Rebound

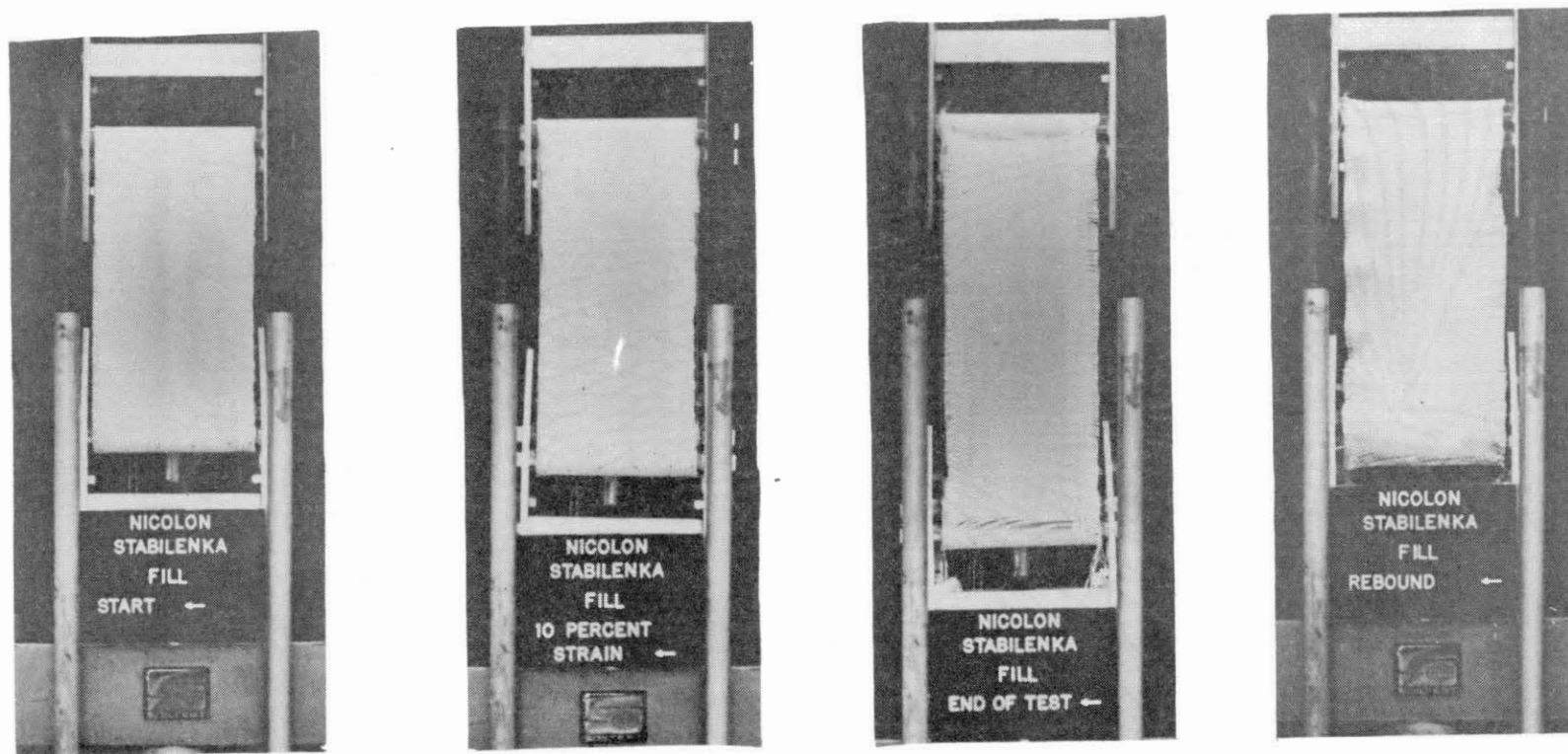


Figure 52. Photographs of Stabileika 200-Fill Direction in Tension Testing at (Left to Right) Start, 10 Percent Strain, Failure, and After "Elastic" Rebound

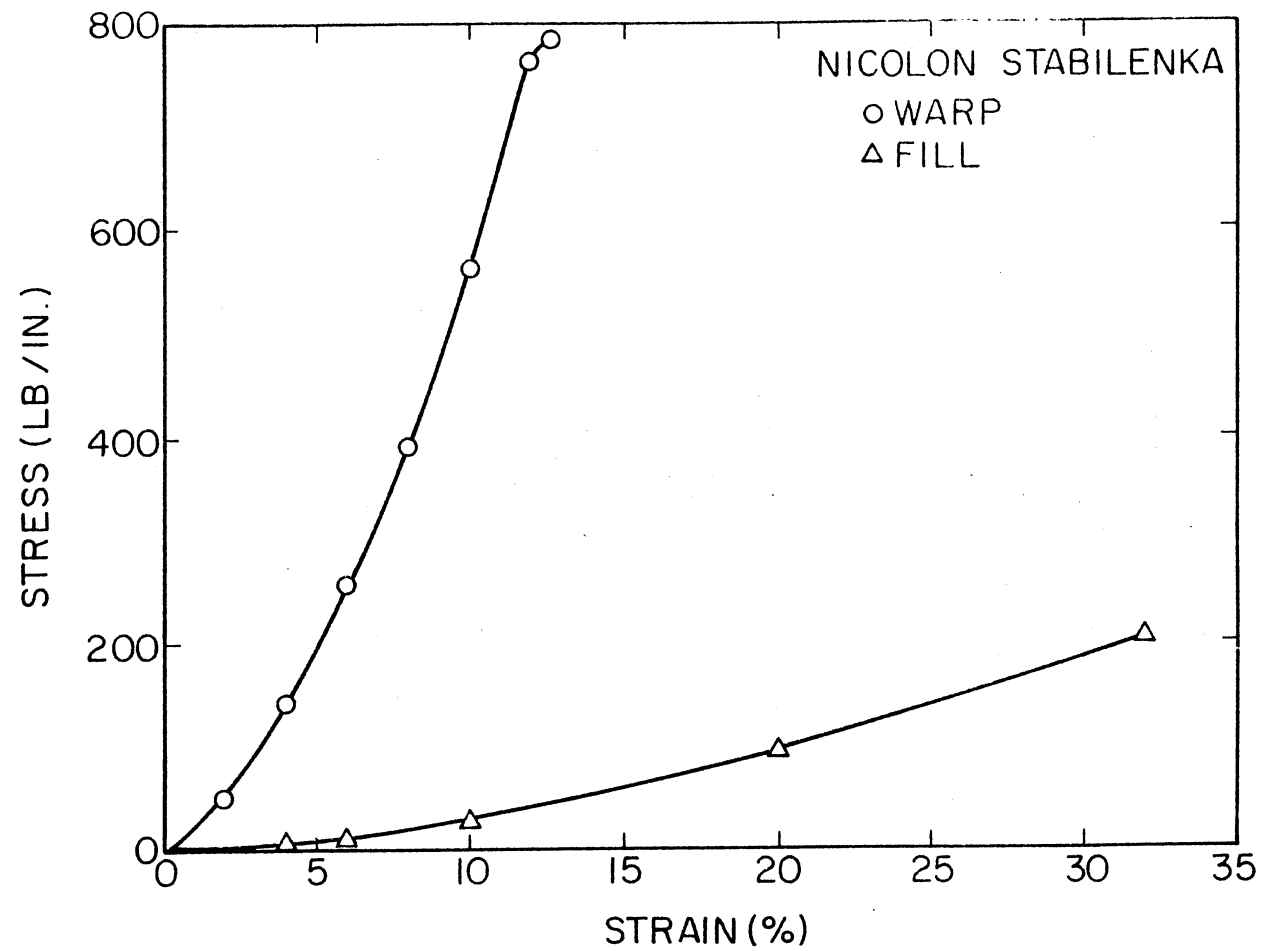


Figure 53. Stress-Strain Data for Stabilenka 200 In Uniaxial Testing



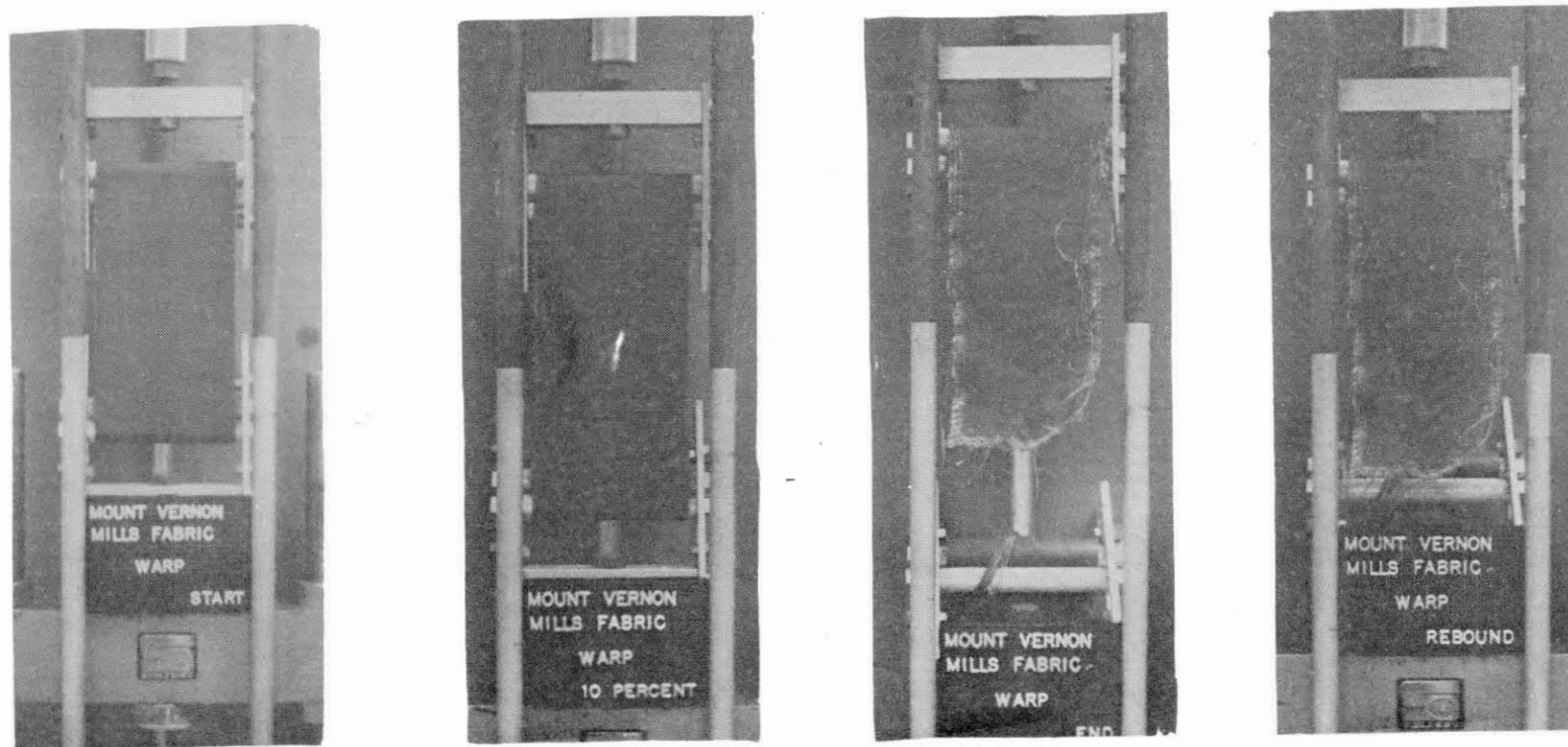


Figure 54. Photographs of Mount Vernon Mills Fabric-Warp Direction in Tension Testing at (Left to Right) Start, 10 Percent Strain, Failure, and After "Elastic" Rebound

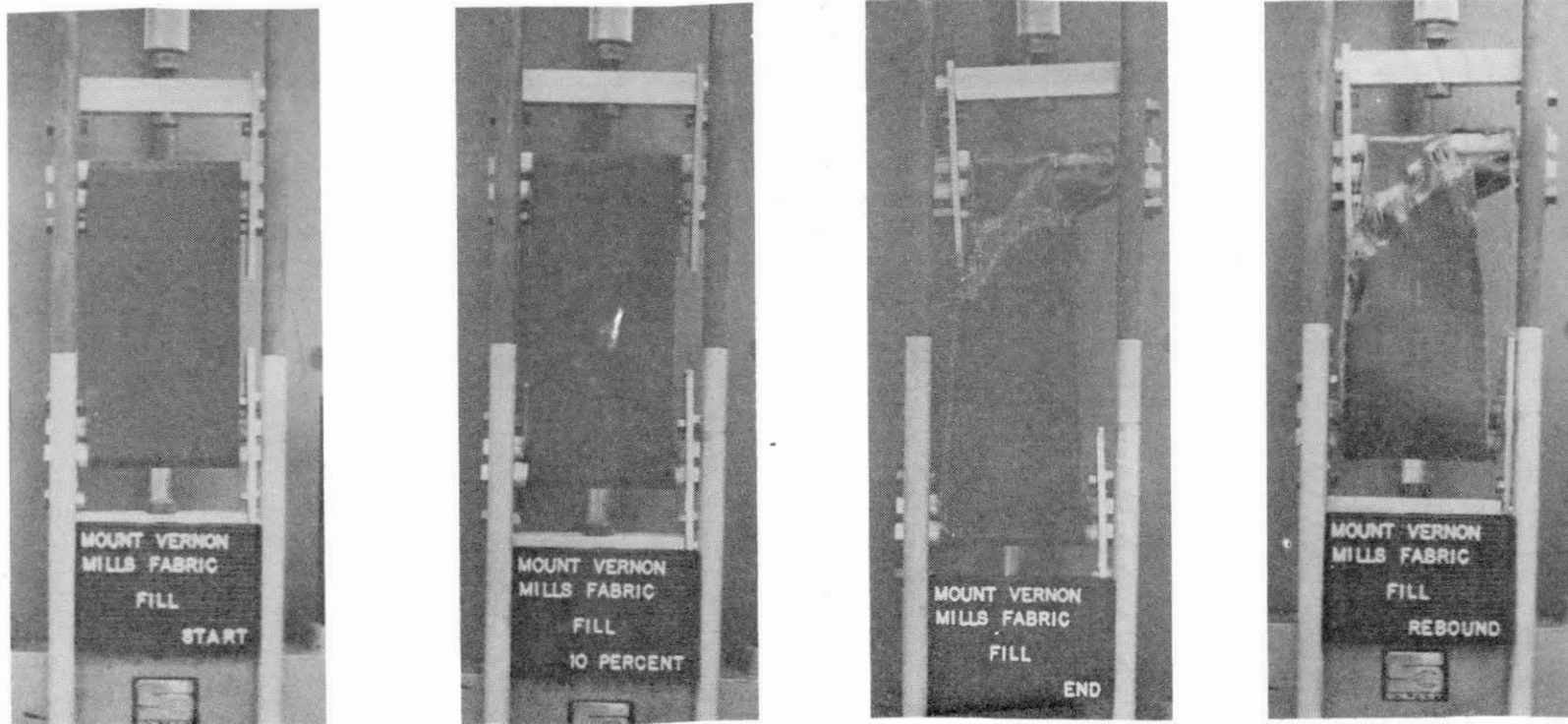


Figure 55. Photographs of Mount Vernon Mills Fabric-Fill Direction in Tension Testing at (Left to Right) Start, 10 Percent Strain, Failure, and After "Elastic" Rebound

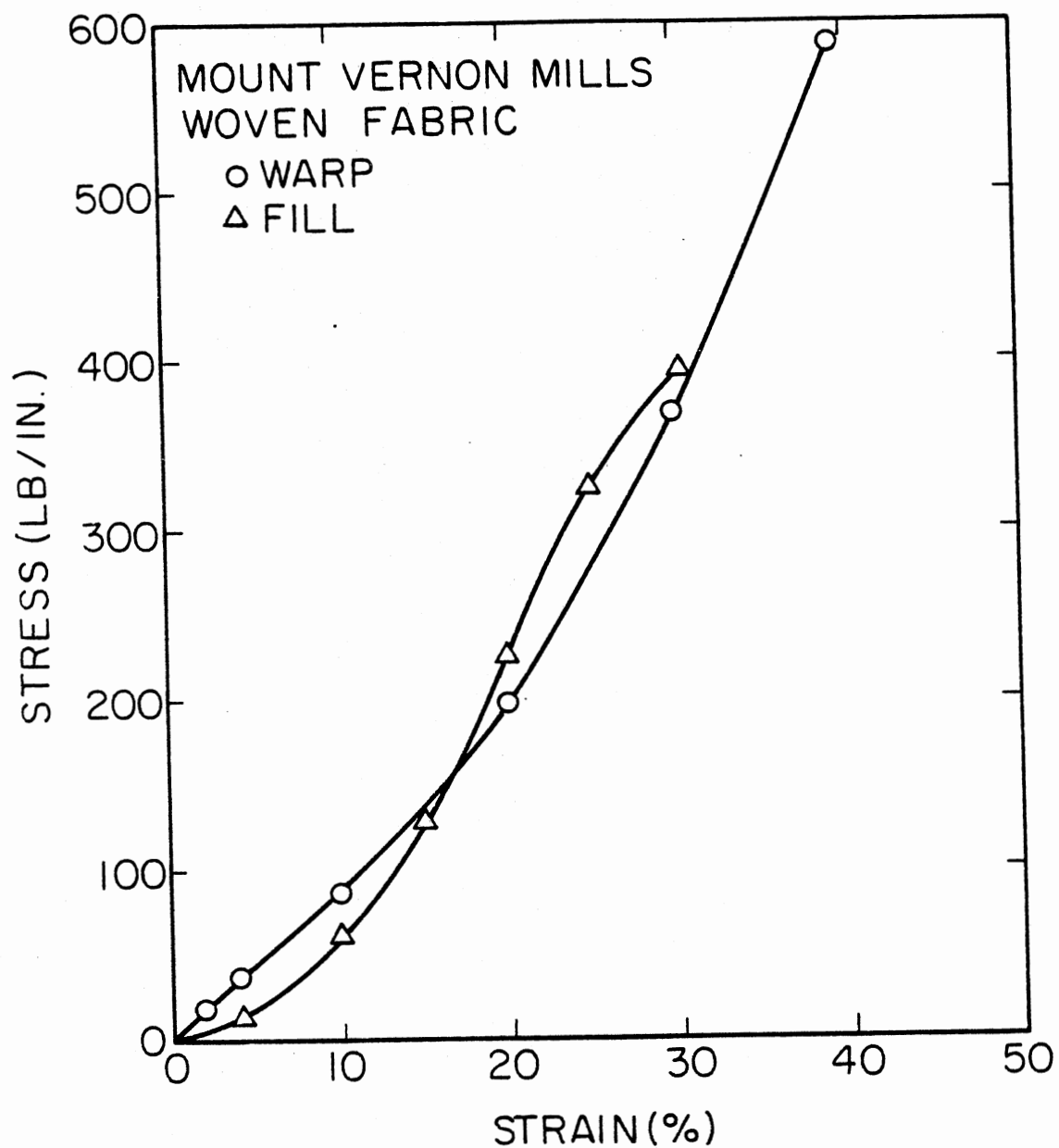


Figure 56. Stress-Strain Data for Mount Vernon Mills Fabric in Uniaxial Testing

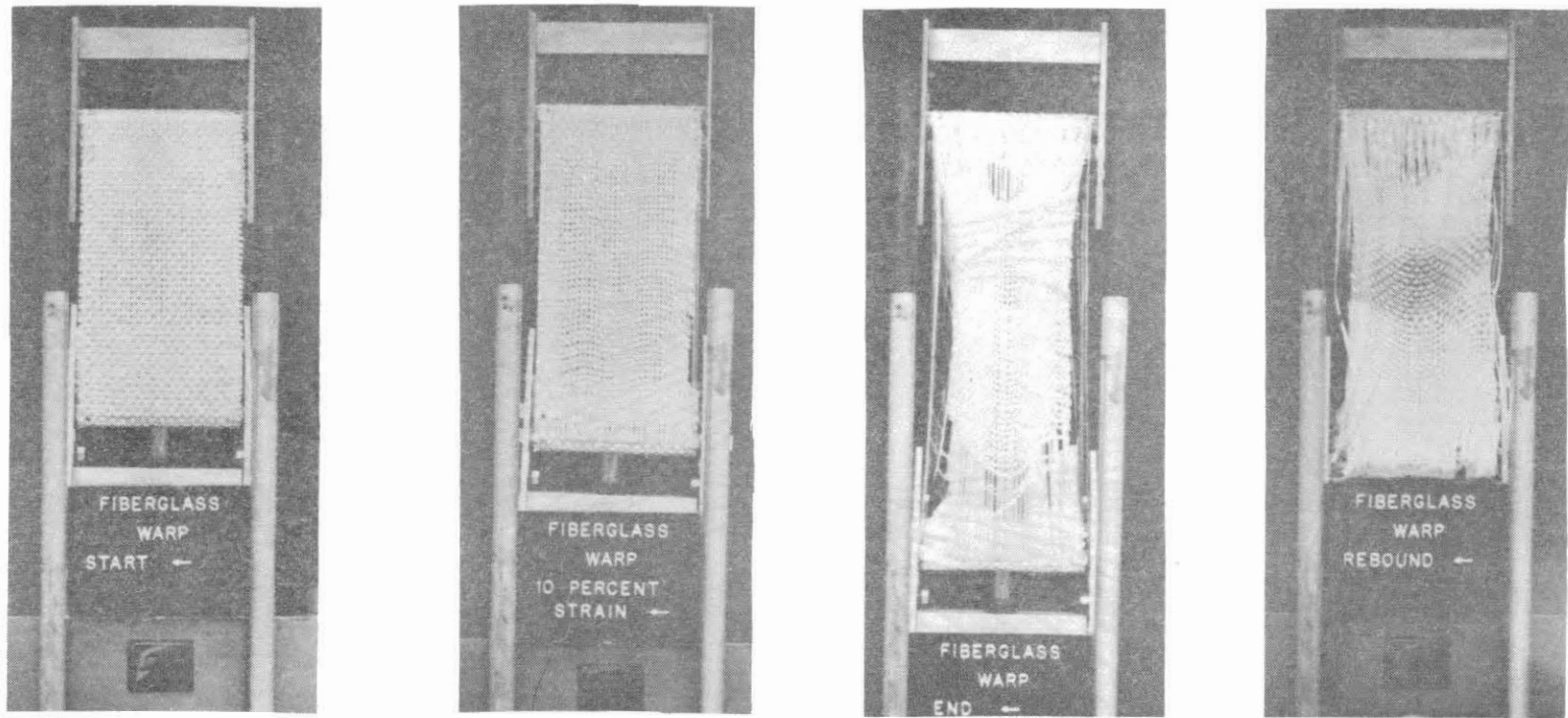


Figure 57. Photographs of Corning Fiberglass Fabric-Warp Direction in Tension Testing at (Left to Right) Start, 10 Percent Strain, Failure, and After "Elastic" Rebound

## VITA<sup>2</sup>

John Kevin King

Candidate for the Degree of

Master of Science

Thesis: A LABORATORY STUDY OF THE ROLE OF GEOTECHNICAL FABRIC AS A  
SEPARATION MEDIUM IN A SOIL FABRIC SYSTEM

Major Field: Civil Engineering

Biographical:

Personal Data: Born in Tulsa, Oklahoma, November 24, 1956, son of  
Mr. and Mrs. Charlie L. King.

Education: Graduated from Memorial High School, Tulsa, Oklahoma,  
in May, 1975; received the Bachelor of Science in Civil Engi-  
neering Degree from Oklahoma State University, Stillwater,  
Oklahoma, in July, 1979; enrolled in the Graduate Program at  
Oklahoma State University, Stillwater, Oklahoma, in September,  
1979; completed requirements for the Master of Science degree  
in Civil Engineering in July, 1981.

Professional Experience: Undergraduate Teaching Assistant, Civil  
Engineering, Oklahoma State University, January, 1979 to May,  
1979. Undergraduate Research Assistant, Civil Engineering,  
Oklahoma State University, May, 1979 to August, 1979. Graduate  
Research Assistant, Civil Engineering, Oklahoma State University,  
September, 1979, to May, 1980. Full time Project Engineer, June,  
1980 to present, LTM Inc., Tulsa, Oklahoma.

Professional Organizations: Student member of American Society of  
Civil Engineers; Associate member of Oklahoma Society of Pro-  
fessional Engineers; Member Chi Epsilon; Engineer-in-Training  
State of Oklahoma.